Aus dem Institut für translationale Immunologie (TIM)
der Universitätsmedizin der Johannes Gutenberg-Universität Mainz

Interferon-γ loaded dextran-based nanoparticles for the polarization of macrophages
Interferon-γ beladene dextranbasierte Nanopartikel zur Polarisierung von Makrophagen

Inauguraldissertation
zur Erlangung des Doktorgrades der
Medizin
der Universitätsmedizin
der Johannes Gutenberg-Universität Mainz

Vorgelegt von

Carlotta Baumhöfner
aus Frankfurt am Main

Mainz, 2024

Wissenschaftlicher Vorstand: Univ.-Prof. Dr. Hansjörg Schild

1. Gutachter: Univ.-Prof. Dr. Dr. Detlef Schuppan
2. Gutachter: PD Dr. med. (Ernst)_Friedrich_(Christoph) Foerster

Tag der Promotion: 11. Juli 2024

CONTENTS

I. DIRECTORY I

Abbreviations I
Tables IV
Figures V

II. INTRODUCTION 1

General Introduction 1
Inflammation and Cancer Development 1
Tumour microenvironment 2
Metastasis 2
Tumour associated macrophages 3
Macrophage subtypes and functions 4
Signalling and functions of interferon-γ 6
PEGylated interferon-γ loaded dextran nanoparticles in vitro and vivo 7

III. METHODS AND MATERIALS 8

Cell culture 8
Generation of bone-marrow derived macrophages 8
Cultivation of bone-marrow derived macrophages 8
Polarization to M2 type macrophages 8
Repolarization of M2 polarized macrophages with interferon-γ and lipopolysaccharides 9
Repolarization of M2 polarized macrophages with PEGylated interferon-γ loaded dextran nanoparticles and PEGylated lipopolysaccharide loaded dextran nanoparticles 9
Purification of RNA 9
Reverse transcription quantitative real-time polymerase chain reaction (qPCR) 11
Taqman real-time quantitative polymerase chain reaction 12
Fluorescence-activated cell sorting 13
Enzyme-linked immunosorbent assay 13
Injection of interferon-γ-dextran nanoparticles in healthy C57BL/6 mice and C57BL/6 mice with B16F10 liver metastasis 14
Viability resazurin assay 14
Statistical analyses 15
Dextran based nanoparticles 15
Reagents, consumables and devices 16

IV. RESULTS 22

In vitro analysis 22
1. In vitro toxicity of dextran nanoparticles 22
2. Cellular uptake of dextran nanoparticles 23
3. M2 Polarization 25
4. Dextran-based nanoparticle dependent changes of macrophage populations characterized morphologically 26
5. Optimization of real-time quantitative PCR - DNAse treatment 28
6. Interferon-γ, lipopolysaccharides and Dextran nanoparticle dependent changes of macrophage populations characterized via relative quantification of gene expression by real-time quantitative PCR 29
7. Fluorescence-activated cell sorting analysis of macrophage subtypes after interferon-γ, lipopolysaccharides and dextran-based nanoparticle treatment 40
8. Enzyme-linked immunosorbent assay (ELISA) for cytokines 54
In vivo studies 55
Healthy mice 55
Mice with B16F10 liver metastasis 58

V. DISCUSSION 64

Interferon-γ alone fails to polarize and repolarize bone marrow derived macrophages 64
PEGylated interferon-γ-loaded dextran-nanoparticles polarized bone marrow derived macrophages towards and M1-phenotype only in combination with LPS 64
PEGylated interferon-γ loaded dextran-based nanoparticles in combination with LPS trigger proinflammatory cytokine production 65
PEGylated interferon-γ loaded dextran nanoparticles could change macrophages to a MHCII^{high} and CD206^{low} phenotype 66
Reverse transcription quantitative real-time PCR 67
Attempt to explain the lack of effect of PEGylated interferon-γ loaded dextran nanoparticles in vivo 67
Mouse model 68
Conclusion 68

VI. SUMMARY 70

VII. ZUSAMMENFASSUNG 72

VIII. LITERATURE 74

IX. ACKNOWLEDGEMENTS 83

X. CURRICULUM VITAE 84

I. DIRECTORY

Abbreviations

7-AAD	7-Aminoactinomycin D
A	Area
Ac-Dex	Acetalated dextran polymer
AP-1	Activator protein 1
APC-Cy7-A	APC-A Allophycocyanin
Arg1	Arginase 1
BMDM	Bone marrow derived macrophages
c-Myc	Cellular-Myelocytomatosis
CCL17	C-C Motif Chemokine Ligand 17
CCL22	C-C motif chemokine ligand 22
CCL24	C-C motif chemokine ligand 24
CD11b	Integrin αM
CD11b/CD18	Macrophage-1 antigen; CR3; Complement receptor type 3
CD163	Cluster of Differentiation 163
CD206	Cluster of Differentiation 206; Mannose receptor, *cd206*
CD38	Cluster of Differentiation 38; Cyclic ADP ribose hydrolase, *cd38*
CD45	Cluster of Differentiation 45; Leucocyte common antigen
CD68	Cluster of Differentiation 68; Macrosialin; Glycosylated type I transmembrane glycoprotein, *cd68*
CD80	Cluster of Differentiation 80
CD86	Cluster of Differentiation 86
cDNA	Complementary Deoxyribonucleic acid
Comp-7 AAD-A	Compensation-7-Aminoactinomycin D
Comp-APC-Cy7-A	Compensation-APC-A Allophycocyanin
Comp-FITCH	Compensation-Fluorescein-5-isothiocyanat
Comp-PE	Compensation-Phycoerhtrin
C_q	Quantification cycle
CR3	Complement receptor type 3
C_T	Threshold cycle
CTLs	Cytotoxic T-lymphocytes
dd	Double distilled
DMSO	Dimethyl sulfoxide $(CH_3)_2SO$
DNase	Desoxyribonuclease I;D
DNMTs	DNA methyltransferases
DNP(s)	Dextran-nanoparticle(s)
DPBS	Dulbecco's Phosphate-Buffered Saline
dsDNA	Double stranded Deoxyribonucleic acid
ECM	Extracellular matrix
EDTA	Ethylenediaminetetraacetic acid
Egr2	Early growth response protein, *egr2*

EIA	Enzymgekoppelter Immunadsorptionstest
ELISA	Enzyme linked immunosorbent assay
EMT	Epithelial-mesenchymal transition
EtOH	Ethanol
F4/80	EMR1; EGF-like module containing, mucin-like, hormone receptor-like sequence 1
FACS	Fluorescence-activated cell sorting
FBS	Fetal bovine serum
Fig.	Figure
FITCH	Fluorescein-5-isothiocyanat
Fizz1	Found in inflammatory zone
Fpr2	Formyl peptide receptor 2
FSC	Forward scatter
GM-CSF	Granulocyte-macrophage colony-stimulating factor
Gpr18	G-protein coupled receptor 18
HRP	Horseradish peroxidase
IFN-γ	Interferon-γ
IFN-γ-DNP(s)	Interferon-γ loaded dextran-based nanoparticle(s)
IHC	Immunohistochemistry
IL-10	Interleukin-10, *il10*
IL-12	Interleukin-12
IL-13	Interleukin-13
IL-18	Interleukin-18
IL-1ra	Interleukin-1 receptor antagonist
IL-1β	Interleukin-1β
IL-23	Interleukin-23
IL-4	Interleukin-4
IMDM	Iscove's Modified Dulbecco's Medium
iNOS	Inducible nitric oxide synthase, *inos*
IRF1	Interferon regulatory factor 1
JAK	Januskinase
KCl	Potassium chloride
KH_2HPO_4	Monopotassium phosphate
LPS	Lipopolysaccharide
LPS-DNP(s)	Lipopolysaccharide dextran-nanoparticle(s)
Ly6c	Lymphocyte antigen 6 complex, *ly6c*
M-CSF	macrophage colony stimulating factor
M1	M1-type macrophages
M2	M2-type macrophages
Mac-1	Complement receptor type 3
MFI	Mean fluorescence intensity
MHCII	Class II major histocompatibility complex molecules, *mhc2*
MMP	Matrix metalloproteinases

MMR	Macrophage mannose receptor
Mph	Macrophages
Mrc1	Mannose receptor, Cluster of Differentiation 206, *mrc1*
Na_2HPO_4	Sodium hydrogen phosphate
NaCl	Sodium chloride
NF-κB	Nuclear factor kappa B
PBS	Phosphate-buffered saline
PE	Phycoerhtrin
PEG	Polyethylene glycol
Pen-strep	Penicillin-Streptomycin
PPAR-y	Peroxisome proliferator–activated receptor-y
QPCR; qPCR	Reverse transcription quantitative real-time polymerase chain reaction; quantitative Echtzeit-Polymerase-Kettenreaktion
RNA	Ribonucleic acid
RNase	Ribonuclease
RT-PCR	Reverse transcription-Polymerase chain reaction
SOCS3	Suppressor of cytokine signaling 3
SSC	Size and side (90°, SSC) scatter
STAT1	Signal transducer and activator of transcription 1
STAT3	Signal transducer and activator of transcription 3
STAT6	Signal transducer and activator of transcription 6
T reg.	Regulatory T-cells
TAM	Tumour associated macrophage
TC treated plates	Tissue-culture treated plates
TGF-β1	Transforming growth factor β1
Th1	T-helper-cells type 1
Th2	T-helper-cells type 2
TMB	3,3',5,5'-Tetramethylbenzidine
TNFα	Tumour necrosis factor α, *tnfa*
TLR	toll-like receptor
VEGF	Vascular endothelial growth factor

Tables

Table **1**: M1 and M2 polarization macrophage marker 6

Table **2**: DNase I treatment 10

Table **3**: Reverse transcription – Thermal cycler program 11

Table **4**: Primer for Real-time quantitative PCR 11

Table **5**: QPCR – Syber Green Mastermix 12

Table **6**: Programm - qPCR 12

Table **7**: Fold change Ratio 12

Table **8**: QPCR - Taqman Mastermix 13

Table **9**: QPCR Taqman - Program 13

Table **10**: Reagents, consumables and devices 16

Figures

Figure **1**: In vivo Biodistribution and composition of PEGylated dextran nanoparticles 7

Figure **2**: Viability Resazurin Assay 22

Figure **3**: Cellular uptake of dextran-based nanoparticles by native and treated murine macrophages 24

Figure **4** : Oregon Green® 488-labeled Interferon-γ loaded dextran-based nanoparticles distribute evenly after dispersion in PBS by ultrasound 24

Figure **5**: Cellular uptake time-course of Oregon Green® 488-labeled Interferon-γ loaded dextran-based nanoparticles by native murine macrophages 25

Figure **6**: Arginase 1 indicates alternative polarization of murine macrophages after IL-4 and IL-13 treatment 26

Figure **7**: Phase contrast images of native murine macrophages. 27

Figure **8**: Phase contrast images of murine macrophages M2-polarized with interleukin-4 and interleukin-14. 27

Figure **9**: RNA concentration before and after DNAse I treatment 29

Figure **10**: Representative real-time quantitative PCR results - DNase I treatment .. 29

Figure **11**: Heat map and real-time quantitative PCR data of marker genes in interferon-γ treated murine macrophages 31

Figure **12**: Heat map of marker genes in interferon-γ dextran-nanoparticle treated murine macrophages 34

Figure **13**: Real-time quantitative PCR based analysis of dextran-based nanoparticle treated murine macrophages 35

Figure **14**: Real-time quantitative PCR analysis of dextran-based nanoparticle treated murine macrophages 36

Figure **15**: First taqman real-time quantitative PCR based analysis of dextran-based nanoparticle treated murine macrophages 37

Figure **16**: Second Taqman real-time quantitative PCR based analysis of dextran-based nanoparticle treated murine macrophages 39

Figure **17**: Fluorescence-activated cell sorting of interferon-γ treated murine macrophages – Gating (17.2) 42

Figure **18**: Fluorescence-activated cell sorting of interferon-γ dextran-based nanoparticle treated murine macrophages – Gating (18.2) 45

Figure **19**: Fluorescence-activated cell sorting of interferon-γ dextran-based nanoparticle in combination with lipopolysaccharid treated murine macrophages – Gating (19.2) 48

Figure **20**: Fluorescence-activated cell sorting of dextran-based nanoparticle treated murine macrophages (20.2) 51

Figure **21**: Fluorescence-activated cell sorting of dextran-based nanoparticle treated murine macrophages 53

Figure **22**: TNFα-ELISA of cell culture supernatant 54

Figure **23**: IL10- ELISA of cell culture supernatant 55

Figure **24**: Biometric data after intravenous injection of Interferon-γ loaded dextran-based nanoparticles in healthy C57BL/6 mice 56

Figure **25**: Characterisation of liver tissue macrophage populations after intravenous injection of interferon-γ loaded dextran-based nanoparticles in healthy C57BL/6 mice via relative quantification of gene expression. 57

Figure **26**: Biometric data after intravenous injection of interferon-γ loaded dextran-based nanoparticles in C57BL/6 mice with B16F10 liver metastasis 59

Figure **27**: Characterisation of liver tissue macrophage population after intravenous injection of interferon-γ loaded DNP in C57BL/6 mice with B16F10 liver metastasis by relative quantification of gene expression 61

Figure **28**: Fluorescence Activated Cell Sorting of murine liver macrophages after intravenous injection of interferon γ-carrying DNP in C57BL/6 mice with B16F10 liver metastasis 62

II. INTRODUCTION

General Introduction

The immune system plays a decisive role in cancer development and progression. This thesis surveyed several participants of the innate and the adaptive immune system focusing on macrophages and investigating how they are affected by interferon-γ loaded dextran nanoparticles (IFN-γ-DNP).
In 1863 Rudolf Virchow was the first who drew a connection between chronic inflammation and cancer development and progression (1). The current status of research supports his hypothesis and has furthermore identified crucial players. Cancer-related inflammation in the tumour microenvironment is maintained by cytokines, growth factors and the interaction between the responsible immune cells (2). Macrophages play a fundamental role in tumour progression and patient prognosis (3).
Macrophages can either be natural constituents of organs, such as Kupffer cells in liver, or derive from the bone marrow, especially, these monocyte-derived macrophages home to organs where, e.g., an infection or chronic inflammation occurs. Tissue resident and freshly recruited macrophages can then differentiate into subtypes with diverse functions depending on the target tissue (4, 5). Regarding malignant tumours, which can be described as 'inflammatory wounds that do not heal' two main groups of macrophages can be differentiated: On the one hand tumour associated macrophages (TAMs) which modulate the tumour microenvironment to suppress the immune system, promote tumour cell growth, angiogenesis, immunosuppression and metastasis (M2-type), and on the other hand proinflammatory (M1-type) macrophages inducing a defence mechanism via CD8+ cytotoxic T-cell recruitment and activation (6, 7).
This ambivalent effect is caused by the ability to respond to signals from the microenvironment including the tumour cells themselves, by the expression of either pro- or anti-tumour functions (8). Over the approaches influencing this differentiation, the terms polarization and repolarization have been coined (9).
So far the suitability of IFN-γ-loaded DNP (dextran nanoparticles) to repolarize TAMs from tumour promoting M2-type towards anti-tumour M1-type macrophages, and assessment of their therapeutic effect *in vitro* and *in vivo* has been unknown. The intention of this work was to study how far IFN-γ-DNP affect the polarization of murine bone marrow derived macrophages towards an M1-type and whether they exert anti-cancer effects in a murine melanoma model in vivo.

Inflammation and Cancer Development

Above all, tumour-promoting inflammation in the early states of cancer development seem to be an important determinant of tumour progression (10). Furthermore neoplastic tissues need to be understood as "complex tissues with distinct cell types" which form the tumour microenvironment (6). In recent decades this concept has expanded, as expressed by Hanahan and Weinberg (11), who postulated that the

hallmarks of cancer are the following: “Evading growth suppressing activation, resisting cell death, enabling replicative immortality, invasion and metastasis, inducing angiogenesis, and sustaining proliferative signalling”(6). At least the last three abilities appear to be directly related to the tumour microenvironment and the supporting cells within the stroma.

Tumour microenvironment

Decisively the tumour microenvironment is influenced by the tumour itself, producing cytokines and growth factors and the adjacent or recruited “normal” cells, which start supporting the cancer progress, manipulated by neoplastic cells (7).
Sustaining proliferative signalling is mediated amongst other things by growth factors binding cell-surface receptors, especially transmembrane tyrosin kinases, including auto- and paracrine proliferative stimulation, largely also via signals from neighbouring non-transformed activated cells supplying cancer cells with vascular supply and nutrients, or growth factors (12). Here, apart from the cancer cells, also ‘switched’ immune cells infiltrating tumours or even premalignant lesions help to promote angiogenesis (13).
Thus, on the one hand immune competence appears to be a key feature shielding the organism from developing malignant neoplasia (14), while immunosuppressed individuals, particularly those with a deficiency of innate immune cells, are at risk of developing cancers (15).
On the other hand tumour-infiltrating myeloid immune cells, among them “alternatively-activated“ macrophages and tolerogenic dendritic cells, promote tumour growth, antagonizing the anti-tumour immune response (8). This seems to by an inconsistent reaction of the body, but can be explained by the diverse functions of immune cells: promoting acute inflammation to fight pathogenic agents and de novo occurring neoplastic cells, but also dampening chronic inflammation to prevent organ disassembly, helping to rebuild the tissue by activating fibrogenesis, supplying growth factors and promoting neo angiogenesis (16). Thus, since the cells of the tumour microenvironment are often more stable than tumour cells themselves, they are suggested a promising new target in tumour therapy (4).

Metastasis

One determinant of tissue integrity that prevents invasion and metastasis is the attachment of cells to the extracellular matrix (ECM) by cell-cell and cell-ECM adhesion molecules like E-cadherin and certain integrins, respectively, which are usually downregulated in invasive carcinomas (17). Immune cells of the microenvironment, like macrophages, are switched towards an M2-phenotype that supports invasive growth, metastasis and promotes the epithelial-mesenchymal transition (EMT) transition of the cancer cells, resistance to apoptosis and metastasis by by supplying extracellular matrix degrading enzymes (18).
Metastasis consists of two major steps: dissemination and macroscopic tumour growth. A paracrine interaction between tumour cells and macrophages via the induction of synergistic migration has been suggested for many years (19).

Hageman et al. found tumour necrosis factor α (TNFα)-dependent matrix metalloproteinases (MMP) production and therefore increased tumour cell invasiveness when co-culturing macrophages with tumour cells (20).
It is known that cells can disseminate early in tumour growth (21) indicating the importance of the interplay between cancer cells and the supporting stroma, not only for primary tumour growth, but also for metastasis (6). This also explains the often insufficient long-term response to anti-tumour therapy such as radiation (22).

Tumour associated macrophages

As critical mediator of tissue homeostasis macrophages represent an attractive target for tumour immunotherapy (23, 24). TAMs have the ability to regulate T-cell recruitment, promote neoangiogenesis, and interfere with cells of the ECM to indirectly promote cancer growth by providing growth factors for fibroblasts (cancer associated fibroblasts (25), such as TGFβ1 and vascular endothelial growth factor (VEGF) (4, 26, 27).
In several studies, the presence of TAMs could be associated with poor prognosis due to their effect on tumour growth and metastasis and by promoting tumour angiogenesis (10, 28-30). In addition, TAMs have been shown to suppress the response to standard anti-tumour therapies such as chemotherapy, radiation (31-34), and even anti-angiogenetic agents and checkpoint inhibitors (22, 26, 33). For example, subsequent relapses due to adaptive (T cell mediated) tumour resistance after treatment with targeted drugs, such as checkpoint inhibitors, are often associated with the number of TAMs (35, 36). These activities combine with physical barriers in solid tumours reduce the therapeutic effect of immunotherapies (37).
Thus, re-educating TAMs for cancer therapy seems to be a way to avoid the limiting effects described above. Consequently, targeting multiple cells and drivers appears to be required to consistently inhibit tumour growth (6). Therefore, TAM-reducing or modulating therapies can act in concert with chemotherapy and immunotherapy (38).
Tissue macrophages can originate from two different sources: embryonic organ-resident cells persisting until adulthood, or adult hematopoietic stem cell (HSC) progenitor cells that circulate as monocytes (16, 19, 25). Thus, TAMs in pancreatic ductal adenocarcinoma have both embryonic and HSC origin and different roles in tumour progression depending on this origin (26, 39).
As mentioned above, functions of macrophages concerning tumour immunity and tumour growth change with the diversity and development of the macrophage subtypes. Specification appears to depend on developmental origin, tissue of residence, the interaction with other cells like fibroblasts and endothelia, and the ECM (26).
In conclusion, macrophages, especially TAMs, seem to be a promising target to stimulate the anti-tumour immune response, and preclinical studies hypothesize therapeutic success by repolarizing macrophages to a tumour-suppressing or killing phenotype (40, 41).

Macrophage subtypes and functions

The beginning of research in macrophages and their functions in induction and resolution of inflammation and tissue repair was in the early twentieth century. In 1983 Nathan et al. confirmed the classic activation in human macrophages by interferon-γ (IFN-γ) (42). One year later IFN-γ was identified as a stimulator of tumouricidal activity in bone marrow derived mouse macrophages (43). Meanwhile Stein et al. discovered interleukin-4 (IL-4) inducing an alternative macrophage activation and an increased expression of macrophage mannose receptor (MMR) in contrast to a decrease of this receptor in response to INF-γ (44). Similar to IL-4, interleukin-13 (IL-13) enhances class II major histocompatibility complex molecules (MHCII) expression as well as MMR, supporting tissue repair and inhibiting inflammatory reaction (45).

Consequently, the nomenclature of macrophages followed that of T-helper cells type 1 (Th1) and T-helper cells type 2 (Th2), which produce IFN-γ and IL-4 and IL-13 (15), respectively, leading to the central assumption that macrophages can be divided into two main groups: on the one hand classical activated M1-type macrophages (M1), which support proinflammatory and anti-tumour functions, and on the other hand alternative activated macrophages (M2-type macrophages (M2)), which suppress T-cell function, promote angiogenesis and therefore tumour growth and metastasis (46).

In the last 2 decades this categorization turned out to be too simplistic, since the heterogeneous phenotypes and functions of macrophages *in vivo* are more a fluent and diverse system which develops over time and being dependent on changes of the surrounding microenvironment, including tumour growth (26).

Nevertheless, *in vitro* under defined conditions the differentiation into extremes of either M1-like or M2-like subpopulations is easily achievable (4, 9, 47) serving as basis for categorization of macrophage subtypes through markers that define the in vitro polaristaion and activation state. In general, the activation state depends on stimulus, feedback and feed forward signals and developmental effects. Under the influence of INF-γ, lipopolysaccharide (LPS) and granulocyte-macrophage colony-stimulating factor (GM-CSF) an interleukin-12 $(IL\text{-}12)^{high}$/ interleukin-10 $(IL\text{-}10)^{low}$ phenotype type producing the cytokines interleukin-1β (IL-1β), TNFα, IL-12, interleukin-18 (IL-18), Interleukin-23 (IL-23) as well as chemokine attracting Th1, develops (47). The M1-type macrophages express the surface markers cluster of differentiation 38 (CD38), CD80, CD86 and class II major histocompatibility complex molecules (MHCII), suppressor of cytokine signaling 3 (SOCS3) and inducible nitric oxide synthase (iNOS) (48). Phenotype changes via INF-γ and LPS are mediated through signal transducer and activator of transcription (STAT1) and nuclear factor-κB (NF-κB) activation (43). This macrophage type directs Th1 and Th17 cells to an inflammatory immune response (44).

IL-13 and IL-4 lead to an IL-10 ^{high}/IL-12 ^{low} type that suppresses T-cell recruitment and activation and promotes growth and tissue repair via producing IL-10, transforming growth factor β1 (TGF-β1) and interleukin-1 receptor antagonist (IL-

1ra). Furthermore, these M2-type macrophages express CD163, MHCII, CD206, arginase1 (Arg1), Found in inflammatory zone (Fizz1), and produce C-C Motif Chemokine Ligand 17 (CCL17), CCL22 and CCL24 (41). IL-13 and IL-4 induce these M2 phenotype changes via STAT3, STAT6 intracellular signal transducers and the peroxisome proliferator–activated receptor-y (PPAR-y) pathway (49), 43, (50). Produced by innate lymphoid cells, adaptive lymphocytes such as Th1 and cytotoxic T cells (CTLs), INF-γ activates Janus kinase (JAK) signalling, STAT1 signalling and interferon-simulated gene induction by binding to interferon-γ receptor 1 and interferon-γ receptor 2, triggering a rapid and transient intracellular JAK-response (69).

In selected tumours the type 2 cytokines IL-4 and IL-13 are major drivers of the M2-like polarization of TAMs (38). Accordingly, the majority of TAMs exhibit M2 characteristics such as neoangiogenesis, tissue repair, growth factor secretion and suppression of inflammation (8). Thus, a high amount of TAMs with an M2 phenotype is considered to be responsible for disease progression and poor outcome (29).

The classification of macrophage subtypes by the characterisic constellation of multiple markers (Table 1) is recommended by Murray et al (9). Apart from the classical markers as mentioned above, Jablonski *et al.* defined further markers such as CD38, G-protein coupled receptor 18 (Gpr18) and Formyl peptide receptor 2 (Fpr2) as M1 and Early growth response protein (Egr2) and c-Myc as M2 specific (51). Still, the in vitro and especially in vivo functionality of macrophages cannot be predicted by their currently used marker profile.

Moreover and in general, there are basic surface markers suitable to distinguish the subtypes of immune cells: leucocyte common antigen (CD45) a receptor tyrosine kinase can used as a marker for all hematopoietic cells except for platelets and erythrocytes, and plays an important role in the function of these cells (52). F4/80 is a mouse macrophage specific membrane glycoprotein, which is necessary to generate antigen-specific regulatory T-cells (T reg.) (53).

As an example, CD11b/CD18, also known as dimeric integrin αMβ2 or Mac-1, is a cell-cell and cell-collagen adhesion receptor and part of the complement receptor type 3 cascade. It is mainly expressed by neutrophils, dendritic cells, monocytes and macrophages which are key antigen presenting cells (54).

Table **1**: M1 and M2 polarization macrophage upregulated marker

M1 upregulated *transcripts*		Reference	M2-upregulated *transcripts*		Reference
Il-6 *il-6*	Interleukin-6	(55)	Egr2 *egr2*	Early growth response 2	(51, 56)
TNFα *tnfa*	Tumour Necrosis Factor α	(57-59)	Mrc1 / CD206 *mrc1*	Mannose receptor C type 1	(51, 60)
Ly6c *ly6c*	Lymphocyte antigen 6 complex	(61)	TGF-β1 /Tgfβ1 *tgfb1*	transforming growth factor β1	(62)
MHCII *mhc2*	Class II major histocompatibility complex molecules	(63)	Il-10 *il-10*	Interleukin-10	(64)
iNOS *inos*	Inducible nitric oxide synthase	(65)	Arg1 *arg1*	Arginase, liver	(66)
CD38 *cd38*	Cyclic ADP ribose hydrolase	(67)	Fizz1 *fizz1*	Found in inflammatory zone	(51)
CD68 *cd68*	Macrosialin; glycosylated type I transmembrane glycoprotein	(69)	CD68 *cd68*	Macrosialin; glycosylated type I transmembrane glycoprotein	(68)

Signalling and functions of interferon-γ

As explained above, INF-γ activates STAT1 signalling and interferon-stimulated gene inductions through binding to interferon-γ receptor 1 and interferon-γ receptor 2, activating rapid and transient JAK-STAT signal transduction (69).
Enhancers control the pro-inflammatory gene expression program in macrophages (70) by binding inflammation activated transcription factors like NF-kB, STATs and activator protein 1 (AP-1) (38) despite of that by over expression of DNA methyltransferases (DNMTs) or the loss of histone deacetylase a genetic priming towards an M2 type is favoured (71, 72).
INF-γ stimulation of macrophages results in their increased responsiveness to pro-inflammatory stimuli (such as LPS) (69, 70). Aside from that INF-γ works as an activator of a subset of proinflammatory genes, by priming pre-existing enhancers and promotors via the recruitment of signal of transducer, STAT1 and interferon regulatory factor 1 (IRF1) (71-73).
A previous study discovers IFN-y mediated repolarization of M2 like TAM to immunstimulatory M1 macrophages in human ovarian cancer (73).

In conclusion, LPS and INF-γ alone and in combination are thought to induce potent tumouricidal activity, leading to the production of high levels of TNF-α and inflammatory responses through Th1 activation and low levels of IL-10 (45).

PEGylated interferon-γ loaded dextran nanoparticles in vitro and vivo

Like described above INF-γ and LPS are (55) able to redirect TAMs through a pro inflammatory phenotype (73). In terms of specific drug delivery to the tumour bearing regions, which is necessary to gain therapeutic success, DNP show up potential thus they are non-toxic, biodegradable (74) and accumulate in macrophages (75) which are able to carry the particles to the tumour affected areas especially the liver. Uptake by macrophages does not appear to be affected by the polarisation state (75). Wang et al. suggest additional beneficial effects using carrier molecules to avoid poor distribution and instability of cytokines and systemic side effects by systemic administration (76). DNP show no relevant organ effects after injection (75). In a previous study Foerster et al. demonstrated that PEGylation improved in vivo accumulation of DNP in the liver (Fig. 1) without influencing the circulation half live (75).
Overall, PEGylated INF-γ-DNPs appear to be promising vehicles for the polarisation of macrophages to the M1 type in the liver.

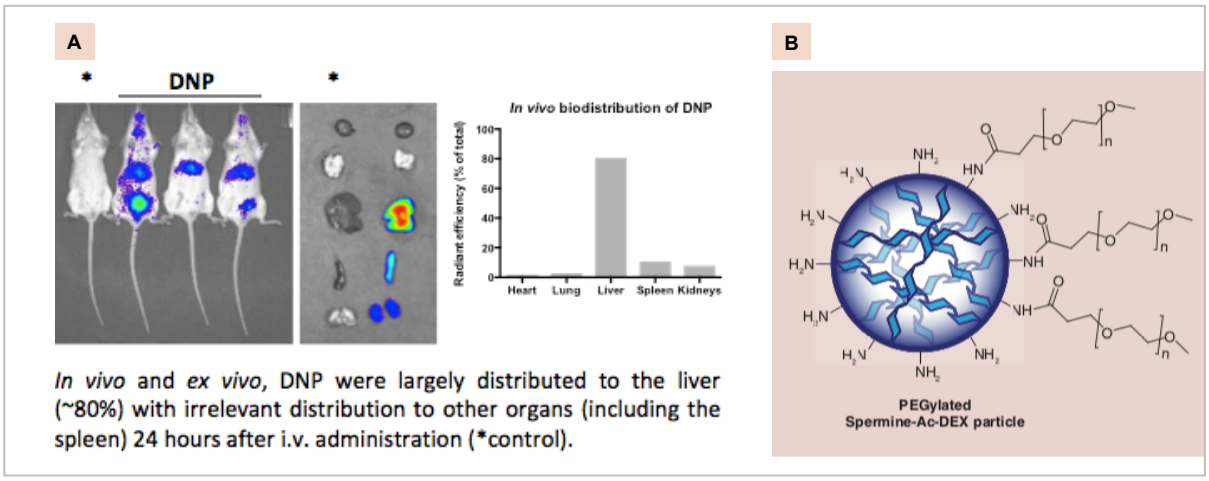

Figure **1**: In vivo Biodistribution and composition of PEGylated dextran nanoparticles (Modified from (75, 77)). In vivo and ex vivo imaging of the biodistribution of dextran nanoparticles (DNP) (A) DNP were mainly distributed to the liver 24 h after intravenous administration (77). Composition of PEGylated DNP (B) (75). PEG: polyethylene glycol; Ac-Dex: aceylated dextran polymer.

III. METHODS AND MATERIALS

Cell culture

Generation of bone-marrow derived macrophages

The generation of murine bone marrow derived macrophages was based of isolation of precursor cells from the bone marrow of tibia, femur and pelvis of male ten weeks old BALB/c and C57BL/6 mice (Charles River Laboratories, Wilmington, Massachusetts, United States). After sacrificing the mice by cervical dislocation, the hind limbs were isolated from the corpus. Then they were disinfected with 65% ethanol (EtOH) for ten minutes and afterwards placed in a plastic centrifugation tube with cell culture media (Iscove's Modified Dulbecco's Medium (IMDM) on ice until further preparation. The bone extraction from muscles and the further bone marrow isolation were practiced under laminar flow to avoid contamination of the isolated cells. Before the opening of the end of the bones they were again left in 65% EtOH for 1 min and afterwards places in IMDM media. The bone marrow was isolated using cannulas (0.5 x 16 mm for the tibia and 0.7 x 30 mm for the femur and pelvis) and the eluted suspension was pipetted over 70 µm cell filter EASYstrainer™. After centrifugation (300 x g, 4°C, 10 min) the cells were diluted into 10 ml IMDM media and counted in with automated cell counter TC10™ using Trypan Blue solution and Counting Slides, Dual Chamber.

Cultivation of bone-marrow derived macrophages

To achieve the specification of bone marrow derived macrophages the precursor cells were cultivated on 94 mm cell culture petri dish in IMDM Media (+penicillin-streptomycin (Pen-strep (2 mM)) + fetal bovine serum (FBS (10%))+ Glutamine (2 mM)) and macrophage colony stimulating factor (M-CSF (25 ng/ml)) at least 7 days in a density of 2-3 million into a humidified incubator at 37°C containing 5% CO_2. The media was changed every third day to remove dead cells.
Before the following treatment the cells were plated out on 100 mm cell-culture petri dishes. The media from the further dishes was collected and after treating them with phosphate-buffered saline (PBS) and 5 mM ethylenediaminetetraacetic acid (EDTA (0.5 M)) and an incubation time of max 10 minutes, controlled under microscope until they start detaching. Then the cells were mixed with the IMDM media and centrifuged (300 x g, 4°C, 10min). Afterwards they were plated out with IMDM Media (+ Pen-strep (2 mM) +FBS (10%)+ Glutamine (2 mM)) and M-CSF (10 ng/ml) on sterile cell culture petri dishes (100mm) for further treatment.

Polarization to M2 type macrophages

To polarize native bone marrow derived macrophages to alternatively activated macrophages the interleukins IL-4 and IL-13 are described to be potent stimulants (44, 45) used in concentration of 20 ng/ml IMDM Media (+ Pen-strep (2 mM) + FBS (10%) + Glutamine (2 mM) + M-CSF (10 ng/ml)). The cells were incubated for 48 h at 37°C.

Repolarization of M2 polarized macrophages with interferon-γ and lipopolysaccharides

Polarization and Repolarization to classically activated (M1 type) macrophages with IFN-γ and LPS like described in several studies (42, 51). The native and the previously treated cells were incubated for 48 h in IMDM Media (+ Pen-strep (2 mM) + FBS (10%)+ Glutamine (2 mM) + M-CSF (10 ng/ml)), after washing with PBS. The used concentration of IFN-γ (ImmunoTools GmbH, Friesoythe, Germany) was 20 ng/ml and LPS (E. coli O111:B4, Merck Millipore) were used in a concentration of 100 ng/ml.

Repolarization of M2 polarized macrophages with PEGylated interferon-γ loaded dextran nanoparticles and PEGylated lipopolysaccharide loaded dextran nanoparticles

The lyophilized DNP (0.5 mg per tube) were diluted in 100 µl PBS vortexed and placed into an ultrasound bath (10 min).
As mentioned above the cells were incubated for 24 h (48 h) in IMDM Media (+ Pen-strep (2 mM) +FBS (10%)+ Glutamine (2 mM) + M-CSF (10 ng/ml)) and as treated, with LPS-DNP (10 µg/ml), IFN-γ-DNP (20 µg/ml) or empty DNP (20 µg/ml).

Purification of RNA

a) *RNA isolation*

For thick homogenate out of two to three pieces of tissue samples, stored on ice, these were left in 1,000 µl of ribozol for homogenization. For thin homogenate 950 µl of ribozol was pipetted in 1.5 ml Eppendorf Safe-Lock Tubes and then 50 µl of the thick homogenate were added and vortexed several times. Further proceeded as described below.
For cell culture samples the protocol for RNA isolation was followed from this point. After the cells / tissue were lysed in 1,000 µl ribozol 300 µl chloroform were added per tube. After vortexing and incubation at room temperature for 15 min, the samples were centrifuged at 13,000 rpm for 15 min (4°C). Then the clear supernatant (400 µl) from the triphasic phenol-chloroform extraction was pipetted carefully into new eppendorf tubes.
After adding Isopropanol (same amount as the supernatant), vortexing and incubation at room temperature for 15 min the samples were centrifuged again at 13,000 rpm for 15 min (4°C) and the supernatant was discarded.
Afterwards the pellet was washed two times with 1000 µl EtOH (75%) and centrifuged in between at 13,000 rpm for 5 min (4°C). The pellet was placed under the laminar flow for drying. The RNA was diluted in 90 µl RNAse-free water on ice and stored at -80°C.

b) *RNA isolation with GeneMATRIX Universal RNA Purification Kit*

Before starting the isolation procedure the activation of the homogenization spin column was performed with 30 µl Buffer A (GeneMATRIX Universal RNA Purification

Kit, EURX, Poland) for ten minutes. To inactivate contaminating RNase 10 µl beta-mercaptoethanol per ml RL buffer (GeneMATRIX Universal RNA Purification Kit, EURX, Poland) was added.
The media was removed from the cell culture dishes and the cells were washed with 1 ml PBS afterwards they were harvested in PBS using a cell-scraper. Subsequently the cells were pelleted by centrifugation in the 2 ml eppendorf tubes (5 min at 1,000 x g) and PBS was replaced by 400 µl RL buffer. After efficient cell disruption by pipetting the lysate was transferred to a homogenization spin-column placed on a receiver tube and centrifuged (2 min 11,000 x g). This step homogenized the sample and removed DNA. Afterwards 250 µl EtOH (100%) was added and everything was transferred on the RNA binding spin-column. After centrifugation (1 min at 11,000 x g) and discarding the flow through 400 µl Wash DN1 buffer was added to the column. The supernatant was discarded and 600 µl Wash RBW (afterwards 300 µl) was added, centrifugation in between (1 min 11,000 x g). Then the RNA was eluted into new eppendorf tubes with 50 µl RNase-free water. If not proceeded immediately the RNA was stored at -80°C. The RNA content was measured using Tecan 2000 monochromator-based microplate reader.

c) *Combination*

After proceeding as described above (RNA isolation, only one wash step) the pellet was dissolved in 350 µl EtOH (70%) and pipetted on the RNA binding column and processed like provided in protocol (EURX, Poland) including the DNaseI (QIAGEN, Netherlands) treatment.

d) *DNaseI treatment*

After mixing the following ingredients (Table 2) the samples were incubated for 30 minutes at 37°C.

Table **2**: DNase I treatment

Mix RNA containing 1µg RNA	**1 - 8 µl**
RNase free water	0 - 7 µl
10 x reaction buffer I	1 µl
DNase I	1 U per 1 µg RNA
Total reaction volume	10 µl

DNase I was inactivated by heat inactivation (65°C, 10 min) in the presence of 20mM EDTA. Alternative Dnase treatment EURx RNase-free DNase I like described in EURX protocol (https://eurx.com.pl/docs/manuals/en/e3598.pdf, August 24th2021, 1:27 pm).

e) *Reverse transcription*

Since RNA is unstable and prone to digestion by RNase, RNA was transcribed to cDNA using reverse transcription-Polymerase chain reaction (RT-PCR). Therefore an equivalent of 500 ng to 1 µg RNA sample was transferred to the volume of RNase-free H2O to reach a total volume of 8 µl. Afterwards 2 µl of qScript SuperMix

(Quantabio, Beverly, USA) in appropriate dilution were added to each tube. Tubes were vortexed, centrifuged and placed in a thermal cycler (Table 3).

Table **3**: Reverse transcription – Thermal cycler program

1 cycle:	22ºC, 5 min
1 cycle:	42ºC, 30 min for transcription
1 cycle:	85ºC, 5 min to inactivate reverse transcriptase

Then the samples were diluted in 90 µl Nucl-free H2O and directly used as an aliquot or stored at -20ºC until proceeding.

Reverse transcription quantitative real-time polymerase chain reaction (qPCR)

For relative quantification of the gene expression reverse transcription quantitative real-time polymerase chain reaction (qPCR) was performed (78). The basic principle of qPCR is repeated amplification of cDNA and the detection of the amplified product using dsDNA binding fluorescence dye. The cycle in which the detected fluorescence signal rises above a defined threshold is called the threshold cycle (C_T) or quantification cycle (C_q). Thus, a low CT value correlates with a high amount of RNA in the sample. The used primers were listed in Table 4.

Table **4**: Primer for Real-time quantitative PCR

Gene		GI	Source	Forward	Reverse	Melting-temp	Product-length	Annealing-temp
Arg1	Mouse	NM_007482	Primerbank	CTCCAAGCCAAAGTCCTTAGAG	AGGAGCTGTCATTAGGGACATC	60.0 / 61.0°C	185	62°C
CD38	Mouse	NM_007646	Primerbank	TCTCTAGGAAAGCCCAGATCG	GTCCACACCAGGAGTGAGC	60.4 / 62.0°C	109	61°C
CD68	Mouse	NM_009853	Primerbank	TGTCTGATCTTGCTAGGACCG	GAGAGTAACGGCCTTTTTGTGA	61.0 / 60.5°C	75	62°C
Egr2	Mouse	NM_010118	Primerbank	GCCAAGGCCGTAGACAAAATC	CCACTCCGTTCATCTGGTCA	61.6 / 61.2°C	154	61°C
GAPDH	Mouse	NM_001289726.1	Primer blast	GGAGAGTGTTTCCTCGTCCC	ACTGTGCCGTTGAATTTGCC	59.8 / 60.0°C	202	58°C
IL-10	Mouse	NM_010548	Primerbank	GCTCTTACTGACTGGCATGAG	CGCAGCTCTAGGAGCATGTG	60.2 / 62.7°C	105	58°C
IL6	Mouse	NM_031168	Primerbank	TAGTCCTTCCTACCCCAATTTCC	TTGGTCCTTAGCCACTCCTTC	60.8 / 61.1°C	118	59°C
iNOS	Mouse	NM_010927.4	M. K.	CTATCTCCATTCTACTACTACCAGATCGA	CCTGGGCCTCAGCTTCTCAT	60.8 / 61.6°C	75	65°C
Ly6c	Mouse	NM_001252055.1	Primer blast	GAGAGGAACCCTTCTCTGAGG	AAAGAAAGGCACTGACGGGT	58.9 / 59,8°C	136	59°C
Tnf	Mouse	NM_013693	Primerbank	CCCTCACACTCAGATCATCTTCT	GCTACGACGTGGGCTACAG	60.9 / 62.1°C	61	60°C

MHC-II	Mouse	NM_010381.2	Hepatology 2011	TCCAGATGCCAACGTGGCCC	TGCGGAAGAGGTGATCGTCCC	65.3 / 64.2°C	200	63°C
Mrc1	Mouse	NM_008625.2	Immunity 2013	ATGCCAAGTGGGAAAATCTG	TGTAGCAGTGGCCTGCATAG	56.3 / 59.8°C	153	58°C
18Sr RNA	Mouse	NR_003278.3	Oncogene 2011	GTAACCCGTTGAACCCCATT	CCATCCAATCGGTAGTAGCG	58.1 /57.9°C	151	61°C
18Sr RNA	Mouse	NR_003278.3	N. R.	GATCAAAACCAACCCGGTGA	GAGTCACCAAGCCGCC	58.4 /57.5°C	70	60°C
Fizz1	Mouse	NM_020509	Primerbank	CCAATCCAGCTAACTATCCCTCC	ACCCAGTAGCAGTCATCCCA	65.0 / 60.0°C	108	61°C

For the qPCR Power SYBR™ Green PCR Master Mix was used and the experiment was set up in a 96-well plate with 13 µl of the mastermix (Table 5), prepared for the required amount of wells, pipetted into each well.

Table **5**: QPCR – Syber Green Mastermix

Syber Green Mastermix	7.5 µl
Primer S	0.5 µl (500 nM)
Primer AS	0.5 µl (500 nM)
Ncl free H_2O	4.5 µl

2 µl (= 10 ng) cDNA were added to each well, to the total reaction volume of 15 µl. Afterward the plate was sealed with MicroAmp™ Clear Adhesive Film. The following program was run on StepOnePlus Real Time PCR “Thermocycler” (Table 6).

Table 6: Programm - qPCR

Stage 1:	95°C, 10 min
Stage 2:	95°C, 15 sec; Annealing temperature of the primer, 1min 40 cycles
Stage 3:	95°C, 15 sec

The relative amount of transcript was calculated with the deltadelta-CT methode, using a housekeeping gene as reference. The fold change Ratio (fc) to a control group was calculated with the following formula (Table 7).

Table **7**: Fold change Ratio

dCT	= CT (gene of interest)- CT (housekeeping-gene)
ddCT	= dCT (treatment)- dCT (control)
fc	$= 2^{-\,\mathrm{ddCT}}$

To proof the statistically reference of the results they were analysed using GraphPad Prism. Assuming a Gaussian distribution an ordinary one-way ANOVA and Dunett`s multiple comparisons test was performed.

Taqman real-time quantitative polymerase chain reaction

In comparison to SYBR-Green based detection Taqman qPCR with TaqMan™ Gene Expression Master Mix uses a fluorogenic probe specific to target gene. So only the amplification of the target gene is detected while accumulates during amplification.

The double amount of the standard protocol was used adding 20 µl total volumes per well of a 96-well plate. Each volume contains a Mastermix prepared like described in Table 8.

Table **8**: QPCR - Taqman Mastermix

Taqman mastermix	5 µl x2	10µl
Primer S	0.25 µl x2	0.5 µl
Primer AS	0.25 µl x2	0.5 µl
Taqman probe	0.20 µl x2	0.4 µl
Ncl free H_2O *add*	2.30 µl x2	4.6 µl
cDNA	2 µl x2	4 µl
	10 µl	20 µl

After adding cDNA, following program was run on on StepOnePlus Real Time PCR "Thermocycler" (Table 9).

Table **9**: QPCR Taqman - Program

Stage 1:	50°C, 9 sec; 95°C, 10 min
Stage 2:	5°C, 15 sec; Annealing temperature of the primer, 1 min 40 cycles

Fluorescence-activated cell sorting

Fluorescence-activated cell sorting (FACS) is able to sort cells by detecting forward scatter (FSC) for the cell size and side (90°, SSC) scatter for granularity and complexity using laser light. In addition fluorescence dye tagged antibodies against specific surface markers can be used to specify the cell subtype.
To perform FACS analysis the cells were washed with PBS twice subsequently harvested with a cell scraper and transferred to FACS tubes placed on ice. Afterwards they were centrifuged (300 x g, 10 min) the supernatant was discarded and placed on an absorbent paper. Then 100 µl FACS buffer was added and Live/dead discrimination was performed with 7-Aminoactinomycin D (7-AAD 1 µl/ 100 ml). Cells were stained with antibodies against the following cell-specific markers as recommended in the manufacturer's instructions for the corresponding cell count: CD45-allophyocyanin (APC)-Cy7 and F4/80-PE; dendritic cells: CD45-APC-Cy7, FITC anti-mouse I-A/I-E Antibody, anti-CD206 followed by the secondary antibodies (15 min, 4°C): Phycoerythrin (PE) anti-mouse IgG and/or Alexa Fluor® 680 anti-rat IgG.

Enzyme-linked immunosorbent assay

TNFα enzyme-linked immunosorbent assay (ELISA) was performed with Mouse ELISA Ready-SET-Go! (Affymetrix/eBioscience, USA) and IL-10 with Mouse IL-10 Incoated ELISA (Invitrogen, Thermo Fischer Scientific, MA, USA) like described in the Immunoassay–TDS Protocol. The wash buffer was prepared out of PBS (1X) and 0.05% Tween-20.

PBS (10X): natriumchlorid (NaCl) 80 g; dinatriumhydrogenphosphat (Na_2HPO_4) 14.4 g; potassium dihydrogen phosphat (KH_2HPO_4) 2.4 g; potassium chloride (KCl) 2 g; H_2O 1 l.
After coating the plate with the capture antibody and overnight incubation at 4°C three times washing and blotting was performed. Afterwards the plate was incubated at room temperature for on hour with ELISA diluent (1x) for blocking. After washing the prepared standards and samples were pipetted on the plate (using a multichannel pipet) and incubated at room temperature for two hours. Five washing steps and covering the plate with the detection antibody provided and incubation for one hour at room temperature followed the previous step. After another five washing steps Avidin-horseradish peroxidase (HRP) was added and incubated for half an hour at room temperature, followed by eight washing steps (divided into three and five, blotting in between), and adding the 3,3',5,5'-Tetramethylbenzidine (TMB) Solution. While the incubation around 15 minutes the control well was checked to at the stop solution (2N H_2SO_4) before colour changing to avoid high background signals.
The measurement was performed with wavelength subtraction of 570 nm from those of 450 nm and the data were analysed.

Injection of interferon-γ-dextran nanoparticles in healthy C57BL/6 mice and C57BL/6 mice with B16F10 liver metastasis

The experimental setup were 5 C57BL/6 wildtype mice per group (age: 10 weeks) from (Charles River Laboratories, Wilmington, Massachusetts, United States). After anaesthesia by isoflurane inhalation mice were treated with retro orbital vein injection of 200 µl IFN-γ-DNP (200 µg carrying 200 ng IFN-γ) at 0 and 24 hours. The sacrifice by cervical dislocation and organ harvest was performed after 48 hours. The control group was treated with 200 µl PBS containing 10 µg/ml IFN-γ (dose: 2 µg IFN-γ per animal per injection). B16F10 murine melanoma cell liver metastasis in C57BL/6 mice was initiated by 300,000 B16F10luc cells intrasplenic injection and followed by splenectomy as described in the paper published by Foerster *et al.* (79, 80).
The C57BL/6 mice with B16F10 liver metastasis (n = 5 mice per group (age: 8 weeks)) were treated with retroorbital injection of 400 µg IFN-γ-DNP (carrying 400 ng IFN-γ in 300 µl PBS) on day 1, 3, 5, 7, 9. The sacrifice by cervical dislocation and organ harvest was performed on day 14. In the control group the injection was performed with 300 µl PBS containing 1.33 µg/ml IFN-γ-DNP (dose: 400 ng IFN-γ per animal per injection).
Animal experiments were performed according to the German law for the protection of animals and approved by the local ethics committee on animal care (reference number 23177-07/G13-1-002, Government of Rhineland-Palatinate, Germany).

Viability resazurin assay

The resazurin assay indicates the amount of living cells through the produced red fluorescent dye (resorufin) by the mitochondrial respiratory chain. The non-fluorescent blue resazurin is oxidized to resorufin.

The cells were seeded into F-bottom plates (TC treated) using 5000 cells and 200 µl media per well. The polarization for 24 hours started the day after to ensure proper cell attachment. All groups were run in 6 replicates including a medium control and dead control after dimethyl sulfoxide (DMSO 10%) treatment. After the treatment with IFN-γ, LPS, IFN-γ-DNP and LPS-DNP for another 24 hours resazurin salt (0,3 mg/ml in DPBS) stock solution (final dilution of 50x) was added to the wells. The fluorescence was measured after 60 min (Ex 544/20nm; Em 590/20 nm). For data analyses from every sample the mean of media control was subtracted as blank measurement and then the results were normalized to the mean of untreated samples as 100 percent.

Statistical analyses

All statistical analyses were performed in Prism 6 or Prism 8 for Mac OS X (GraphPad Software, CA, USA). All numeric values are expressed as means ± standard deviation. ANOVA and Dunnett's multiple comparisons were used to calculate p-values if not indicated otherwise. P-values <0.05 were considered statistically significant. Asterisks were used to illustrate statistical significance: *p < 0.05, **p < 0.01, ***p < 0.001, ****p < 0.0001; ns: not significant.
All cell culture experiments were performed in triplets for each group.

Dextran based nanoparticles

The method of preparing the DNP was described previously (81, 82) the PEGylation and further modifications followed the descriptions as published by Foerster et al. (75). The following passage was taken from the publication (Foerster et al., Nanomedicine (Lond.) 2016)(75)). In 800 µl ice-cold dichloromethane (DCM, Sigma-Aldrich) an acetalated and spermine-functionalized dextran (10 mg, size of unmodified dextran 9–11 kDa) was dissolved and 100 µl PBS or 100 µl PBS with interferon-γ or LPS (equivalent to 20 and 100 ng/ml) was added to prepare the primary water-in-oil emulsion by sonication. The following water-in-oil-in-water emulsion was prepared by sonication for 20 sec after adding 4 ml polyvinyl alcohol (PVA) solution (3% in PBS, 13–23 kDa, 87–89% partly hydrolyzed). After stirring the emulsion over night and followed ultracentrifugation (45,000 × g, 20 min) the DNP pellet was removed by adding double distilled (dd) H2O (adjusted to pH 8).
For PEGylation (attached PEG-chains (2 kDa)) Methoxy- PEG-N-hydroxysuccinimide ester (NHS-PEG; 2 Da, 10× molar excess; 50 mg/ml, Rapp Polymere, Tübingen, Germany) dissolved in PBS was added drop wise to the in PBS (pH 8) suspended DNP (2mg/ml). Then they were incubated for 2h, while stirring and after ultrazentrifugatin (45,000 × g, 20 min) rinsed with dd H_2O (pH 8). PVA solution (0.3% in dd-H_2O, pH 8, 10 µl/ 1mg nanoparticle) was added as cryoprotectant before lipolization.
For imaging the DNPs were loaded with fluorescence dye Oregon Green® 488 (MW Life Technologies)(75).
Dr. … (Institute of Pharmacy and Biochemistry, Johannes Gutenberg-University, Mainz) kindly provided the DNPs, synthesized and PEGylated as described above.

Reagents, consumables and devices

The BALB/c mice and C57BL/6 mice come from Charles River Laboratories, Wilmington, Massachusetts, USA.

Table **10**: Reagents, consumables and devices

Product	Company	Number (cat.; CAS; EC)
7-Aminoactinomycin, e-Bioscience™ 7-AAD	ThermoFischer scientific, Waltham, MA, USA	cat.no. 00-6993-5
ACSCanto II flow cytometer	BD Biosciences, Franklin Lakes, New Jersey,U.S.	
Analytical balance, CPA225D-OCE	Satorius, Göttingen, Germany	cat.no. p2697
Arginase Activity Assay Kit	Sigma-Aldrich, Missouri, USA	cat.no. MAK112-1KT
Automated cell counter TC10™	Bio-Rad Laboratories, Inc., Hercules, California, USA	cat.no. 1450001
BD Microlance™ Stainless Steel Needles 0.45 x 13 mm	Thermo Fisher Scientific, Waltham, MA, USA	cat.no. 10753785
BD Microlance™ Stainless Steel Needles 0.9 x 25 mm	Thermo Fisher Scientific, Waltham, MA, USA	cat.no. 10030464
Beta-Mercaptoethanol (2-Sulfanylethan-1-ol)	Thermo Fisher Scientific, Waltham, MA, USA	cat.no. 21985023
BioScience-grade, Nuklease-frei und autoklaviert, DEPC-behandeltes Wasser	Carl Roth GmbH + Co. KG, Karlsruhe, Germany	cat.no. T143.3
CD- 45 / APC-Cy7-A	Biolegend, CA, USA	cat.no. 103115
CD206 / AF647	BD Biosciences, CA, USA	cat.no. 568809
Cell filter70µm EASYstrainer™	Geiner bio-one, Kremsmünster Austria	cat.no. 542 070
Cell scraper, 28 cm long, blue, sterile	Geiner bio-one, Kremsmünster Austria	cat.no. 541070
Cell-culture petri dish 100mm (Cellstar)	Geiner bio-one, Kremsmünster Austria	cat.no. 664160
Cell-culture petri dish 94 mm (without vents)	Geiner bio-one, Kremsmünster Austria	cat.no. 632181
Chloroform; Trichloromethane $CHCl_3$	PanReac AppliChem, ITW Reagents, Darmstadt, Germany	cat.no. 133101.1611
Counting Slides, Dual Cham-	Bio-Rad Laboratories, Inc.,	cat.no. 145-0011

ber	Hercules, California, USA	
Dextran, acetalated and spermine-functionalized (10 mg, size of unmodified dextran 9–11 kDa)	Sigma-Aldrich, Missouri, USA	CAS no. 9004-54-0 EC-no. 232-677-5 cat.no. D9360-10G
Dextran, Oregon Green® 488,10,000 MW	Life Technologies, California, USA	
Dichloromethane (DCM) CH_2Cl_2	Sigma-Aldrich, Missouri, USA	CAS no. 75-09-2 EC-no. 200-838-9 cat.no. L090000-2.5L
Dinatriumhydrogenphosphat, Na_2HPO_4,	Merck KGaA, Darmstadt, Germany	CAS-no. 7558-79-4 EC-no.: 231-448-7 cat. no. 106586
Disposable Glass Pasteur Pipettes, 150mm	VWR International, Radnor, Pennsylvania, USA	cat.no. 612-1701
DMSO; Dimethyl sulfoxide $(CH_3)_2SO$	Sigma-Aldrich, St. Louis, Missouri, Vereinigte Staaten	cat.no. 200-664-3
DNase1; Desoxyribonuclease I;1500 Kunitz units EC 3.1.21.1	QIAGEN, Venlo, Netherlands	cat.no. 1023460
DNaseI 1000 U (5U/µl) Desoxyribonuclease I; EC 3.1.21.1	EURX, Gdańsk, Poland	cat.no. E1345-01
Dubelco`s Phosphate Bufferd Saline	Sigma-Aldrich, St. Louis, Missouri, USA	cat.no. D8537-500ML
Elisa HydroSpeed™ plate washer	Tecan Group, Männedorf,Switzerland	
Eppendorf Safe-Lock Tubes, 0,5 mL, Eppendorf Quality™	Eppendorf AG, Hamburg, Germany	cat.no. 0030121023
Eppendorf Safe-Lock Tubes, 1,5 mL, Eppendorf Quality™	Eppendorf AG, Hamburg, Germany	cat.no. 0030120086
Eppendorf Safe-Lock Tubes, 2,0 mL, Eppendorf Quality™	Eppendorf AG, Hamburg, Germany	cat.no. 30120094
Eppendorf® Microcentrifuge 5415	Eppendorf AG, Hamburg, Germany	
ErgoOne® 12-Channel Pipette, 0,5 – 10 µl	Starlab International GmbH, Hamburg, Germany	cat.no. S7112-0510
ErgoOne® 12-Channel Pipette, 10 – 100 µl	Starlab International GmbH, Hamburg, Germany	cat.no. S7112-1100
ErgoOne® Single-Channel Pipette, 0,1 – 2,5 µl	Starlab International GmbH, Hamburg, Germany	cat.no. S7100-0125
ErgoOne® Single-Channel Pipette, 0,5 – 10 µl	Starlab International GmbH, Hamburg, Germany	cat.no. S7100-0510

ErgoOne® Single-Channel Pipette, 10 – 100µl	Starlab International GmbH, Hamburg, Germany	cat.no. S7100-1100
ErgoOne® Single-Channel Pipette, 100 – 1000µl	Starlab International GmbH, Hamburg, Germany	cat.no. S7100- 1000
ErgoOne® Single-Channel Pipette, 2 – 20 µl	Starlab International GmbH, Hamburg, Germany	cat.no. S7100- 0220
ErgoOne® Single-Channel Pipette, 20 – 200 µl	Starlab International GmbH, Hamburg, Germany	cat.no. S7100- 2200
Ethanol; Ethylalkohol C_2H_6O, microbiology grade 500ml	Sigma-Aldrich, St. Louis, Missouri, USA	cat.no. 64-17-5
F4/80-PE	Biolegend, CA, USA	cat.no. 123109
FACS buffer; Cell Staining Buffer	Biolegend, CA, USA	cat.no. 420201
Falcon® 5 mL Round Bottom PP Test Tube, without Cap, Nonsterile	Falcon; Corning, NY 14831 USA	cat.no. 352002
Fetale Bovine Serum	Biochrome AG, Berlin, Germany	cat.no. S0115
Fisherbrand™ Mini-Centrifuge 100-240V, 50/60Hz Universal Plug	Thermo Fisher Scientific™, Waltham, MA, USA	cat.no. 15358266
FITC anti-mouse I-A/I-E Antibody (MHCII–FITC)	Biolegend, CA, USA	cat.no. 107605
Fresco™ 21 Microcentrifuge	Thermo Fisher Scientific™, Waltham, MA, USA	cat.no. 75002555
GeneMATRIX Universal RNA Purification Kit	EURX, Gdańsk, Poland	cat.no. E3598
Iscove's Modified Dulbecco's Medium (IMDM) gibco®	Thermo Fisher Scientific, Waltham, MA, USA	cat.no. 21056023
Isopropyl alcohol, 4 litres	Sigma-Aldrich, St. Louis, Missouri, USA	cat.no. I9030
L-Glutamine (200 mM)	Thermo Fisher Scientific, Waltham, MA, USA	cat.no. 25030081
LPS, E. coli O111:B4	Sigma-Aldrich, Merck Millipore, MilliporeSigma, Burlington, Massachusetts, United States	LPS25, GTIN: 4053252324598
Macroplate, 6 Well, Ps, Clear, Lid, Vents	Geiner bio-one, Kremsmünster Austria iner bio-one, Austria	cat.no. 657102
MicroAmp® Fast 96- Well Reaction Plate (0.1mL)	Thermo Fisher Scientific, Waltham, MA, USA	cat.no. 4346907

MicroAmp™ Clear Adhesive Film	Thermo Fisher Scientific, Waltham, MA, USA	cat.no. 4306311
Microplate, 96 well, PS, F-Bottom, clear, Microlon®, high binding	Geiner bio-one, Krems-münster Austria greiner bio-one, Austria	cat.no. 655061
Mouse IL-10 Incoated ELISA	Invitrogen, Thermo Fischer Scientific Waltham, MA, USA	cat.no. 88-7105-88
Mouse TNF alpha ELISA Ready-SET-Go!	Affymetrix, eBioscience	cat.no. 88-7324
Natriumchlorid; NaCl	Carl Roth GmbH + Co. KG, Karlsruhe, Germany	CAS no. 7647-14-5 EC-no. 231-598-3 cat. no. 3957.1
Penicillin-Streptomycin (10,000 U/mL) gibco®	Thermo Fisher Scientific, Waltham, MA, USA	cat.no. 15140122
Petri DISH 94x16, Without VENT, with logo, Light ver-sion, Sterile	Geiner bio-one, Krems-münster Austria	cat.no. 632180
Phycoerhtrin (PE) anti-mouse IgG	Jackson Immuno Research, PA, USA	cat.no. 715- 116-151
Pipette tips, yellow, 10 -200 µl	Geiner bio-one, Krems-münster Austria	cat. no.10758432
Pipetus ®	Hirschmann Laborgeräte, Eberstadt, Germany	cat.no. 9907200
Polyvinylalcohol (PVA) solu-tion, [-CH2CHOH-]n (3% in PBS, 13–23 kDa , 87–89% partly hydrolyzed,	Sigma-Aldrich, Missouri, USA	CAS no. 9002-89-5 cat.no. 363170-25G
Potassium chloride; KCl	Carl Roth GmbH + Co. KG, Karlsruhe, Germany	CAS no. 7447-40-7 EC-no. 231-211-8 cat. no. 6781.1
Potassium dihydrogen phos-phat; KH_2HPO_4	Carl Roth GmbH + Co. KG, Karlsruhe, Germany	CAS No. 7778-77-0 EC-Nr. 231-913-4
Power SYBR™ Green PCR Master Mix	Thermo Fisher Scientific, Waltham, MA, USA	cat.no. 4367659
Primer	meatbion international AG, Planegg, Germany	
Promega CellTiter-Blue™ Cell Viability Assays	Fisher scienfic,	cat.no. PR-G8081
qScript SuperMix	Quantabio, Beverly, MA, USA	cat.no. 101414-108
RibozolTM RNA Extraction	Amresco Solon, VWR life	cat.no. N580-200ML

Reagent	science, OH, USA	
rm IL-13 (50 µg)	ImmunoTools GmbH, Friesoythe, Germany	cat.no. 1240135
rm IL-4 (50 µg)	ImmunoTools GmbH, Friesoythe, Germany	cat.no. 12340045
rm INF-y	ImmunoTools GmbH, Friesoythe, Germany	cat.no. 12343536
rm M-CSF (250 µg)	ImmunoTools GmbH, Friesoythe, Germany	cat.no. 12343117
RNase-Free DNase Set, 1500 Kunitz units Desoxyribonuclease I; EC 3.1.21.1	QINAGEN GmbH, Germany	Mat. No 102346-0
Rneasy® Plus Mini Kit (50)	QIAGEN, Germantown, MD 20874, USA	cat.no. 74134
Sapphire Pipette Tip, 10 µl, natural, non-sterile, 1000 pcs./bag	Geiner bio-one, Kremsmünster Austria	cat.no. 771350
Serological Pipett Cellstar®, sterile, 10ml	Geiner bio-one, Kremsmünster Austria	cat.no. 607160
Serological Pipett Cellstar®, sterile, 25ml	Geiner bio-one, Kremsmünster Austria	cat.no. 760160
Serological Pipett Cellstar®, sterile, 5ml	Geiner bio-one, Kremsmünster Austria	cat.no. 606180
StepOnePlus Real Time PCR "Thermocycler" 272005818	Applied Biosystems®	S/N: 272005818
Sulfuric acid; H_2SO_4 ROTIPURAN® 96 %	Carl Roth GmbH + Co., D-76185 Karlsruhe	cat.no. 4623.1
T100 Thermal Cycler	BIO-RAD	cat.no. 1861096
TaqMan™ Gene Expression Master Mix	Thermo Fisher Scientific, Waltham, MA, USA	cat.no. 4369016
Tecan Infinite® M200 Pro	Tecan Group, Männedorf, Switzerland	cat.no. 30017581
Tryptan Blue solution	Sigma-Aldrich, St. Louis, Missouri, Vereinigte Staaten	cat.no. T8154-20ML
Tubes Cellstar®, PP, graduated, conical botton, blue screw cap, sterile, 15 ml	Geiner bio-one, Austria	cat.no. 188271
Tween® 20 for synthesis, Polyoxyethylen(20)-sorbitanmonolaurat, pH 6 - 8 (50 g/l, H_2O, 20 °C)	Merck KGaA, Darmstadt, Germany	cat.no. 8221841000

Ultratip, Pipette tips, blue, 200 -1000 µl	Geiner bio-one, Austria	cat.no. 11739542
Universal RNA purification Kit	Roboklon, Berlin, Germnay	cat.no. E3598
Vortex-Genie	Scientific industries	
Water, (For RNA Work) (DEPC-Treated, DNASE, RNASE free/Mol. Biol.), Fisher BioReagents™	Fisher Scientific; Thermo Fisher Scientific, Waltham, MA, USA	cat.no. BP561-1
Zeiss LSM 710 NLO laser scanning microscope	Carl Zeiss Microscopy, Jena Germany	

IV. RESULTS

In vitro analysis

1. In vitro toxicity of dextran nanoparticles

The resazurin assay measures the amount of living cells through the produced red fluorescent dye (resorufin) by the mitochondrial respiratory chain. The non-fluorescent blue resazurin is oxidized to resorufin. Fluorescence was measured after 60 min (Ex 544/20nm; Em 590/20 nm). For data analyses from every sample the mean of media control was subtracted as blank measurement and the results were normalized to the mean of untreated samples as 100%.
M0 Macrophages treated with INF-y-DNP (300%), LPS-DNP (250%), LPS (230%), combination of LPS-DNP with INF-y-DNP (300%) and INF-y with LPS (220%) show a significant increased absorbance relative to untreated macrophages, indicating an increased metabolic activity (Fig.2A). The metabolic activity of M2 macrophages increased to a lesser extent with significant results only in macrophages treated with INF-y-DNP (175%) and LPS-DNP plus INF-y (157%) (Fig.2B). Compared to the mean of untreated samples (PBS), empty DNP (eDNP) did not increase the fluorescence signal. This assay largely exclude a relevant toxicity of DNP *in vitro*.

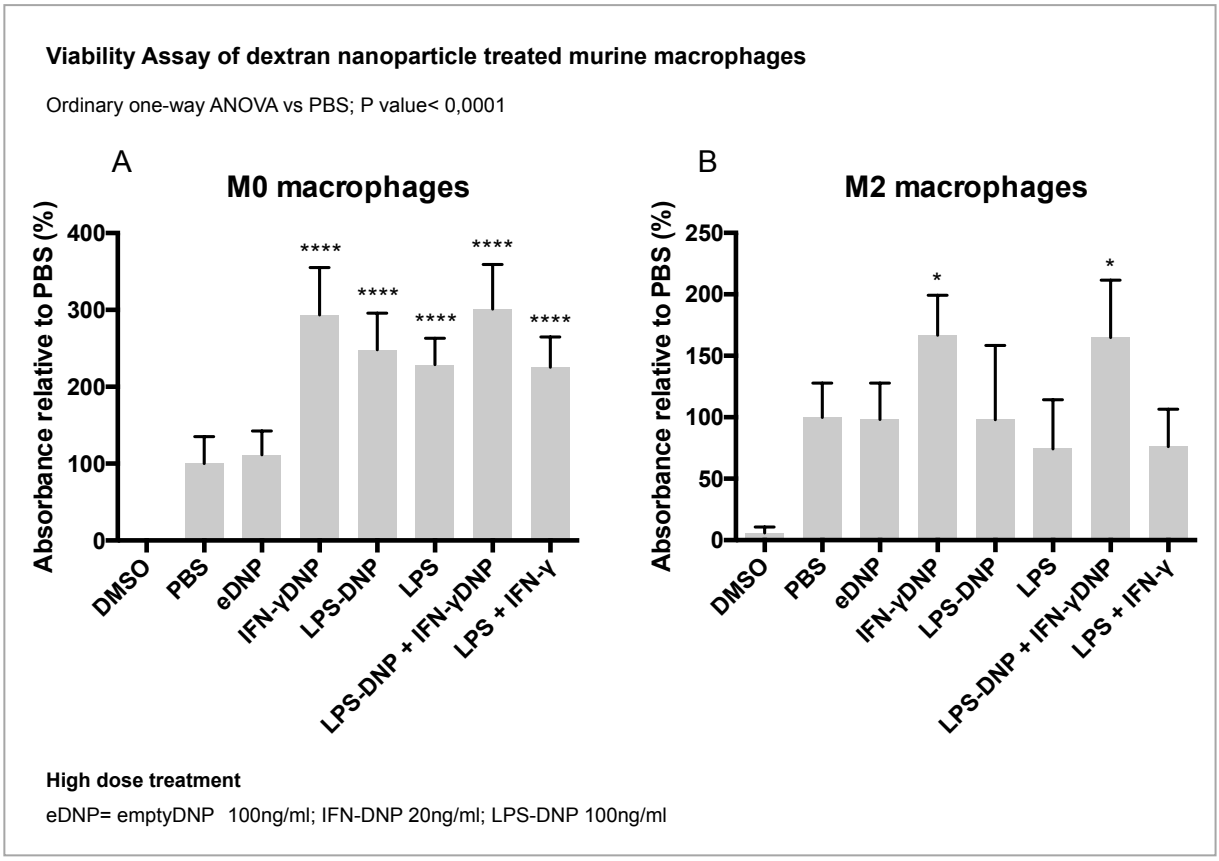

Figure **2**: Viability Resazurin Assay

The cell viability was tested using a Resazurin assay in 96 well formats in 6 replicates. In advance M2 polarization of bone marrow derived murine macrophages was induced with IL-4/IL-13 for 24 h. Afterwards the macrophages were incubated with DNP / cytokines for 48 h and on the harvest day the Resazurin assay performed as described above. Dead control after DMSO (10%) treatment. The experiment indicates no toxicity of dextran-based

nanoparticles further more increased metabolic activity of IFN-γ-DNP and LPS-DNP treated macrophages (M0 Figure 2A and M2 Figure 2B) compared to exclusive IFN- γ and LPS treatment Changes of viability were calculated relative to PBS treatment and to proof statistical relevance Ordinary one-way ANOVA and Dunnett's multiple comparisons test were performed. Asterisks were used to illustrate statistical significance: *p < 0.05, **p < 0.01, ***p < 0.001, ****p < 0.0001; eDNP: empty DNP; DNP: Dextran-based nanoparticles; DMSO: Dimethylsulfoxide; IFN-γ-DNP: interferon-γ-DNP, LPS: Lipopolysaccharide

2. Cellular uptake of dextran nanoparticles

After incubation with titrated concentrations of Oregon Green® 488-labeled DNP the uptake of nanoparticles was analysed by flow cytometry one hour, three and nine hours after treatment (Fig. 3A). The uptake of empty and INF-y-loaded DNP by native (Fig. 3A), as well as by M2 polarized (Fig. 3B) macrophages was shown by increased mean fluorescence intensity over time. The signal of the LPS-DNP group appeared low over the whole period of time.
Oregon Green® 488-labeled INF-y-DNP show a regular distribution in PBS (Fig. 4), after dispersion in an ultrasound bath.

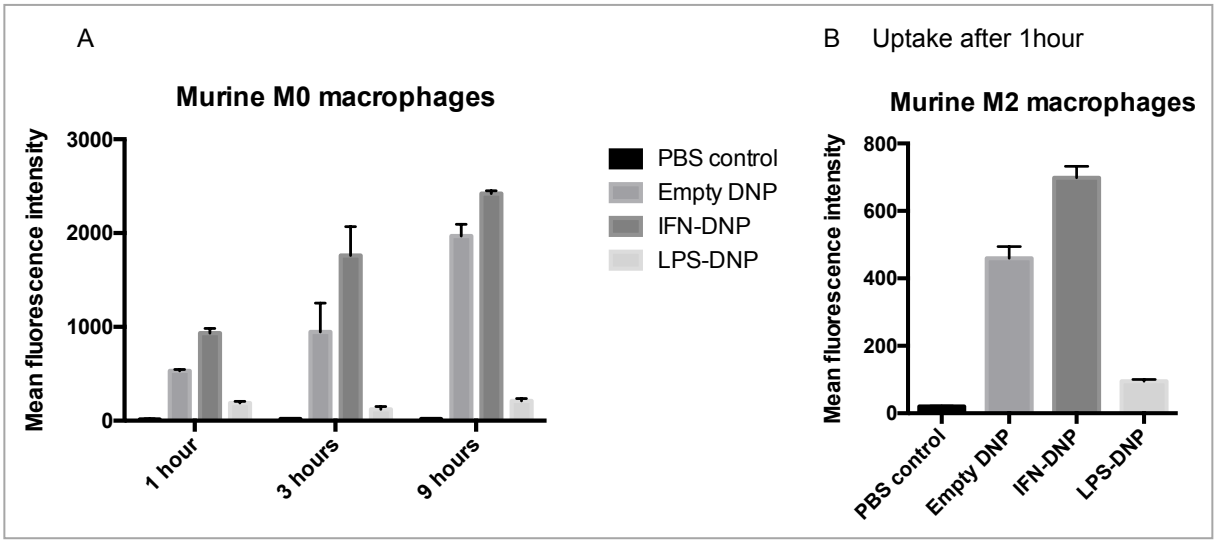

Figure **3**: Cellular uptake of dextran-based nanoparticles by native and treated murine macrophages

The experiment was performed in 6 well formats with bone marrow derived murine macrophage in two groups of either native (A) or M2 (B) polarized macrophages. In advanced M2 polarization of bone marrow derived murine macrophages was induced with IL-4/IL-13 for 24 h. Afterwards the macrophages were incubated with titrated concentrations of Oregon Green® 488-labeled DNP for one hour, three hours up to nine hours. Uptake of DNP was analysed by flow cytometry at different time points after treatment. The mean fluorescence intensity of live Oligo Green 488-fluorescent cells is shown. empty DNP: empty dextran nanoparticles; IFN-DNP: Interferon γ-carrying dextran nanoparticles; LPS-DNP: lipopolysaccharid carrying dextran nanoparticles

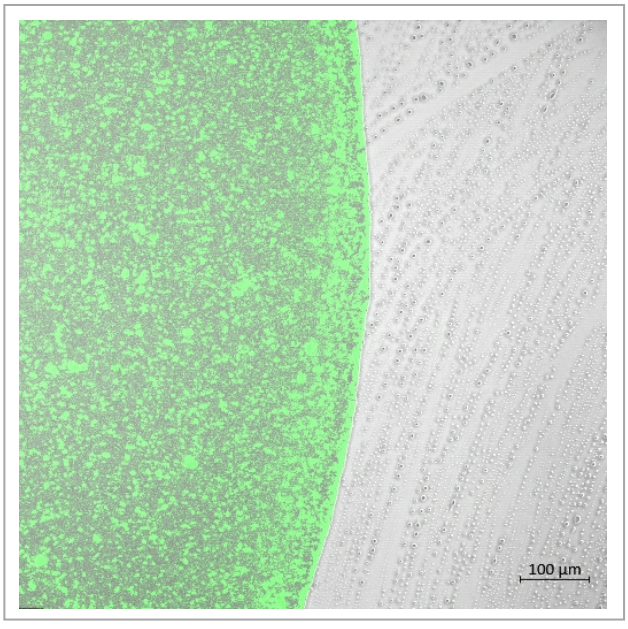

Figure **4** : Oregon Green® 488-labeled Interferon-γ loaded dextran-based nanoparticles distribute evenly after dispersion in PBS by ultrasound

Phagocytosis of Oregon Green® 488-labeled INF-γ-DNP by bone marrow-derived macrophages imaged with a Zeiss LSM 710 NLO laser scanning microscope (Carl

Zeiss Microscopy, Jena, Germany) began after 10 minutes (Fig. 5). Over the time course a complete phagocytosis could be shown, indicating effective uptake by macrophages.

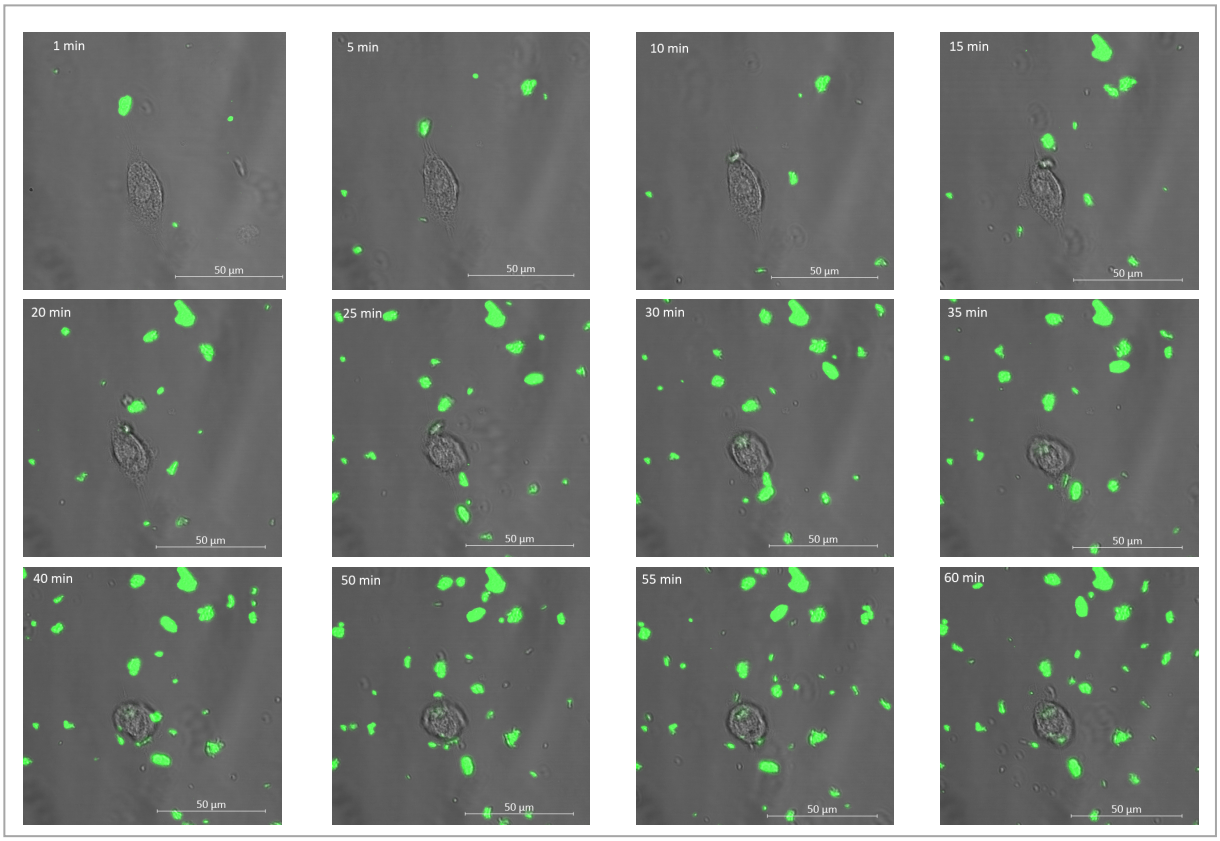

Figure **5**: Cellular uptake time-course of Oregon Green® 488-labeled Interferon-γ loaded dextran-based nanoparticles by native murine macrophages

After isolation and cultivation from male C57BL/6 mice bone marrow derived macrophages were incubated with titrated concentrations of Oregon Green® 488-labeled DNP. The distribution and cellular uptake of the particles was followed under the microscope. A regular distribution of the particles could be shown. Between five and ten minutes the phagocytosis of the particles begun.

3. M2 Polarization

To induce an alternative activation of murine bone marrow derived macrophages (45) they were treated with IL-4/IL-13 for 24h. The significant increase transcription of Arginase 1 (*arg1)* as a marker of M2-type macrophages (50) confirmed in vitro M2 polarization (Fig. 6).

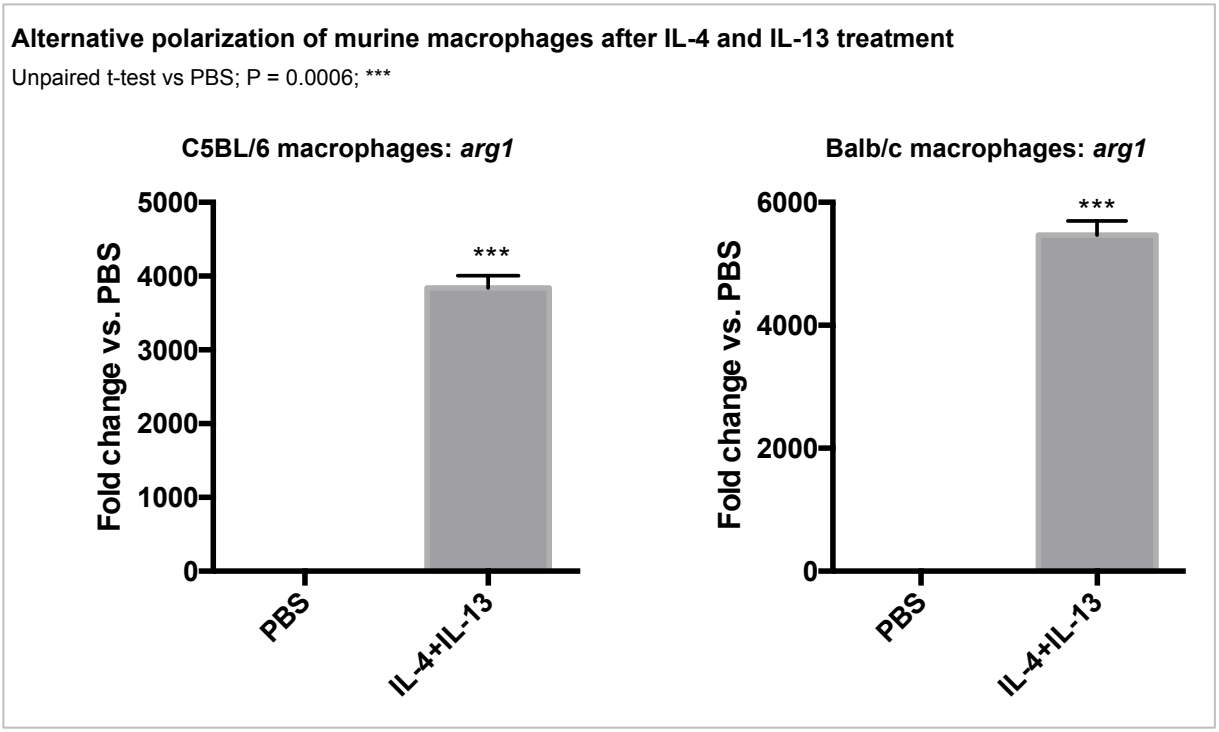

Figure **6**: Arginase 1 indicates alternative polarization of murine macrophages after IL-4 and IL-13 treatment

After cultivation murine bone marrow derived macrophages were incubated with IL-4/IL-13 for 24h for M2 polarization. QPCR was performed to quantify Arginase 1 expression as a marker for alternative polarized macrophages. Statistical significance was tested by unpaired t-test versus PBS control. Asterisks were used to illustrate statistical significance: *p < 0.05, **p < 0.01, ***p < 0.001, ****p < 0.0001; *arg1*: Arginase 1; IL4: interleukin-4; interleukin-13

4. Dextran-based nanoparticle dependent changes of macrophage populations characterized morphologically

Native (Fig. 7) and previously M2-type polarized (Fig. 8) macrophages show morphological changes after treatment with INF-γ, INFγ-DNP, LPS, and LPS-DNP for 24 h in comparison to the cells of the control group treated with PBS, which were more rounded, they were adherent and well spread. The treated cells were more elongated with long branched processes, building more cell clusters as PBS treated cells.

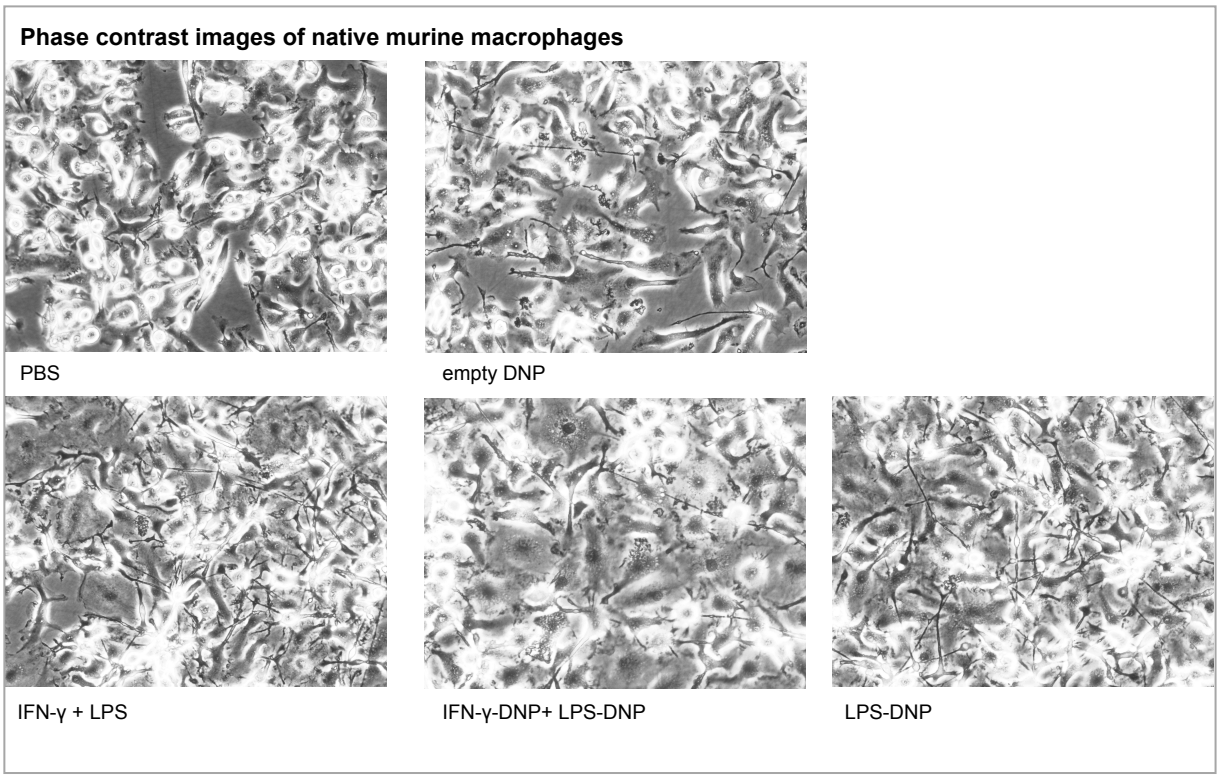

Figure **7**: Phase contrast images of native murine macrophages.

Treated with PBS: Phosphate-buffered saline, empty DNP: empty dextran-nanoparticle, IFN-γ: Interferon-γ, IFN-γ-DNP: Interferon-γ loaded dextran-based nanoparticles, LPS: Lipopolysaccharide, and LPS-DNP: LPS loaded dextran-based nanoparticles for 24 h.

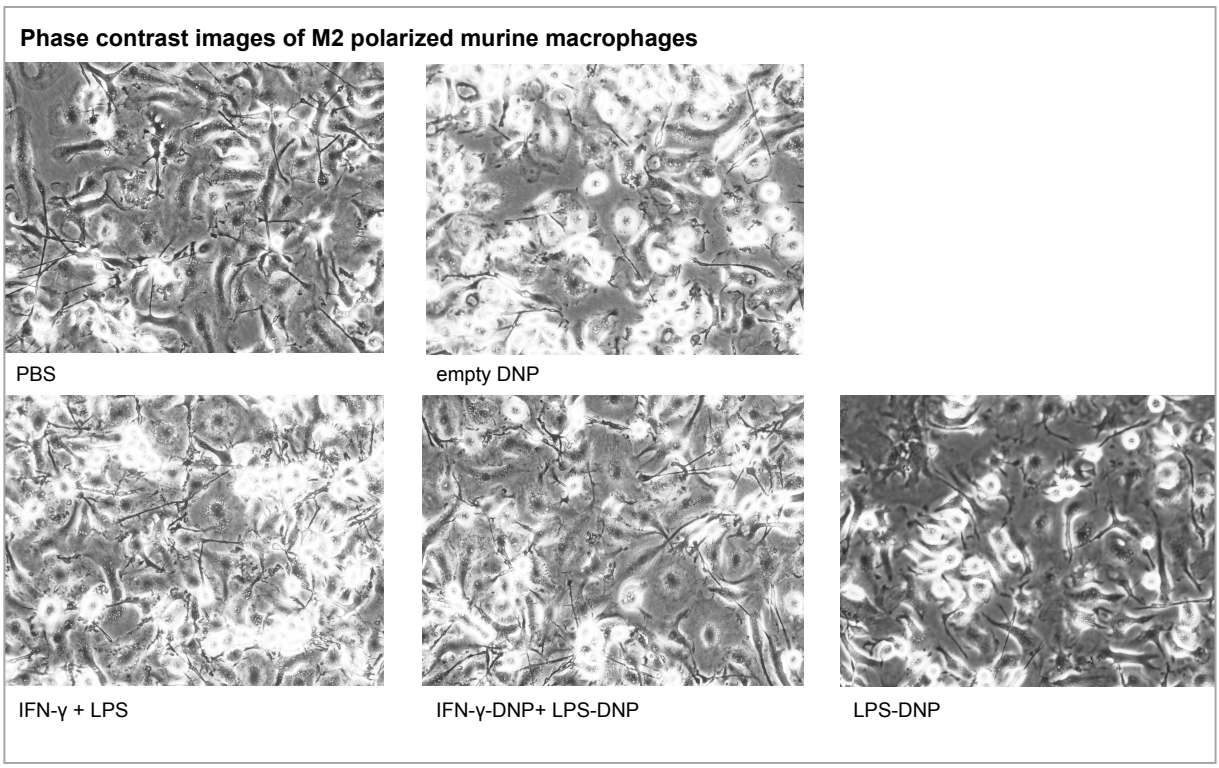

Figure **8**: Phase contrast images of murine macrophages M2-polarized with interleukin-4 and interleukin-14.

Treated with PBS empty DNP, IFN-γ, IFN-γ-DNP, LPS and LPS-DNP for 24 h. Abbreviations see Figure 7.

5. Optimization of real-time quantitative PCR - DNAse treatment

The activation/polarization state and cell lineage of macrophages can be characterized by size and shape, surface markers and cytokines/chemokines through Immunohistochemistry (IHC), secretome ELISA, FACS and transcriptomer analysis. For the relative quantification of the gene expression qPCR was performed. The delta-delta method, using the expression of the gene glyceraldehyde 3-phosphate dehydrogenase (GAPDH) as a reference, was run to analyse the data. Reference genes are also known as housekeeping genes (78). 18S ribosomal RNA is also used as a reference gene because of its invariant expression in tissues and cells (83). GAPDH is a key enzyme in glycolysis hence it is a commonly used reference gene (84). If not indicated otherwise GAPDH is the commonly used reference gene in the following experiments. Common marker genes for M1 and M2 type macrophages were assessed as described above (50, 7).
QPCR is a widely used technology that provides rapid and specific results based on the amplification of a transcript. Thus, several steps are necessary, which carry potential sources of error with them. One is contamination with genomic DNA. DNAse digestion is strongly recommend as a routine step for qPCR, especially when using primers that do not discriminate between genomic DNA and reverse transcribed cDNA (81). The disadvantage of this step could be a lower RNA concentration in the samples especially after incubation at 37 °C, which has been proven in my experiments (Fig. 9). The experimental results though seem to be more reliable (Fig. 10). Thus, in all experiments on-column-DNase I treatment following the EURX protocol as described above was performed. To avoid low RNA concentration the incubation was done at room temperature.

Sample	Conc ng/µl	Conc ng/µl after DNAse treatment	Ratio
M0 macrophage PBS 1	265,6	51,25	1,93
M0 macrophage PBS 2	305,76	84,22	1,95
M0 macrophage PBS 3	174,29	77,1	1,71
M0 macrophage LPS 1	258,64	62,94	1,93
M0 macrophage LPS 2	150,86	80,45	2,05
M0 macrophage LPS 3	132,48	90,85	2,05

Figure **9**: RNA concentration before and after DNAse I treatment

Measurement by Tecan 2000; M0: Unpolarized macrophages; LPS: Lipopolysaccharide

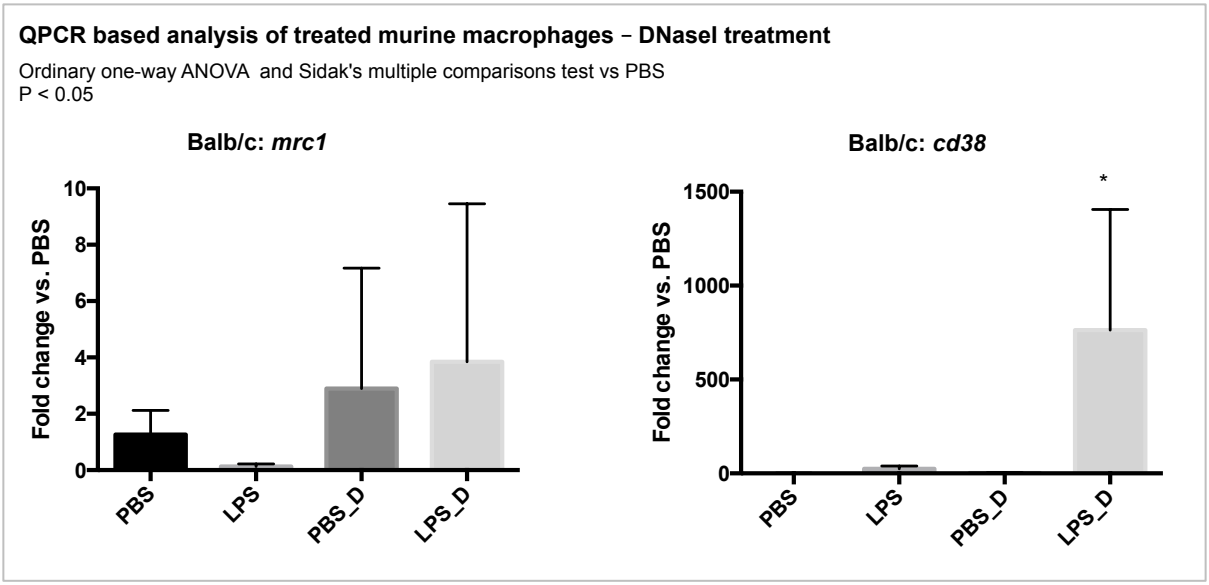

Figure **10**: Representative real-time quantitative PCR results - DNase I treatment

LPS: Lipopolysaccharide; D: DNAse I; *cd38*: Cluster of Differentiation 38; *mrc1*: Mannose receptor; PBS_D and LPS_D: DNase I treatment and without DNase 1 treatment (PBS; LPS) previous

6. Interferon-γ, lipopolysaccharides and Dextran nanoparticle dependent changes of macrophage populations characterized via relative quantification of gene expression by real-time quantitative PCR

a) *Interferon-γ and lipopolysaccharide in combination are able to polarize and re-polarize bone marrow derived murine macrophages*

After M0 and M2 polarization (achieved with IL-4/IL-13 treatment for 24 h) polarization and repolarization of bone marrow derived macrophages (BMDM) of C57BL/6 mice with IFN-γ (20ng/ml) and LPS (100ng/ml) for 48 hours was started. qPCR was performed as described above. Statistical significance was calculated by one-way ANOVA with PBS as reference group ($P<0.05$) and Holm-Sidak's multiple comparisons test, indicated by asterisks and colour. The heatmap (Fig. 11A) visualizes by different shades of red increase and blue decrease of commonly used markers. LPS and IFN-γ in combination with LPS showed a significant increase of

the M1 specific marker genes *tnfa* (P= 0,0014; LPS**; IFN-γ + LPS**), *il6* (P=0,0223; LPS*) and *cd38* (not significant) in unpolarized and M2-polarized macrophages *tnfa* (P= 0,0045; LPS**; IFN-γ + LPS**), *il6* (P=0,0203; LPS*). In addition, a significant decrease of the M2 specific marker genes *mrc1* (P=0,0073; LPS*; IFN-γ + LPS *) in M0 and *egr2* (P=0,0290; LPS*; IFN-γ + LPS*) in M2 polarized macrophages could be verified (Fig. 11 B).

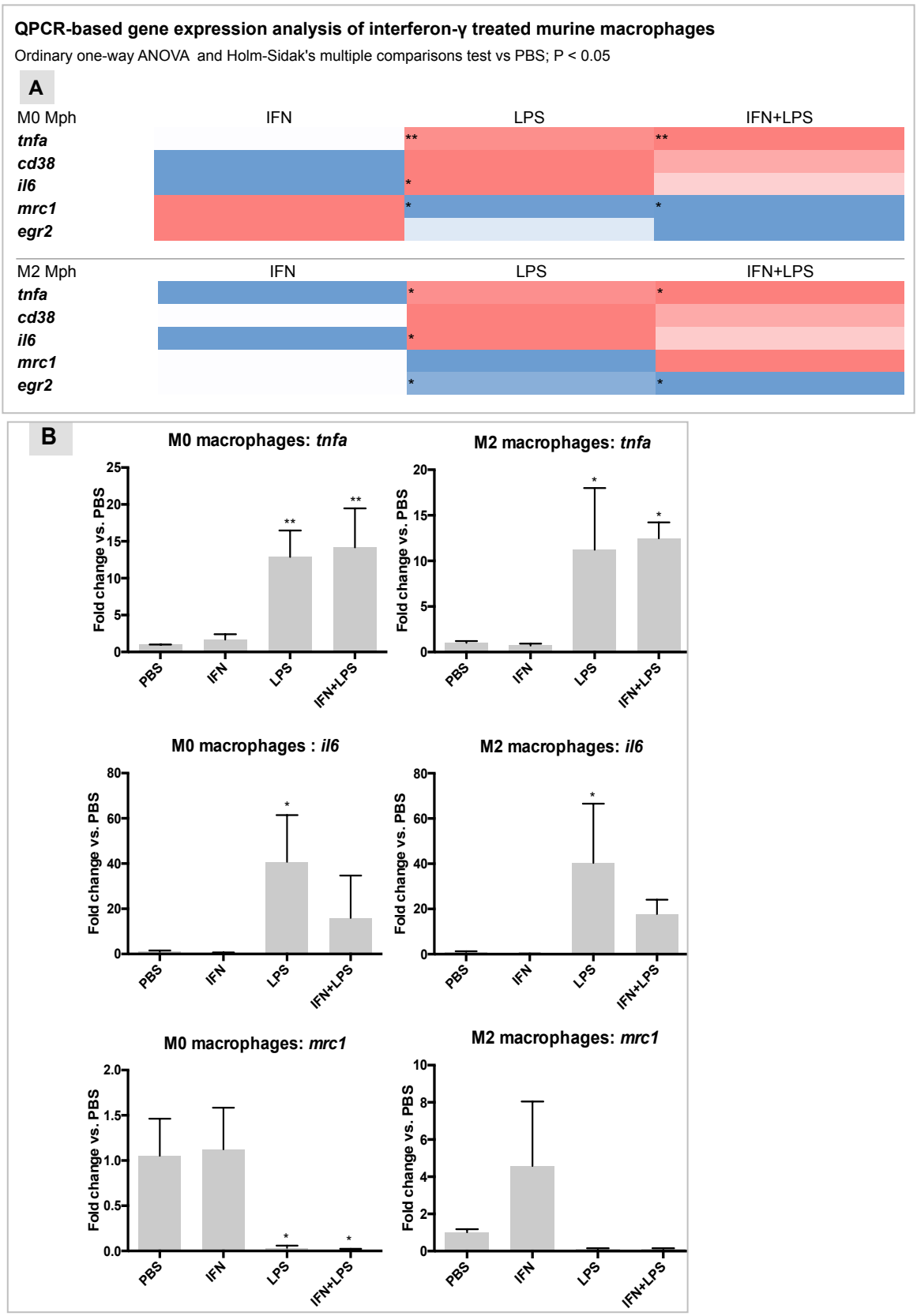

Figure **11**: Heat map and real-time quantitative PCR data of marker genes in interferon-γ treated murine macrophages

(A): The heatmap displays the expression of M1- and M2- polarization marker genes, measured in unpolarized and M2-polarized macrophages by qPCR in relation to PBS

treatment. The bone marrow derived macrophages (BMDM) from C57BL/6 mice were treated with IFN-γ and LPS for 48h. M2-polarization was achieved with IL-4/IL-13 treatment for 24 h. Statistical significance was calculated by one-way ANOVA with PBS as reference group and is indicated by asterisks and colour. Different shades of red indicate an increase and of blue a decrease.

(B): Expression of M1- and M2-polarization marker gens measured in unpolarized and M2-polarized macrophages by qPCR in relation to PBS treatment. The BMDM from C57BL/6 mice were treated with IFN-γ and LPS for 48h. M2-polarization was achieved by IL-4/IL-13 treatment for 24 h. Statistical significance was calculated by one-way ANOVA with PBS as reference group and is indicated by asterisks. Asterisks were used to illustrate statistical significance: *p < 0.05, **p < 0.01, ***p < 0.001, ****p < 0.0001. LPS: Lipopolysaccharide IL4: Interleukin-4; IL-13: Interleukin-13; Mph: Macrophages; *tnfa*: Tumour necrosis factor α; *cd38*: Cluster of Differentiation 38; *il6*: Interleukin-6; *mrc1*: Mannose receptor; *egr2*: Early growth response protein; IFN-γ: Interferon-γ.

b) *Dextran nanoparticles loaded with interferon-γ in combination with lipopolysaccharides are capable of polarization/repolarization of bone marrow derived macrophages*

The described experiment followed the same procedure as described above, but differ in the isolation of the RNA using an RNA purification kit (EURX ®, Polska) and Rneasy® Plus Mini Kit (50) (QIAGEN, Germantown, MD 20874, USA) including on column DNase treatment, hypothesizing better results as with standard purification. Statistical significance was calculated by one-way ANOVA with PBS as negative control and Dunett's multiple comparisons were performed. The DNPs used in the following experiments were prepared with attached PEG-chains (2 kDa) as described above.

The heatmap (Fig. 12) visualizes by different shades of red increase and blue decrease of commonly used markers. A significant (ANOVA summary: P=<0,0001) increase of TNFα and MHCII expression as M1-polarization marker genes for the groups treated with IFN-γ-DNP plus LPS (only *tnfa*** p< 0.01) the combination of LPS-DNP and IFN-γ-DNP (*tnfa****p < 0.001; *mhc2*** p< 0.01) and a decrease of *mrc1* (M2-specific marker) for a treatment with empty DNP plus IFN-γ (*p < 0.05), LPS-DNP (*p < 0.05), LPS-DNP plus IFN-γ (*p < 0.05) and IFN-γ plus LPS (** p< 0.01) in unpolarized macrophages. In M2 polarized macrophages the groups treated with LPS-DNP and IFN-γ-DNP show an increase of M1 markers (*tnfa**** p < 0.05; *cd38**p < 0.05; *ly6c**p < 0.05; *mhc2****p < 0.001) and decrease of *mrc1*. In addition to *il10* and *mrc1* (*p < 0.05) an increase after LPS-DNP with IFN-γ-DNP (M0; *il10* (** p< 0.01; *mrc1* (*p < 0.05)) and IFN-γ plus LPS (M2; *il10**p < 0.05) treatment could be shown.

For further analysis statistical significance was calculated by one-way ANOVA with empty DNP as reference group and Dunett's multiple comparisons were performed. Data thus obtained (Fig. 13) indicate a significant (ANOVA summary: P=<0,0001), increase of *tnfa*, *cd38* and *mhc2* expression as M1-polarization marker genes for the groups treated with IFN-γ-DNP plus LPS (only *tnfa****p < 0.001) the combination of IFN-γ and LPS (only *tnfa****p < 0.001 and *mhc2**p < 0.05) and the combination of

LPS-DNP and IFN-γ-DNP (*tnfa****p < 0.001; *cd38**p < 0.05; *mhc2****p < 0.001) in unpolarized macrophages. In M2 polarized macrophages (ANOVA summary: P=<0.0001 for *tnfa*), LPS-DNP together with IFN-γ-DNP achieved a clear result (*tnfa****p < 0.001; *cd38****p < 0.001; *mhc2****p < 0.001). Also a significant increase of *tnfa* expression after treatment with IFN-γ-DNP plus LPS (*cd38**p < 0.05) could be shown.
Comparing treatment with DNP only to treatment with LPS-DNP plus IFN-γ-DNP and to IFN-γ + LPS as reference group (Fig. 14), a significant increase of M1 specific markers in M0 (*tnfa***p < 0.01; *cd38**p < 0.05; *mhc2***p < 0.01) and M2 macrophages (*tnfa****p < 0.001; *cd38****p < 0.001; *mhc2****p < 0.001) could be shown. Also a significant increase of *tnfa* expression after treatment with IFN-γ-DNP plus LPS could be shown (**p < 0.01; Fig. 14).
The previous finding was further consolidated in two additional cell culture experiments in which gene expression was analysed by taqman real-time quantitative qPCR with TaqMan™ Gene Expression Master Mix (Thermo Fisher Scientific, Waltham, MA, USA) using a fluorogenic probe specific to target gene, leading to a more specific analysis. (Fig.15; Fig. 16) The BMDM from C57BL/6 mice were treated with IFN-γ, LPS, empty DNP, LPS-DNP and IFN-γ-DNP for 48h. M2-polarization was achieved with IL-4/IL-13 treatment for 24 h previously.
The first experiment (Fig.15) confirmed the increased expression of *tnfa* (M0 P<0.0001; M2 P<0.0001), *cd38* (M0 P=0.0010; M2 P<0.0001), *mhc2* (M0 P=0.0079; M2 P<0.0001) and *ly6c* (M0 P=0.0011; M2 P<0.0001) as M1 polarization marker genes by treatment with LPS-DNP (M0: *cd38*; M2: *tnfa*, *cd38*, *ly6c*), the combination of IFN-γ and LPS-DNP (M2: *tnfa*, *cd38*, *ly6c*), IFN-γ and LPS (M0: *tnfa*, *mhc2*; M2: *tnfa*, *cd38*, *ly6c*, *mhc2*) and the combination of LPS-DNP and IFN-γ-DNP (M0: *tnfa*, *cd38*, *ly6c*; M2: *tnfa*, *cd38, ly6c, mhc2).*
The data of the second experiment shown in Fig. 16 indicated a significant increase of *tnfa* (ANOVA summary M0 P<0,0001; M2 P=0,0246), *inos* (M0 P<0,0001; M2 P<0,0001) and *ly6c* (M0 P= 0,0006; M2 P=0,0251) expression for the groups of native and M2 polarized macrophages treated with LPS-DNP (M0: *tnfa*, *inos*, *ly6c*; M2: *tnfa* = ns, *inos*, *ly6c*=ns), the combination of IFN-γ and LPS (M0: *tnfa*, *inos*, *ly6c*; M2: *tnfa* = ns, *inos*, *ly6c*=ns), the combination of LPS-DNP and IFN-γ-DNP, as well as an decrease of M2-specific marker *mrc1* significant for each treatment (ANOVA summary M0 P=0,0027; M2 P=0,0071) (Fig.16).
The results of Dunett's multiple comparisons for each marker and treatment are plotted in Figures 15 and 16. In both experiments comparing native and polarized macrophages, polarized macrophages appeared more responsive to treatment, especially the groups treated with the combination of LPS-DNP and IFN-γ-DNP (Fig. 15, Fig. 16).

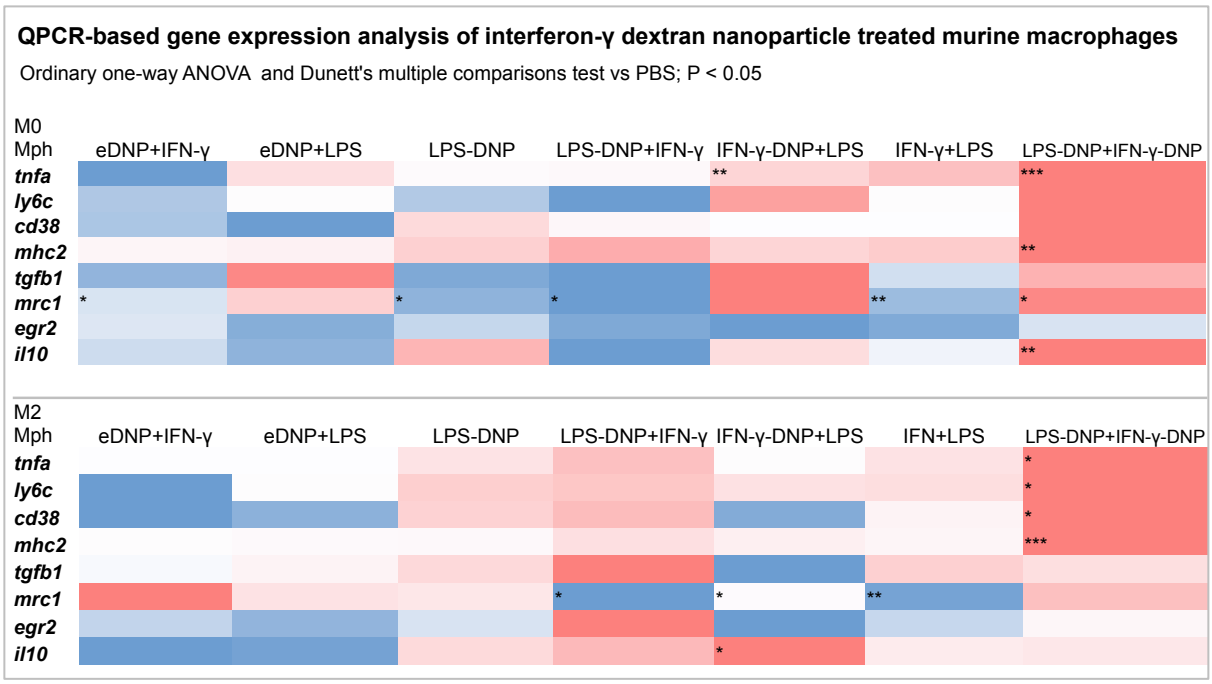

Figure **12**: Heat map of marker genes in interferon-γ dextran-nanoparticle treated murine macrophages

The heatmap displays the expression of M1- and M2- polarization marker genes, measured in unpolarized and M2-polarized macrophages by qPCR in relation to PBS treatment. The bone marrow derived macrophages (BMDM) from C57BL/6 mice were treated with IFN-γ, LPS, IFN-γ-DNP,LPS-DNP and eDNP and the combination of them for 48h. M2-polarization was achieved with IL-4/IL-13 treatment for 24 h. Statistical significance was calculated by one-way ANOVA with PBS as reference group and is indicated by asterisks and colour. Different shades of red indicate an increase and of blue a decrease. LPS: Lipopolysaccharide; IL4: Interleukin-4; IL13: Interleukin-13; *tnfa*: Tumour necrosis factor α; *cd38*: Cluster of Differentiation 38; *il10*: Interleukin-10; *mhc2*: Class II major histocompatibility complex molecules; IFN-γ: Interferon-γ; eDNP: empty dextran-nanoparticle, IFN-γ-DNP: Interferon-γ loaded dextran-based nanoparticles, LPS-DNP: LPS loaded dextran-based nanoparticles; *ergr2*: Early growth response protein; *ly6c*: Lymphocyte antigen 6 complex; *tgfb1*: transforming growth factor β1.

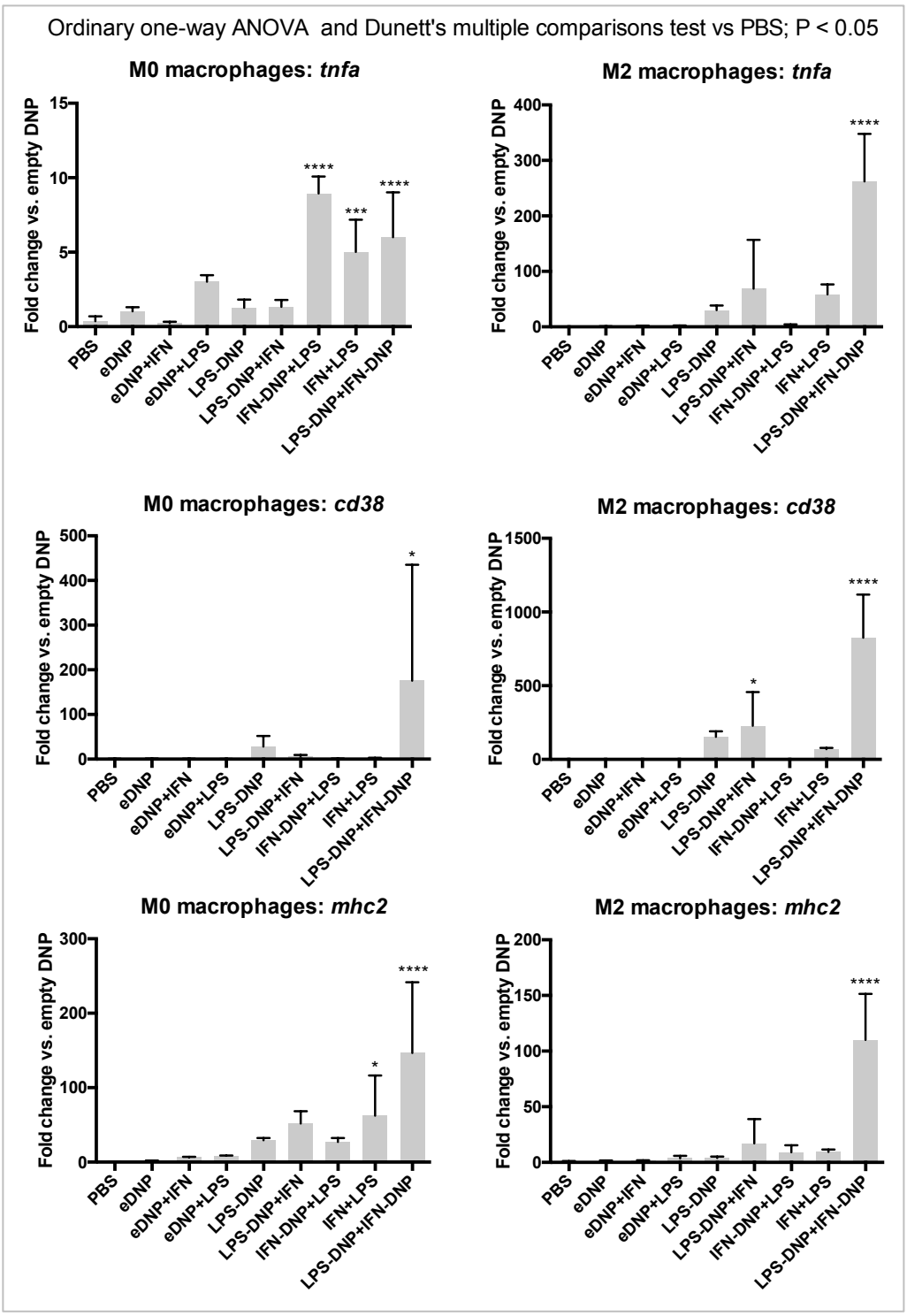

Figure **13**: Real-time quantitative PCR based analysis of dextran-based nanoparticle treated murine macrophages

Expression of M1- and M2- polarization marker genes, measured in unpolarized and M2-polarized macrophages by qPCR in relation to PBS treatment. The BMDM from C57BL/6 mice were treated with IFN-γ, LPS, empty DNP, LPS-DNP and IFN-γ-DNP for 48h. M2-polarization was achieved with IL-4/IL-13 treatment for 24 h. Statistical significance was calculated by one-way ANOVA with empty DNP as reference group (Fig. 13)/ IFN-γ and LPS as reference group (Fig. 14). Asterisks were used to illustrate statistical significance: *p < 0.05, **p < 0.01, ***p < 0.001, ****p < 0.0001. Abbreviations see Figure 12.

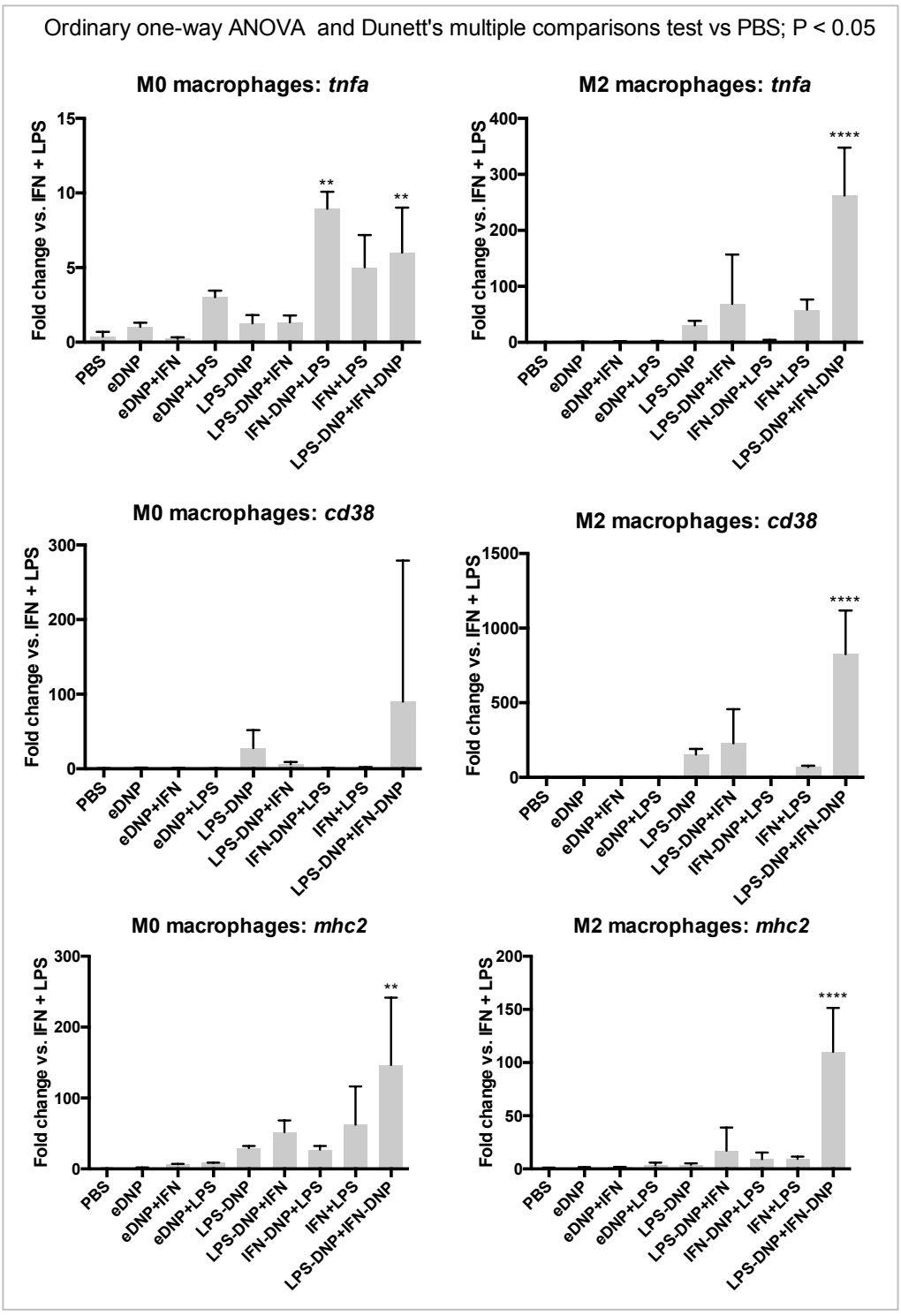

Figure **14**: Real-time quantitative PCR analysis of dextran-based nanoparticle treated murine macrophages

Expression of M1- and M2- polarization marker genes, measured in unpolarized and M2-polarized macrophages by qPCR in relation to PBS treatment. The BMDM from C57BL/6 mice were treated with IFN-γ, LPS, empty DNP, LPS-DNP and IFN-γ-DNP for 48h. M2-polarization was achieved with IL-4/IL-13 treatment for 24 h. Statistical significance was calculated by one-way ANOVA with empty DNP as reference group (Fig. 13)/ IFN-γ and LPS as reference group (Fig. 14). Asterisks were used to illustrate statistical significance: *p < 0.05, **p < 0.01, ***p < 0.001, ****p < 0.0001. Abbreviations see Figure 12.

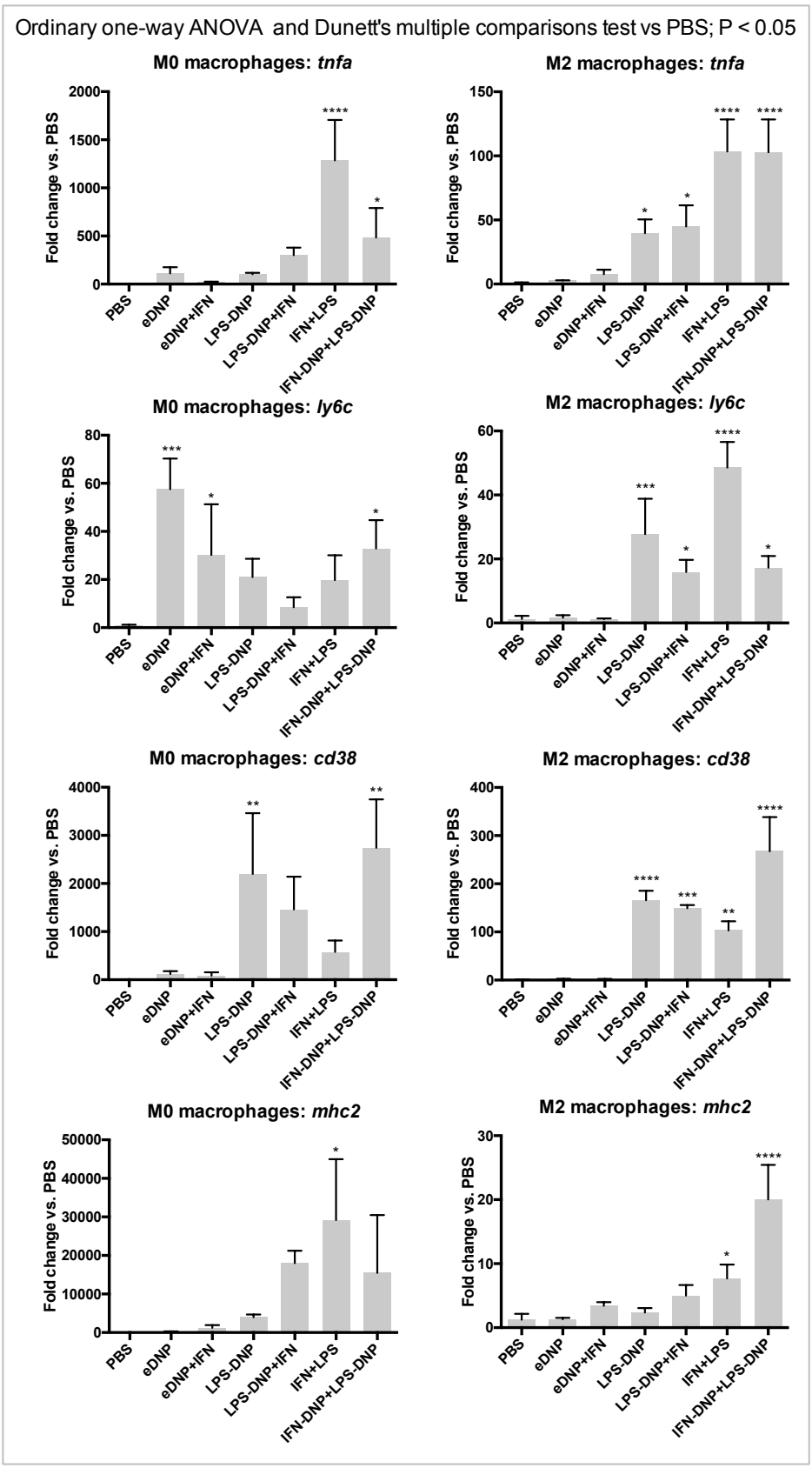

Figure **15**: First taqman real-time quantitative PCR based analysis of dextran-based nanoparticle treated murine macrophages

Expression of M1- and M2- polarization marker gens measured in unpolarized and M2-polarized macrophages by Taqman qPCR in relation to PBS treatment. The BMDM from

C57BL/6 mice were treated with IFN-γ, LPS, empty DNP, LPS-DNP and IFN-γ-DNP for 48h. M2-polarization was achieved with IL-4/IL-13 treatment for 24 h. Statistical significance was calculated by one-way ANOVA with PBS as reference group and is indicated by asterisks. Asterisks were used to illustrate statistical significance Dunnett`s multiple comparisons: *p < 0.05, **p < 0.01, ***p < 0.001, ****p < 0.0001. *mrc1*: Mannose receptor; *ly6c*: Lymphocyte antigen 6 complex; *inos*: Inducible nitric oxide synthase. Remaining abbreviations see Figure 12.

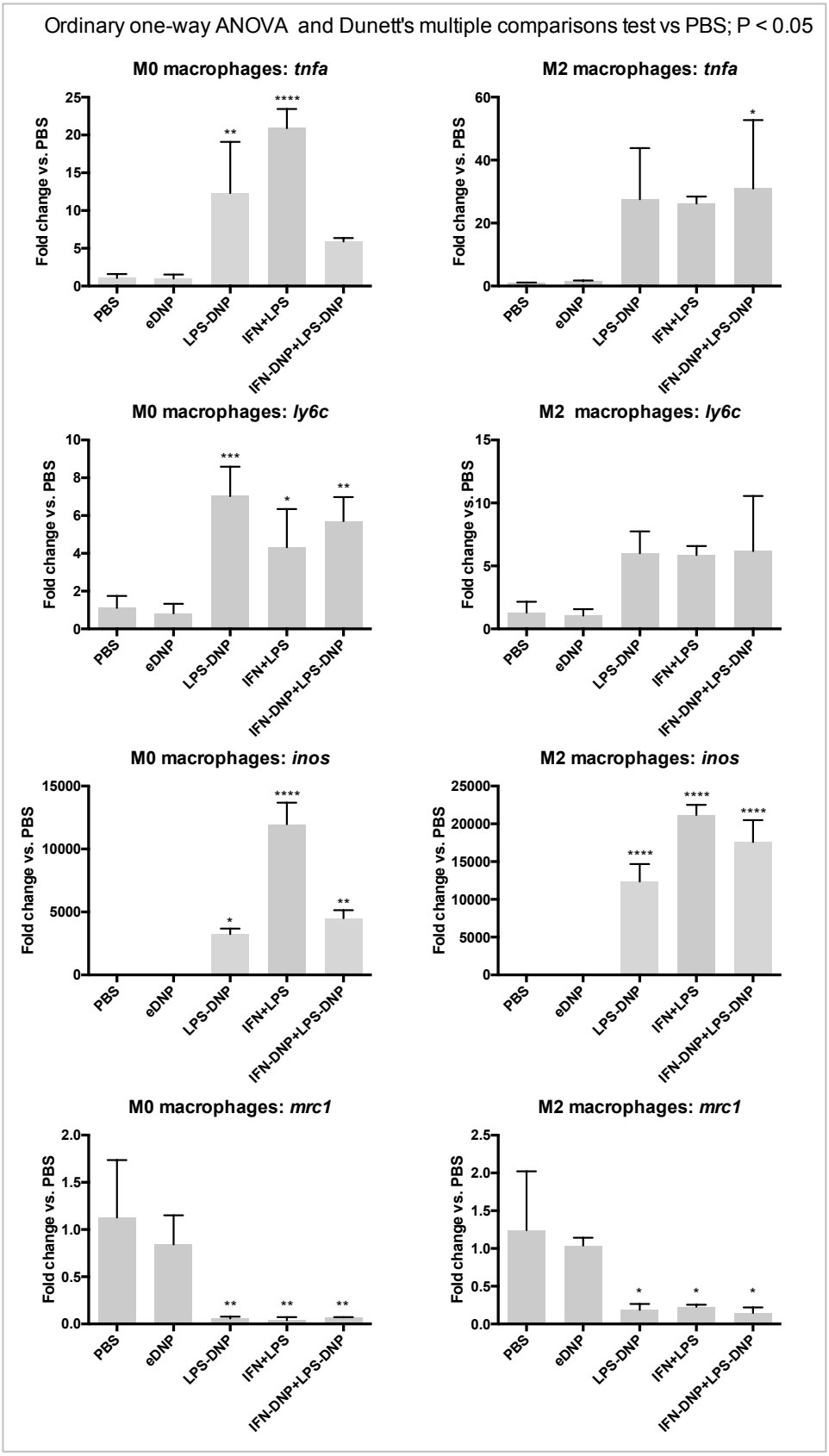

Figure **16**: Second Taqman real-time quantitative PCR based analysis of dextran-based nanoparticle treated murine macrophages

Abbreviations and description see Figure 15 and Figure 12.

7. Fluorescence-activated cell sorting analysis of macrophage subtypes after interferon-γ, lipopolysaccharides and dextran-based nanoparticle treatment

FACS is able to sort cells by detecting forward (FSC) for the cell size and side (90°, SSC) scatter for granularity and complexity using laser light. In addition, fluorescence dye tagged antibodies against specific surface markers are used to specify the cell subtype. 7-Aminoactinomycin D (7-AAD) distinguish live and dead cells, because it can be excluded by live cells, but not by damaged or dead ones. CD45 (leucocyte common antigen) can be used as a marker for all hematopoietic cells except of platelets and erythrocytes. As described in (52) this receptor tyrosine kinase plays an important role in the function of hematopoietic cells. F4/80 is a mouse macrophage specific membrane glycoprotein, which is necessary to generate antigen-specific regulatory T-cells (Tregs) (53).
To separate the macrophage subpopulation marking with APC-A Allophycocyanin (APC) linked antibodies for the CD206 mannose receptor which is highly expressed by TAMs (26) (M2 like phenotype) and with fluorescein-5-isothiocyanate (FITC) linked antibodies for the more M1 type specific MHCII was performed (Gating Fig. 17-19).
The cells sorted Live/CD45+/F480+/MHCII show a significantly increased mean fluorescence intensity percentage of control group PBS as well as an increase of the mean fluorescence intensity for previously unpolarized and polarized macrophages treated with: empty DNP in combination with LPS, IFN-γ loaded DNP in combination with LPS, LPS loaded DNP with IFN-γ, IFN-γ-DNP in combination with LPS-DNP, single LPS and single IFN-γ loaded DNP treatment (Fig. 20A; 20B).
The cells sorted Live/CD45+/F480+/CD206 show a significantly decreased mean fluorescence intensity percentage of control group PBS as well as a decrease of the mean fluorescence intensity for previously unpolarized and polarized macrophages treated with: empty DNP in combination with LPS, IFN-γ loaded DNP in combination with LPS, LPS-DNP with IFN-γ, IFN-γ-DNP in combination with LPS-DNP, single LPS, single IFN-γ and single IFN-γ-DNP treatment (Fig. 20C; 20D).
Summing up treatment with IFN-γ and LPS loaded DNP, as well as the pure IFN-γ and LPS treatment increased the generation of classically activated M1-type macrophages and at the same time decreased alternatively activated M2-type macrophages. Single IFN-γ treatment did not lead to a significant increase of MHCII sorted cells but to a decrease of CD206 sorted cells. IFN-γ-DNP significantly increased classically activated macrophages and decreased alternatively activated macrophages (Fig. 17-20).

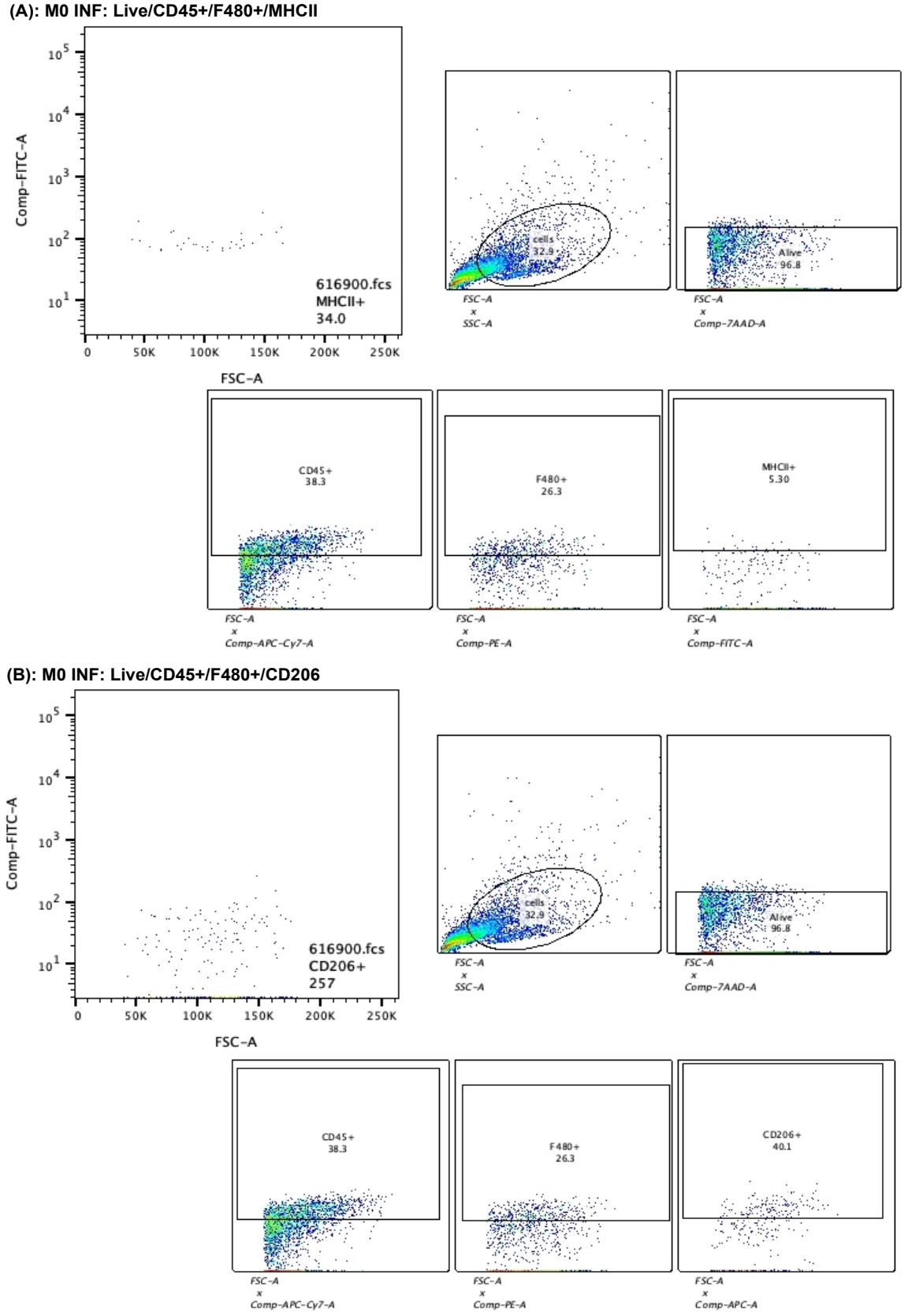

Figure **17**: Fluorescence-activated cell sorting of interferon-γ treated murine macrophages – Gating (17.1, continued on page 42)

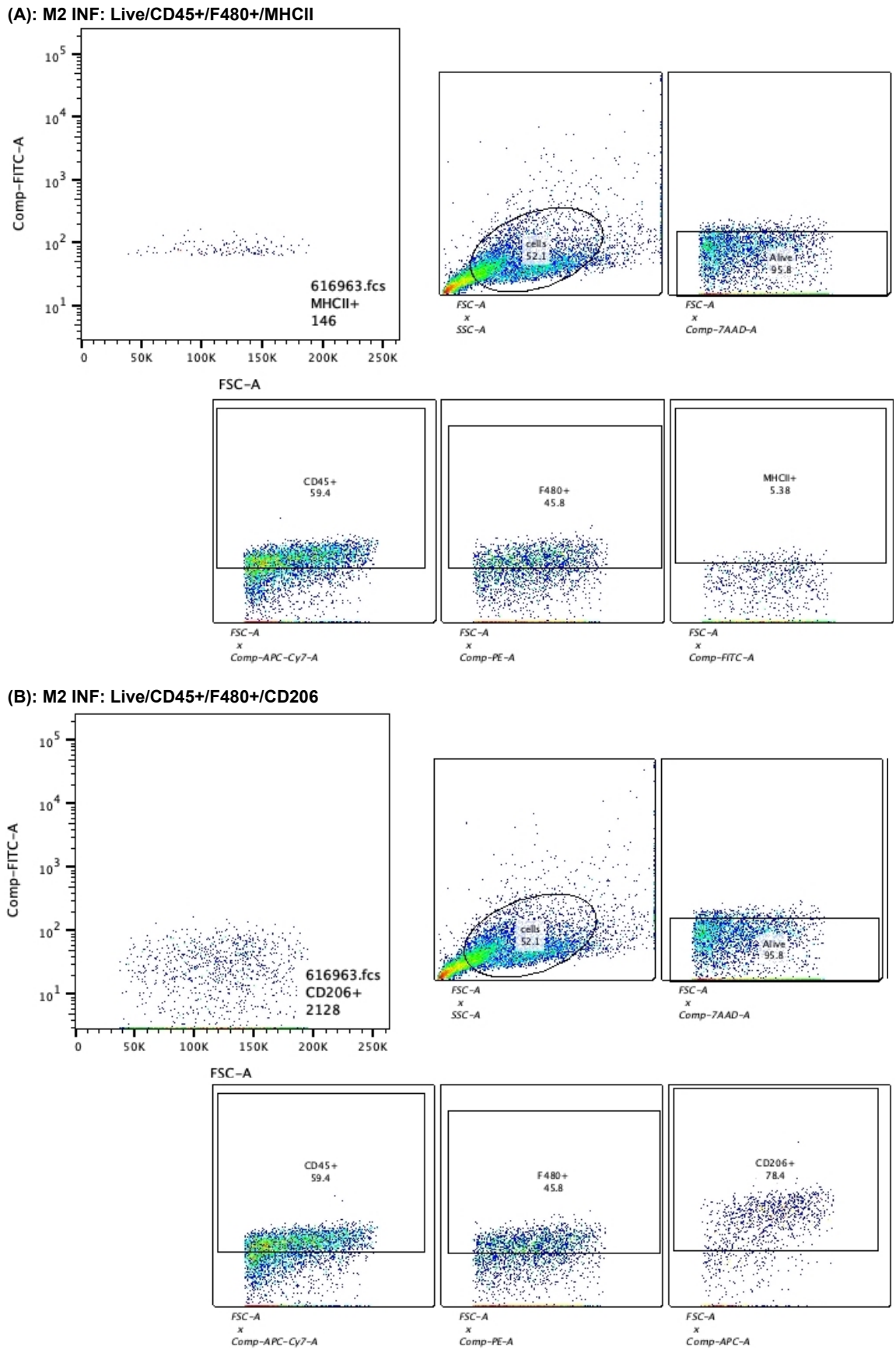

Figure **17**: Fluorescence-activated cell sorting of interferon-γ treated murine macrophages – Gating (17.2)

Previously unpolarized (17.1) and polarized (17.2) macrophages were treated with IFN-γ and gated Live/CD45+/F480+/ MHCII for M1 phenotype (Fig. 17.1A; Fig. 17.2A) and Live/CD45+/F480+/ CD206 for M2 phenotype (Fig. 17.1B; Fig. 17.2B). In the figure above the gating data are shown. The results of the statistical analysis are shown in Figure 20. Comp: compensation; A: Area; FITCH: Fluorescein-5-isothiocyanat; PE: Phycoerhtrin; APC-Cy7-A: APC-A Allophycocyanin; 7-AAD: 7-Aminoactinomycin D; FSC: Forward scatter; SSC: Size and side scatter; MHCII: Class II major histocompatibility complex molecules; CD45: Cluster of Differentiation 45; F4/80: EMR1; EGF-like module containing, mucin-like, hormone receptor-like sequence 1; CD206: Cluster of Differentiation 206; Mannose receptor; IFN-γ: interferon-γ

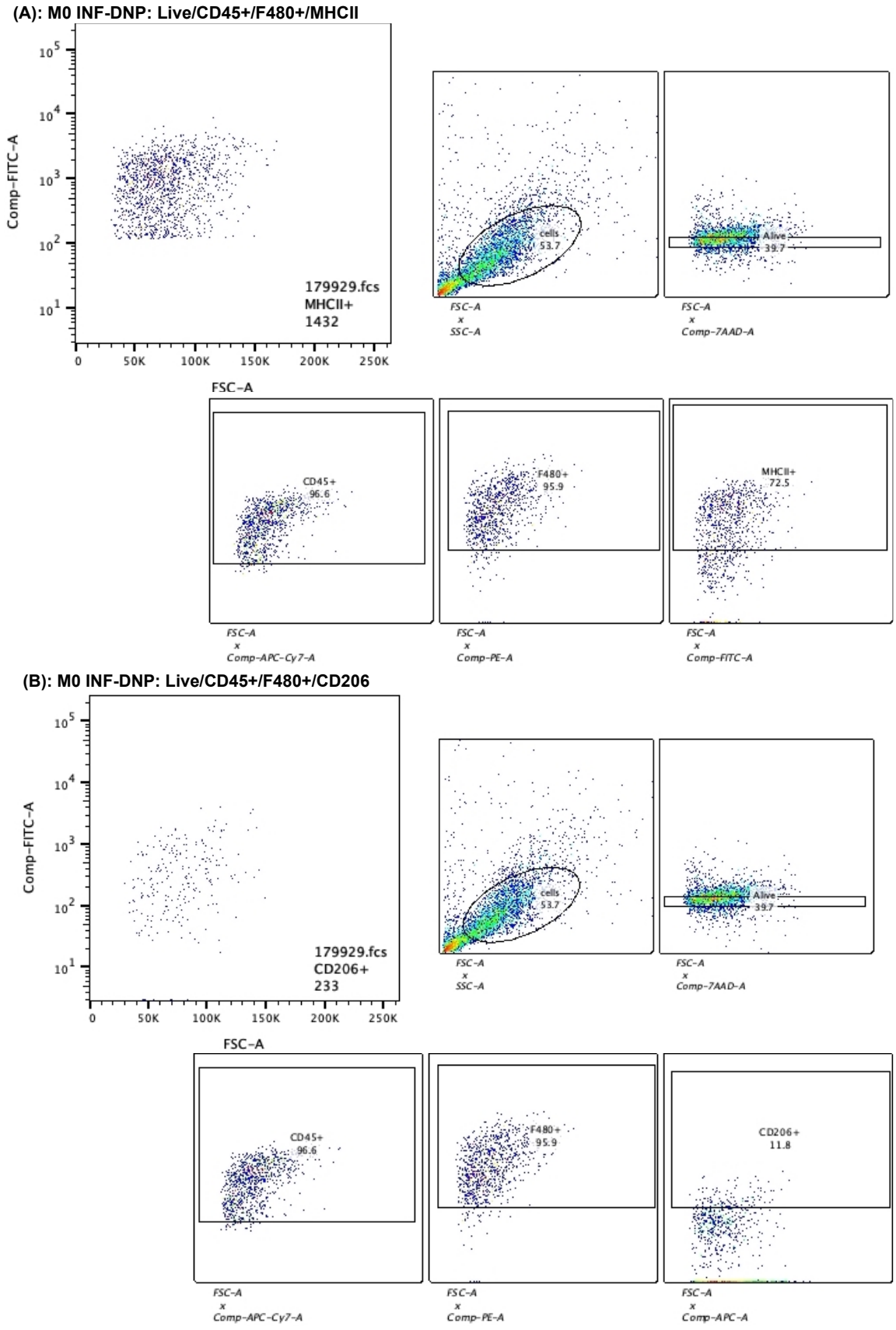

Figure **18**: Fluorescence-activated cell sorting of interferon-γ dextran-based nanoparticle treated murine macrophages – Gating (18.1, continued on page 45)

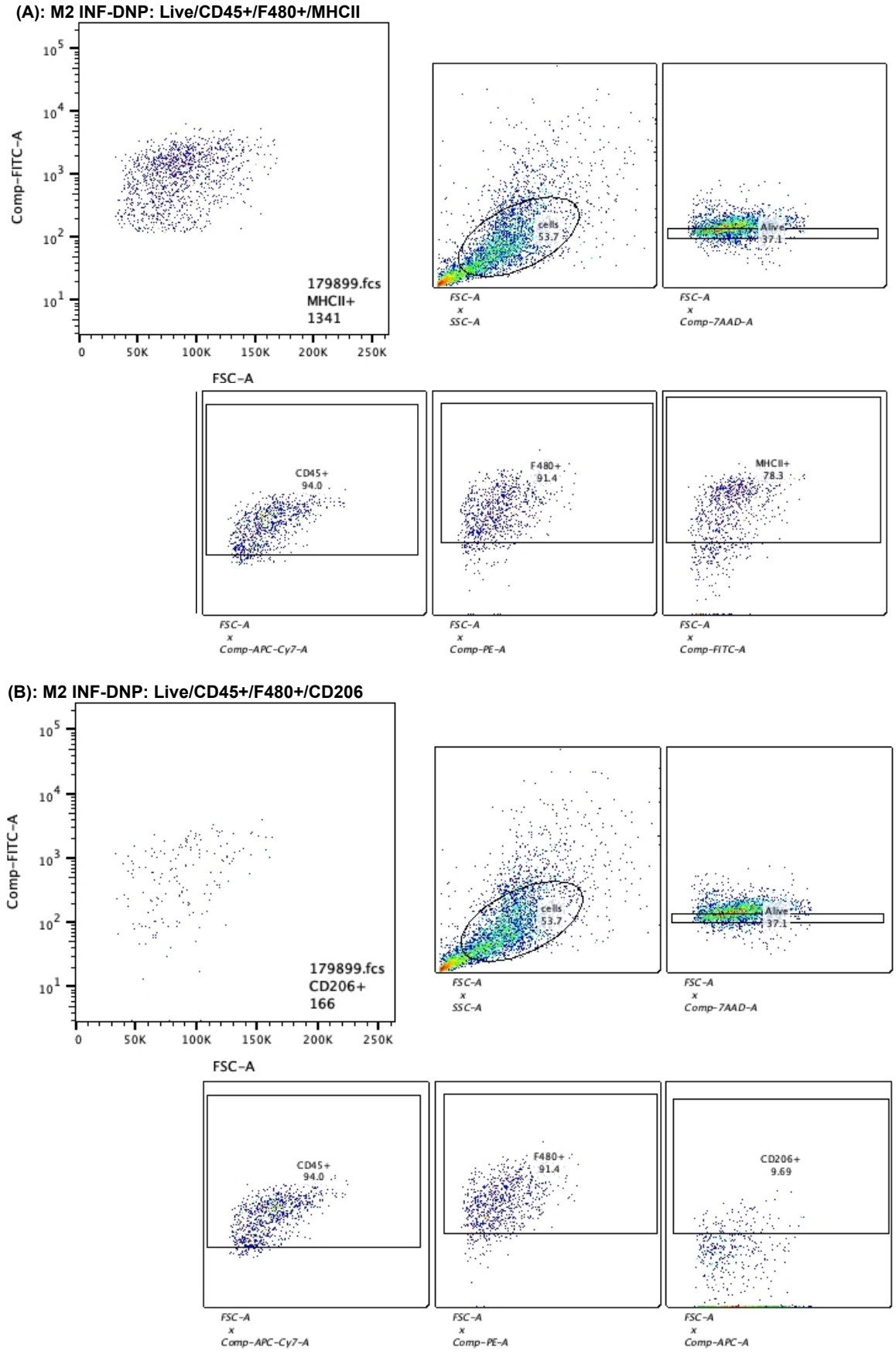

Figure **18**: Fluorescence-activated cell sorting of interferon-γ dextran-based nanoparticle treated murine macrophages – Gating (18.2)

Previously unpolarized (Fig.18.1) and polarized (Fig.18.2) macrophages and treated with IFN-γ-DNP were gated Live/CD45+/F480+/ MHCII for M1 phenotype (Fig.18.1A; Fig18.2A) and Live/CD45+/F480+/ CD206 for M2 phenotype (Fig.18.1B; Fig.18.2B). In the figure above the gating data are shown. The results of the statistical analysis are shown in Figure 20. Abbrevaitions see Figure 17.

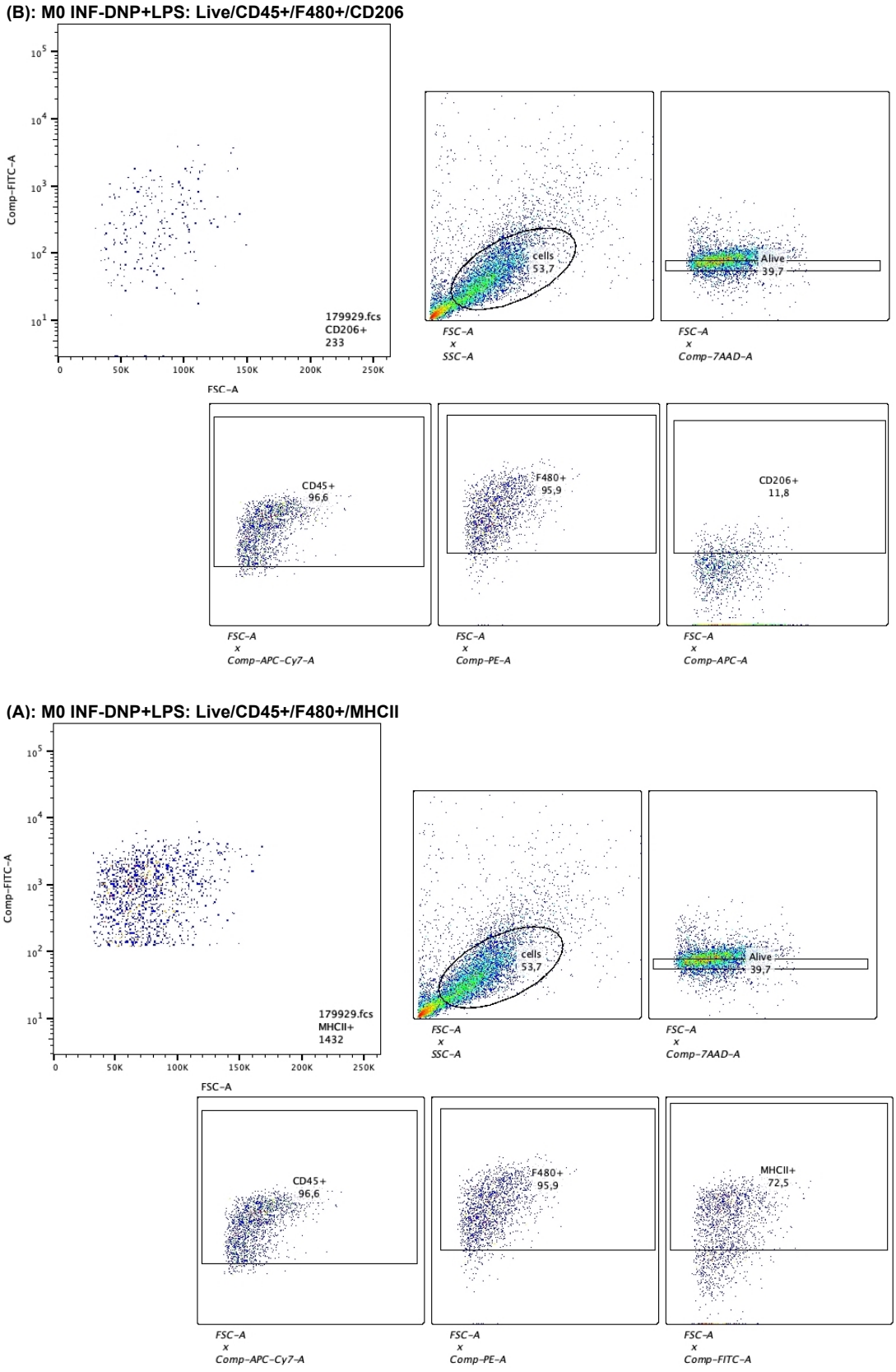

Figure **19**: Fluorescence-activated cell sorting of interferon-γ dextran-based nanoparticle in combination with lipopolysaccharid treated murine macrophages – Gating (19.1, continued on page 48)

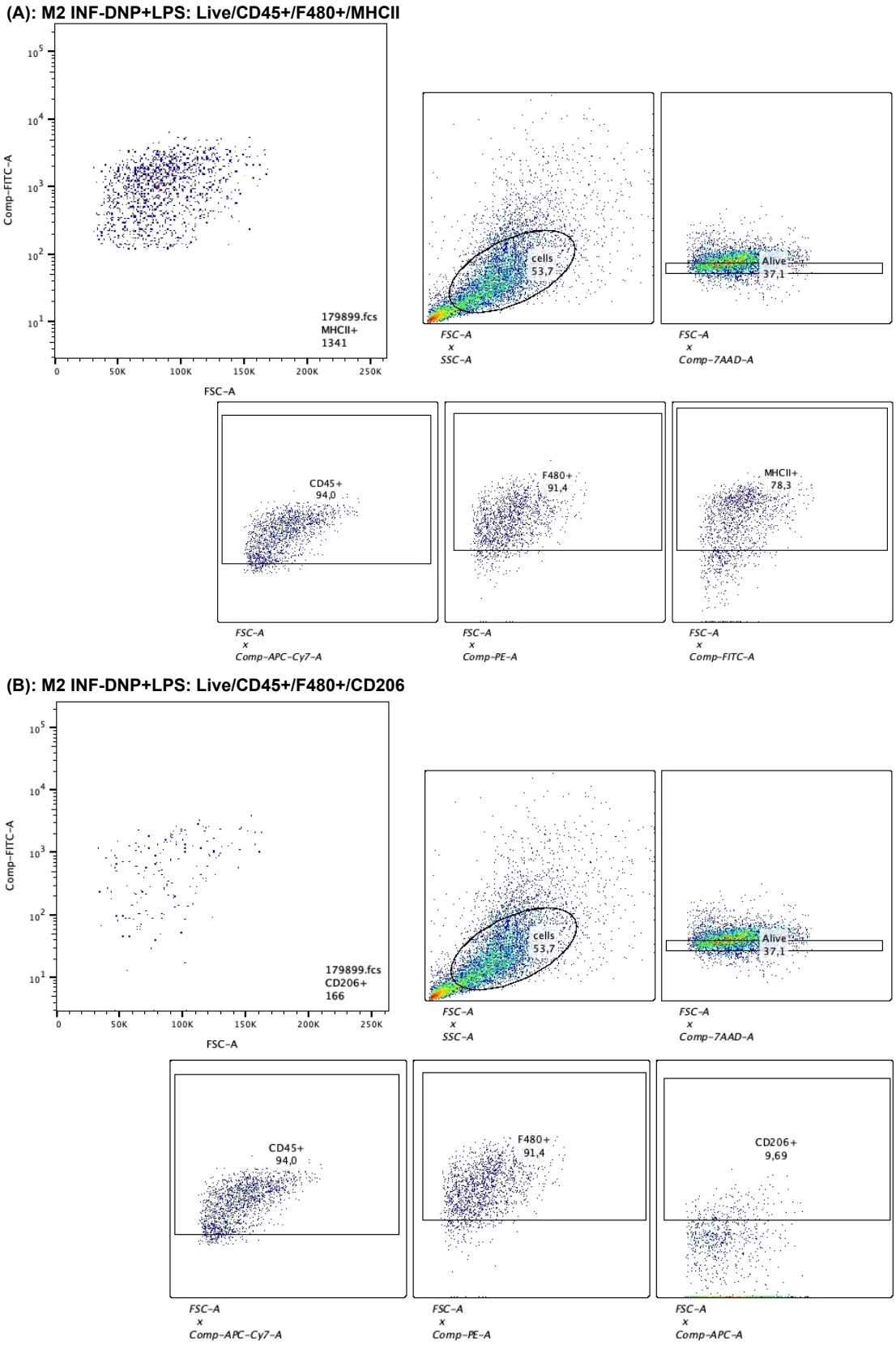

Figure **19**: Fluorescence-activated cell sorting of interferon-γ dextran-based nanoparticle in combination with lipopolysaccharid treated murine macrophages – Gating (19.2)

Previously unpolarized (Fig.19.1) and polarized (Fig.19.2) macrophages and treated with IFN-γ in combination with LPS were gated Live/CD45+/F480+/ MHCII for M1 phenotype (Fig.19.1A; Fig19.2A) and Live/CD45+/F480+/ CD206 for M2 phenotype (Fig.19.1B; Fig.19.2B). In the figure above the gating data are shown. The results of the statistical analysis are shown in Figure 20. Abbrevaitions see Figure 17.

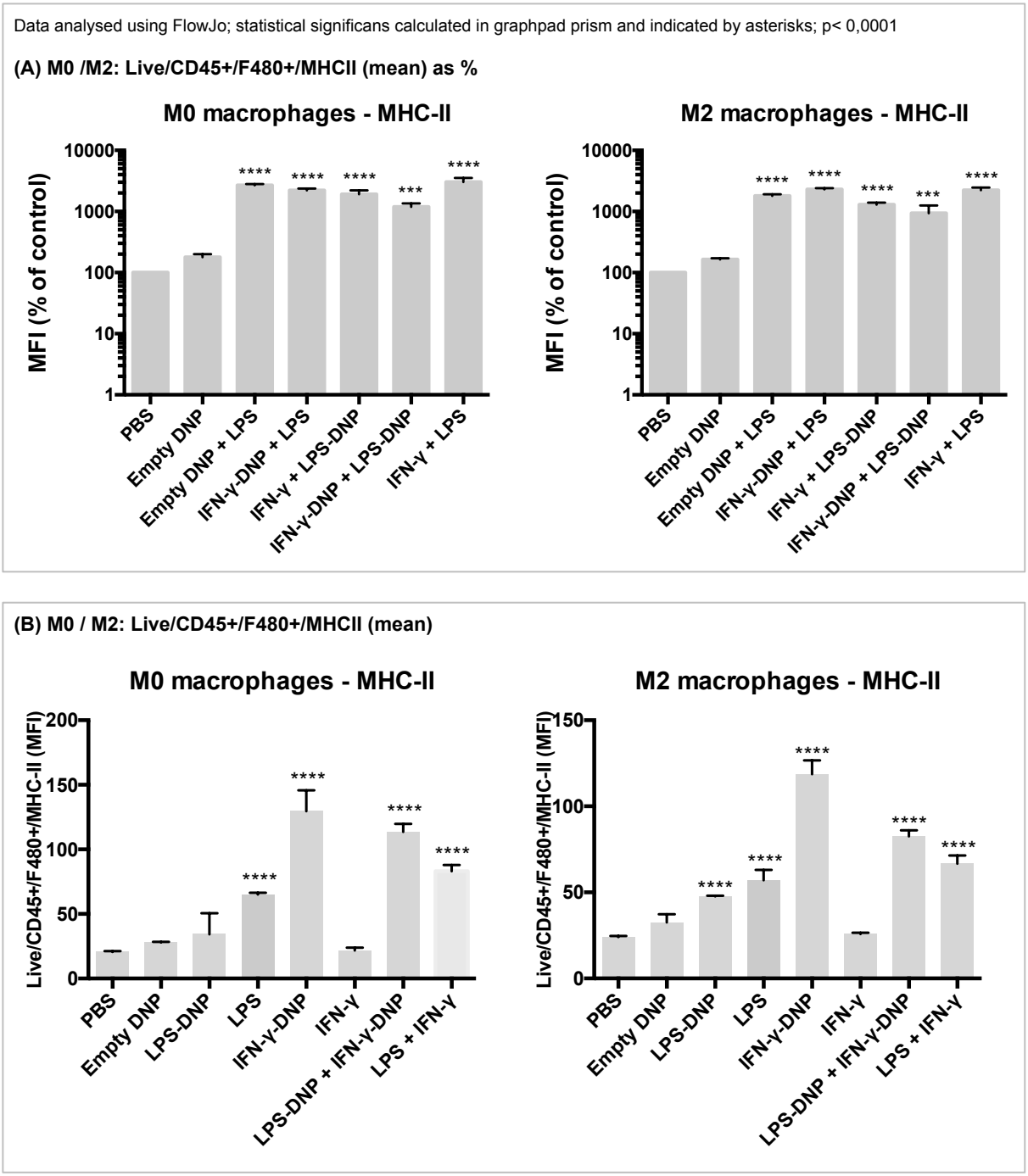

Figure **20**: Fluorescence-activated cell sorting of dextran-based nanoparticle treated murine macrophages (20.1, continued on page 51)

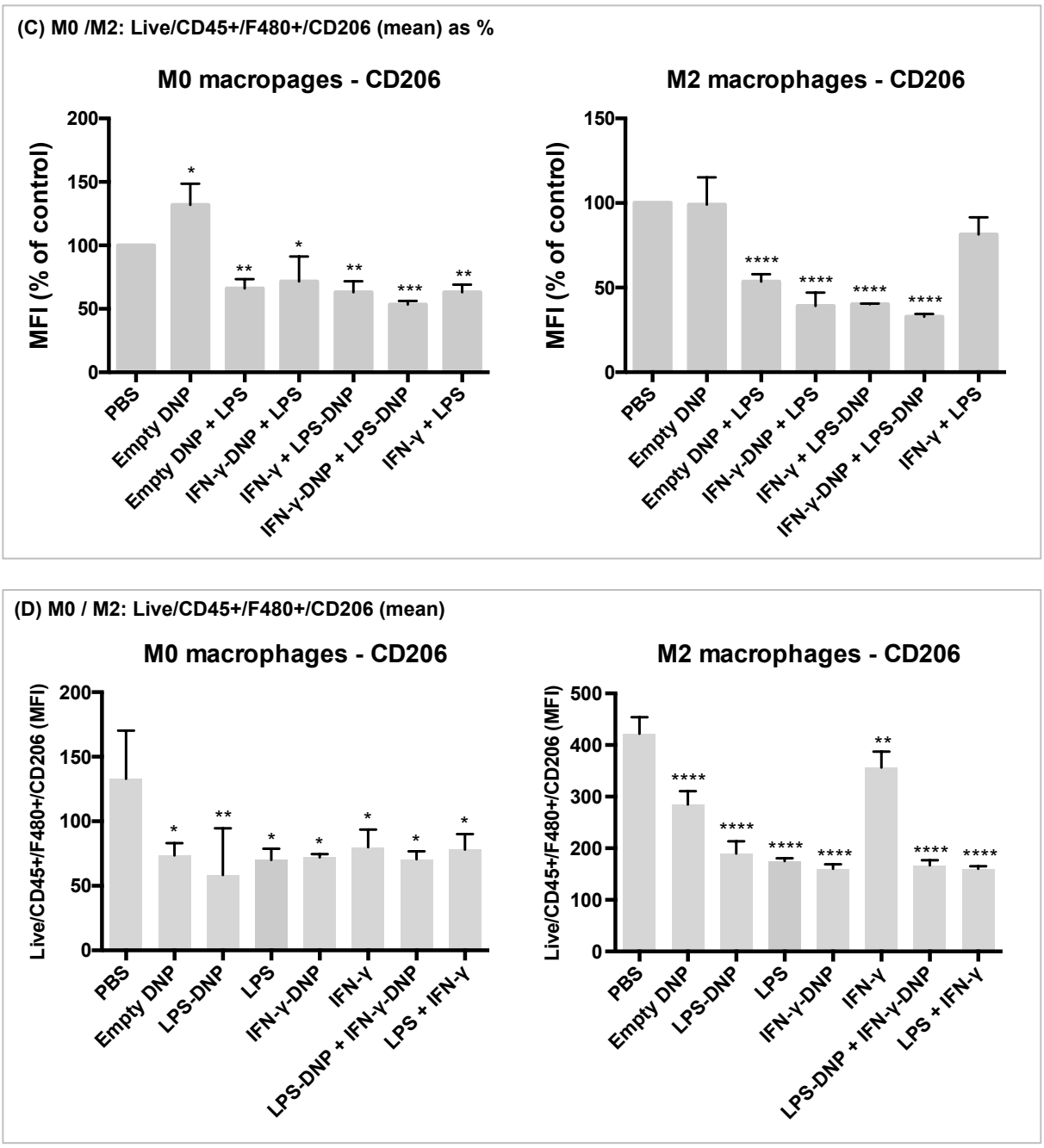

Figure **20**: Fluorescence-activated cell sorting of dextran-based nanoparticle treated murine macrophages (20.2)

The bone marrow derived macrophages from C57BL/6 mice were treated with IFN-γ, LPS, empty DNP, LPS-DNP and IFN-γ-DNP in 6 well formats for 48h. M2-polarization was achieved with IL-4/IL-13 treatment for 24 h. Afterwards FACS- Analysis was performed as described; counting the MHCII positive macrophages representing classically activated macrophages (or CD206, also known as Mrc1 mannose receptor, C type, positive macrophages, representing alternatively activated macrophages). Calculating the percentage of control (Fig. 20.1A;C First experiment) and the cells by mean fluorescence intensity (MFI) (Fig. 20.2B;D Second experiment.) FlowJo and Excel were used. To proof statistical significance one-way ANOVA and Dunnett's multiple comparisons test with PBS as reference group was performed in graph pad prism. Asterisks were used to illustrate statistical significance Dunnett`s multiple comparisons: *p < 0.05, **p < 0.01, ***p < 0.001, ****p < 0.0001. LPS: Lipopolysaccharide; IL4: Interleukin-4; IL-13: Interleukin-13; MHCII: Class II major histocompatibility complex molecules; IFN-γ: Interferon-γ; empty DNP: empty

dextran-nanoparticles, IFN-γ-DNP: Interferon-γ loaded dextran-based nanoparticles, LPS-DNP: LPS loaded dextran-based nanoparticles; CD206: Cluster of Differentiation 206; Mannose receptor; CD45: Cluster of Differentiation 45; F4/80: EMR1, EGF-like module containing, mucin-like, hormone receptor-like sequence 1; MFI: mean fluorescence intensity

An additional analysis was performed comparing the group treated with IFN-γ-DNP against empty DNP (Fig. 21). The Live/CD45+/F480+/MHCII sorted cells showed a significant increase of mean fluorescence intensity for previously unpolarized macrophages treated with: LPS, IFN-γ-DNP, a combination of IFN-γ-DNP and LPS-DNP, and a combination of IFN-γ and LPS, as well as for M2 polarized macrophages: LPS, LPS-DNP, IFN-γ-DNP, a combination of IFN-γ-DNP and LPS-DNP, and IFN-γ and LPS in combination. The cells sorted Live/CD45+/F480+/CD206 showed no significant decrease of mean fluorescence intensity for previously unpolarized macrophages compared to empty nanoparticles. But the control groups with PBS showed increased signals compared to empty DNP. In primary M2 polarized macrophages the treatment with LPS, LPS-DNP, IFN-γ-DNP, IFN-γ-DNP in combination with LPS-DNP and LPS in combination with IFN-γ lead to a significant decrease of the mean fluorescence intensity compared to empty DNP (Fig. 21).

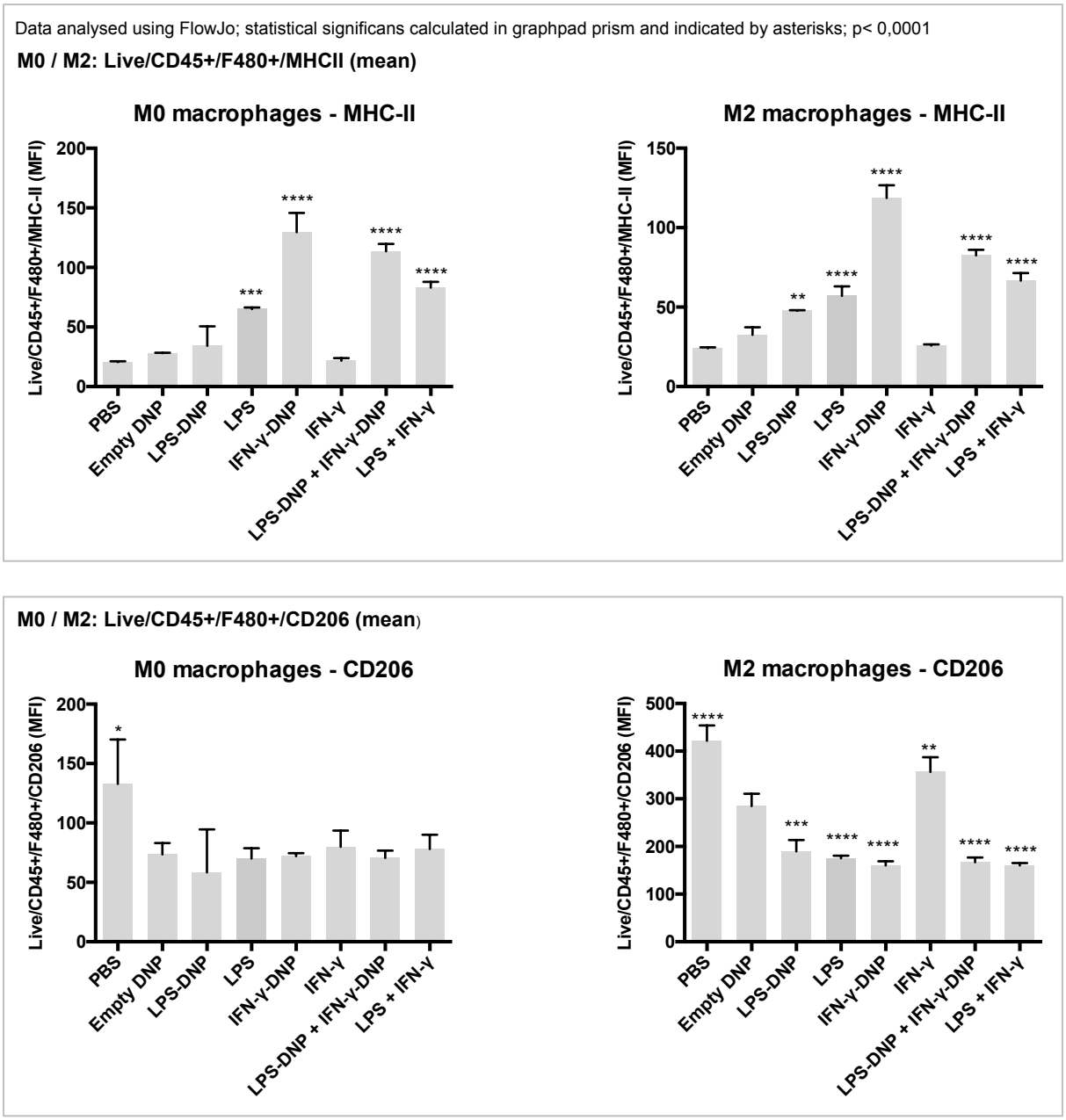

Figure **21**: Fluorescence-activated cell sorting of dextran-based nanoparticle treated murine macrophages

The bone marrow derived macrophages from C57BL/6 mice were treated with IFN-γ, LPS, empty DNP, LPS-DNP and IFN-γ-DNP in 6 well formats for 48h. Afterwards FACS analysis was performed as described counting the MHCII positive macrophages representing classically activated macrophages. FlowJo and Excel were used. To proof statistical significance one-way ANOVA and Dunnett's multiple comparisons test with empty-DNP as reference group was performed in graph pad prism. Asterisks were used to illustrate statistical significance Dunnett`s multiple comparisons: *p < 0.05, **p < 0.01, ***p < 0.001, ****p < 0.0001. Abbreviations see Figure 20.

8. Enzyme-linked immunosorbent assay (ELISA) for cytokines

a) Enhanced TNFα production after treatment with dextran-nanoparticles

A TNFα-Enzyme linked immunosorbent assay (TNFα-ELISA) was used as method for detecting and quantifying TNFα as protein sandwiched two specific anti-TNFα monoclonal antibodies, one immobilized on plastic. TNFα is one of the main players indicating a proinflammatory tumoridical immune reaction (85). The supernatant was used from the previous cell culture experiments. BMDM were polarized with IL-4/IL-13 for 24h towards M2 and then exposed to IFN-γ, LPS, empty DNP, LPS-DNP and IFN-γ-DNP for 48h. LPS with empty DNP, DNP loaded with LPS, in combination with IFN-γ and IFN-γ-DNP lead to a significant upregulation of TNFα. IFN-γ and IFN-γ-DNP alone were not sufficient to induce a pro-inflammatory polarization and/or repolarization as measured by TNFα production (Fig. 22).

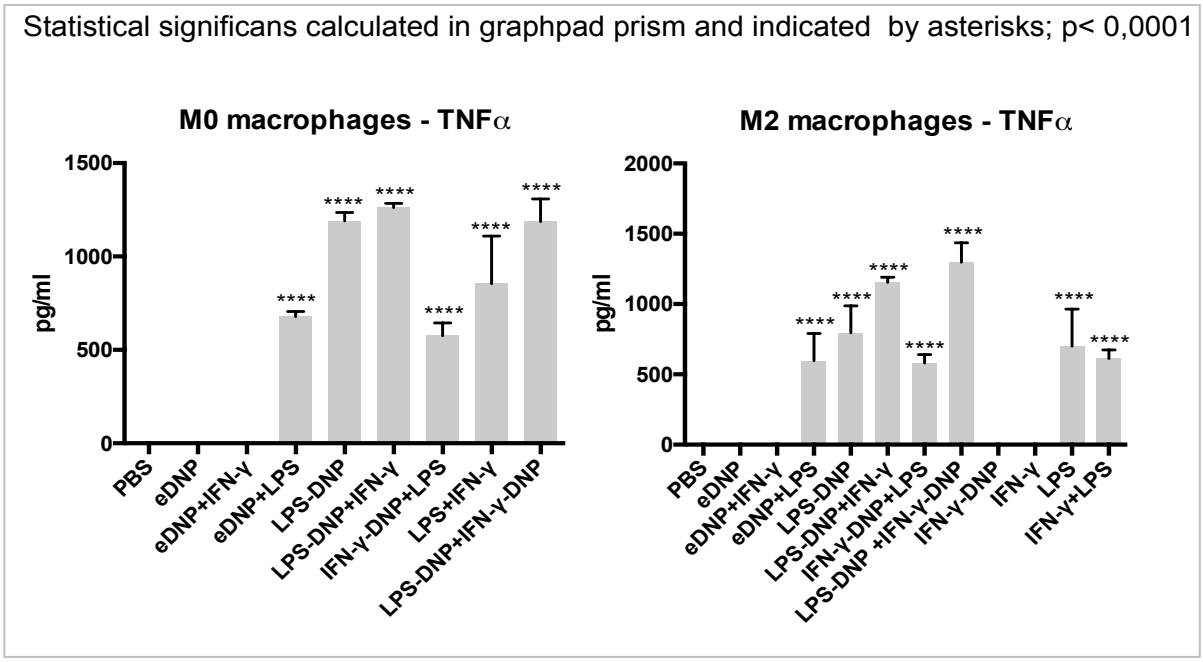

Figure **22**: TNFα-ELISA of cell culture supernatant

The bone marrow derived macrophages from BALB/c/ C57BL/6 mice were treated with IFN-γ, LPS, empty DNP, LPS-DNP and IFN-γ-DNP for 48h. M2-polarization was achieved with IL-4/IL-13 treatment for 24 h. Afterwards an ELISA was performed as described to quantify TNFα in the cell culture supernatant. To proof statistical significance one-way ANOVA and Dunnett's multiple comparisons test with PBS as reference group was performed in graphpad prism. Significance indicated by asterisks (p< 0,0001= ****). LPS: Lipopolysaccharide; IL4: Interleukin-4; IL-13: Interleukin-13; TNF: Tumour necrosis factor α; IFN-γ: Interferon-γ; eDNP: empty dextran-nanoparticle, IFN-γ-DNP: Interferon-γ loaded dextran-based nanoparticles, LPS-DNP: LPS loaded dextran-based nanoparticles.

b) Enhanced IL-10 production after treatment with dextran-nanoparticles

The IL-10 ELISA was performed equivalent to the TNFα ELISA. The treatment with LPS loaded nanoparticles, as well as the combination of IFN-γ and LPS and LPS-DNP and IFN-γ-DNP treatment increased the production of IL-10 (Fig. 23).

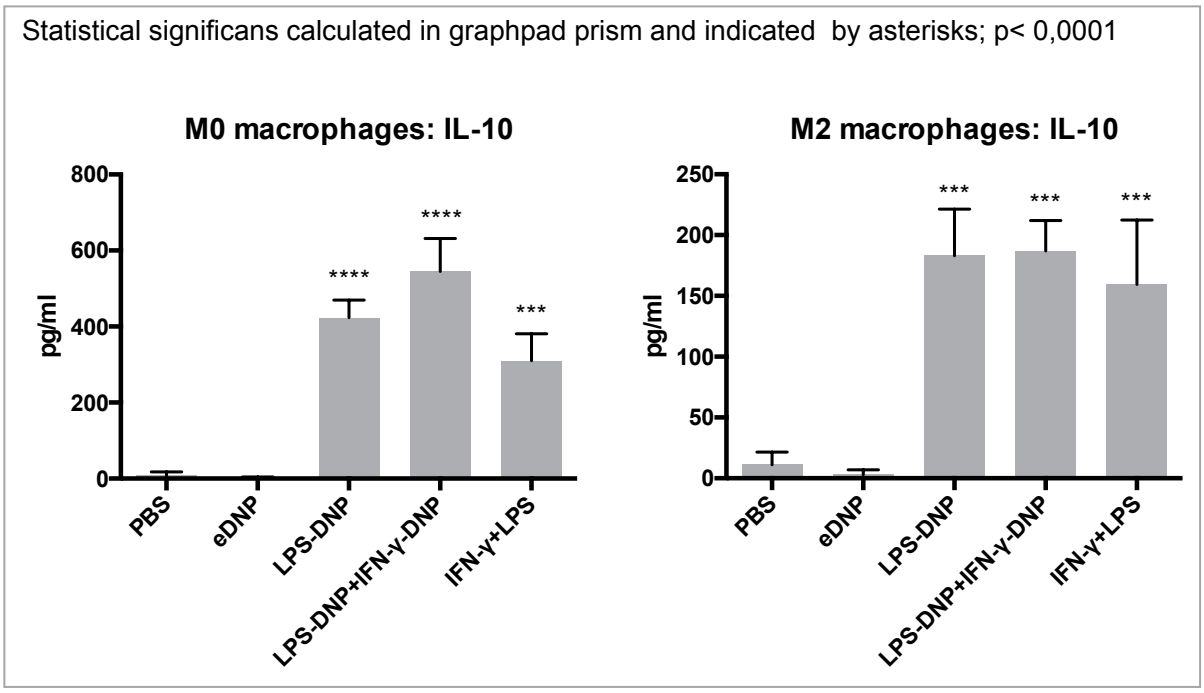

Figure **23**: IL10- ELISA of cell culture supernatant

The bone marrow derived macrophages from C57BL/6 mice were treated with IFN-γ, LPS, empty DNP, LPS-DNP and IFN-γ-DNP in triplets for 48h. M2-polarization was achieved with IL-4/IL-13 treatment for 24 h. Afterwards an ELISA was performed as described to quantify IL-10 in the cell culture supernatant. To proof statistical significance one-way ANOVA and Dunnett's multiple comparisons test with PBS as reference group was performed in graphpad prism. Significance is indicated by asterisks (p< 0,0001= ****). Treatment with LPS loaded nanoparticles, as well as the combination of IFN- γ and LPS and LPS-DNP and IFN-γ –DNP treatment increase the production of IL-10. Abbreviations see Figure 22.

In vivo studies

Healthy mice

a) *Changes of biometric data after intravenous injection of interferon-γ loaded dextran-based nanoparticles in healthy C57BL/6 mice*

Five C57BL/6 healthy mice aged 10 weeks were treated with a retroorbital injection of 200µl PEG-IFN-γ-DNP (200µg carrying 200ng IFN-γ) at 0 and 24 hours. The DNPs were prepared with attached PEG-chains (2 kDa) as described above.
The control group was treated with 200 µl PBS containing 10µg/ml IFN-γ (dose: 2 µg IFN-γ per animal per injection). After 48 h and sacrifice by cervical dislocation body weight, liver weight and liver/body weight ratios were compared showing no significant differences between the two groups (Fig. 24).

n = 5 mice per group (age: 10 weeks)

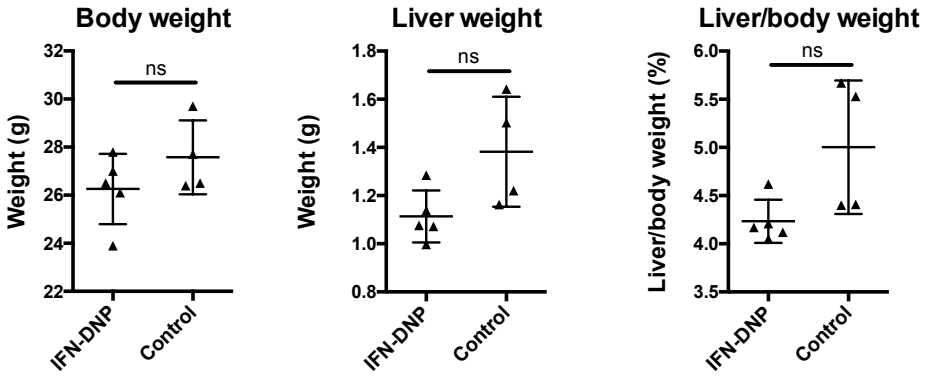

Control: 200 µl PBS containing 10 µg/ml interferon-γ (dose: 2 µg interferon-γ per animal per injection)

Treatment: 200 µl PEGylated interferon-γ loaded DNP (200 µg DNP carrying 200 ng interferon-γ)

Figure **24**: Biometric data after intravenous injection of Interferon-γ loaded dextran-based nanoparticles in healthy C57BL/6 mice

The experimental setup were five C57BL/6 wild type mice per group (age: 10 weeks). They were treated with retroorbital injection of 200 µl PEG-IFN-γ-DNP (200 µg carrying 200 ng IFN-γ) at 0 and 24 hours. The sacrifice by cervical dislocation and organ harvest were performed after 48 hours. The control group was treated with 200 µl PBS containing 10 µg/ml IFN-γ (dose: 2 µg IFN-γ per animal per injection). Biometric data (liver weight, liver to body weight ratio) were recorded and analysed. One mouse in the control group died during the experiment. IFN-γ: Interferon-γ; IFN-DNP/ IFN-γ-DNP: Interferon-γ loaded dextran-based nanoparticles; ns: not significant.

b) *Characterisation of liver tissue macrophage populations after intravenous injection of interferon-γ loaded dextran-based nanoparticles in healthy C57BL/6 mice via real-time quantitative PCR*

Following organ harvest and liver tissue preparation, RNA was purified using the Rneasy® Plus Mini Kit (50) (QIAGEN, USA), and qPCR was performed as described. Statistical significance was calculated by unpaired t-tests with healthy livers of C57BL/6 mice as reference group. Eight commonly used M1 and M2 markers were analysed to characterize the liver tissue macrophage population after intravenous injection of IFN-γ-DNP in healthy C57BL/6 mice by relative quantification of gene expression by qPCR. *Tnfa*, *cd38*, *ly6c* to indicate a pro-inflammatory M1 phenotype and *arg1*, *egr2*, *mrc1* and *tgfb1* to show polarization towards M2 direction, and *cd68* as pan-macrophage marker, none of them show a significant difference between both groups (Fig. 25).
The results show neither toxic effects of DNP carrying IFN-γ compared to IFN-γ injection nor a change in biometric data or qPCR regarding a change in polarization of the tissue macrophage population (Fig. 24, 25).

Fold change relative to healthy livers; IFN-DNP: n=5; Control: n=4; Age: 10 weeks

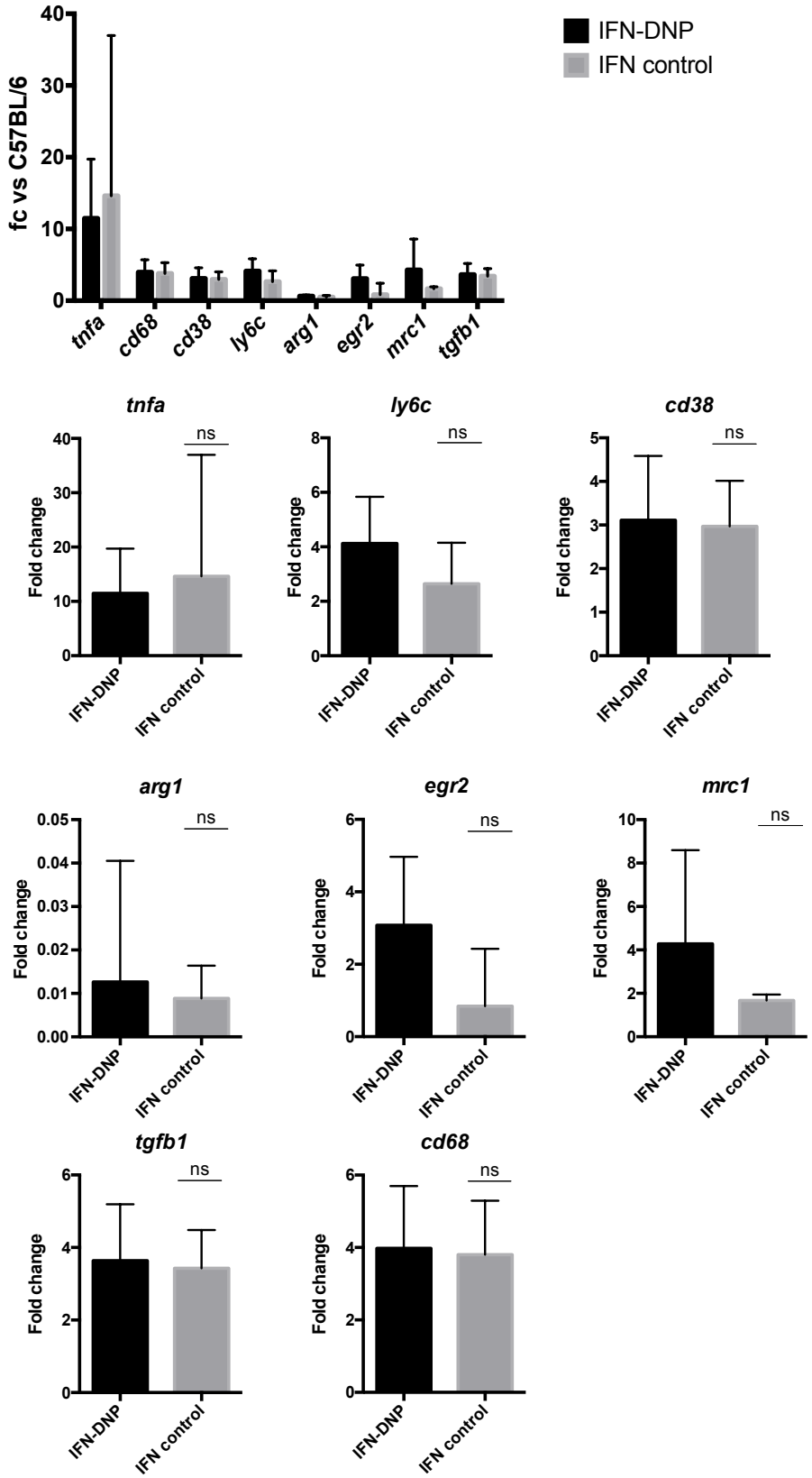

Figure **25**: Characterisation of liver tissue macrophage populations after intravenous injection of interferon-γ loaded dextran-based nanoparticles in healthy C57BL/6 mice via relative quantification of gene expression.

QPCR data of liver tissue from five C57BL/6 mice per group (age: 10 weeks). The mice were treated with retroorbital injection of 200 µl PEG-IFN-γ-DNP (200 µg carrying 200 ng IFN-γ) at 0 and 24 hours. The sacrifice by cervical dislocation and organ harvest were performed after 48 hours. The control group was treated with 200 µl PBS containing 10 µg/ml IFN-γ (dose: 2 µg IFN-γ per animal per injection. Afterwards qPCR was performed as described. Statistical significance was calculated by unpaired t-tests with healthy livers of C57BL/6 as reference group. IFN-γ: Interferon-γ; IFN-DNP/ IFN-γ-DNP: Interferon-γ loaded dextran-based nanoparticles; *tnfa*: Tumour necrosis factor α; *cd38*: Cluster of Differentiation 38; *mrc1*: Mannose receptor; *ly6c*: Lymphocyte antigen 6 complex; *cd68*: Cluster of Differentiation 68; *egr2*: Early growth response protein; *tgfb1*: transforming growth factor β1; ns: not significant.

Mice with B16F10 liver metastasis

a) *Biometric data after intravenous injection of of interferon-γ loaded dextran-based nanoparticles in C57BL/6 mice with B16F10 liver metastasis*

To investigate a potential therapeutic effect on C57BL/6 mice with B16F10 melanoma cell liver metastasis, a previously established metastasis model was employed. Groups of 5 C57BL/6 mice received an intrasplenic injection of 300,000 B16F10luc (luminescence reporter transfected) cells followed by splenectomy like described by Foerster et al. (79) and Box et al. (80). The mice were then treated with retroorbital injection of 400µg PEGylated IFN-γ-DNP (carrying 400ng INF-γ in 300 µl PBS) on day 1, 3, 5, 7, 9 after splenic injection/splenectomy. The DNPs were prepared with attached PEG-chains (2 kDa) as described above. In the control group the injection was performed with 300 µl PBS containing 1.33 µg/ml interferon γ (dose: 400ng IFN-γ per animal per injection).
In the IFN-γ-DNP group two animals had to be sacrificed earlier on day 12, three were sacrificed on day 14. In the control group two animals died during the experiment before day 12, as well two animals had to be sacrificed on day 12, one animal was sacrificed on day 14. Biometric data (liver weight, liver to body weight ratio and liver metastasis) were recorded and analysed indicating no significant difference between the treatment and control group (IFN-γ) (Fig. 26).

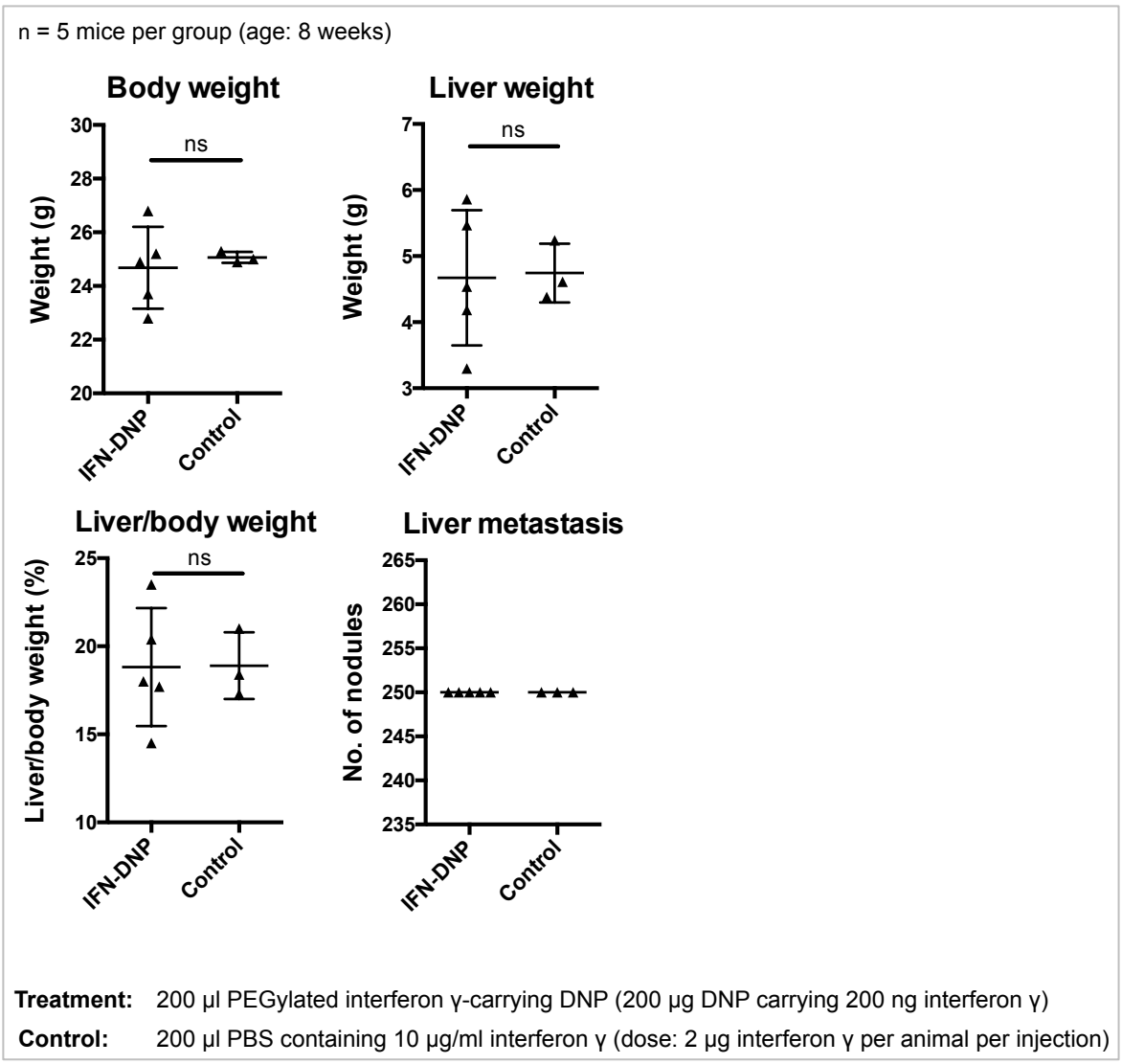

Figure **26**: Biometric data after intravenous injection of interferon-γ loaded dextran-based nanoparticles in C57BL/6 mice with B16F10 liver metastasis

C57BL/6 mice with B16F10 liver metastasis (n = 5 mice per group (age: 8 weeks)) were treated with retroorbital injection of 400 µg PEGylated IFN-γ-DNP (carrying 400ng IFN-γ in 300 µl PBS) on day 1, 3, 5, 7, 9. In the control group the injection was performed with 300 µl PBS containing 1.33 µg/ml IFN-γ (dose: 400ng IFN-γ per animal per injection). The sacrifice by cervical dislocation and organ harvest was performed on day 14. IFN-γ-DNP group: Two animals had to be sacrificed on day 12. Control group: Two animals died during the experiment before day 12, two animals had to be sacrificed on day 12. Biometric data (liver weight, liver to body weight ratio and liver metastasis) were recorded and analysed. IFN-γ: Interferon-γ; IFN-DNP/ IFN-γ-DNP: Interferon-γ loaded dextran-based nanoparticles; ns: not significant.

b) *Characterisation of liver tissue macrophage population after intravenous injection of interferon-γ loaded DNP in C57BL/6 mice with B16F10 liver metastasis by relative quantification of gene expression*

QPCR was performed and statistical significance was calculated by unpaired t-tests compared to healthy livers of C57BL/6 mice as reference group. There was no

significant difference in M1 and M2 specific macrophage markers between the analysed liver tissues (Fig. 27).

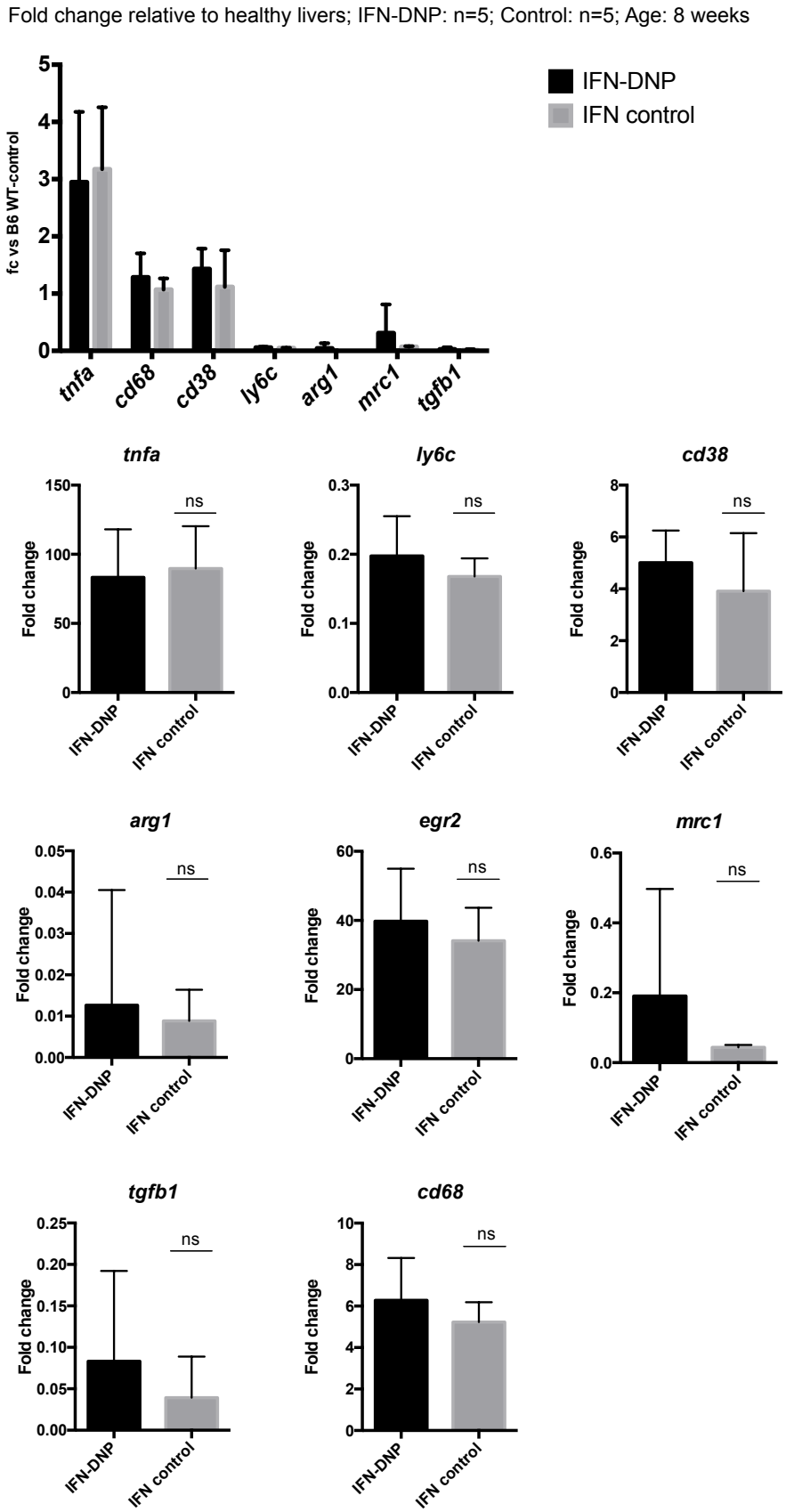

Figure **27**: Characterisation of liver tissue macrophage population after intravenous injection of interferon-γ loaded DNP in C57BL/6 mice with B16F10 liver metastasis by relative quantification of gene expression

QPCR data of C57BL/6 mice with B16F10 liver metastasis (n = 5 mice per group (age: 8 weeks)) treated with retroorbital injection of 400 µg PEGylated IFN-γ-DNP (carrying 400 ng INF-γ in 300 µl PBS) on day 1, 3, 5, 7, 9. In the control group, the injection was done with 300 µl PBS containing 1.33 µg/ml FN-γ (dose: 400 ng interferon γ per animal per injection). The sacrifice by cervical dislocation and organ harvest was performed on day 14. IFN-DNP group: Two animals had to be sacrificed on day 12; Control group: Two animals died during experiment, Two animals had to be sacrificed on day 12. QPCR was performed as described, and statistical significance was calculated by unpaired t-tests with healthy livers of C57BL/6 mice as reference group. IFN-γ: Interferon-γ; IFN-DNP: IFN-γ-DNP: Interferon-γ loaded dextran-based nanoparticles; *tnfa*: Tumour necrosis factor α; *cd38*: Cluster of Differentiation 38; *mrc1*: Mannose receptor; *ly6c*: Lymphocyte antigen 6 complex; *cd68*: Cluster of Differentiation 68; *egr2*: Early growth response protein; *tgfb1*: transforming growth factor β1; ns: not significant.

c) *Differentiation of macrophage subtypes after intravenous injection of interferon-γ loaded dextran nanoparticles in C57BL/6 mice with B16F10 liver metastasis by Fluorescence Activated Cell Sorting*

FACS was performed to count and sort the CD206 positive macrophages representing alternatively activated macrophages, as well as Ly6c-high macrophages, representing classically activated macrophages. To prove statistical significance, one-way ANOVA and Dunnett's multiple comparisons test with PBS as reference group were performed. The FACS analysis did not show any significant difference between the treatment and the control group (Fig. 28).
In conclusion, PEGylated IFN-γ loaded DNP did not inhibit growth of B16F10 liver metastases and did not polarize liver macrophages towards M1 in healthy and metastatic murine livers in vivo.

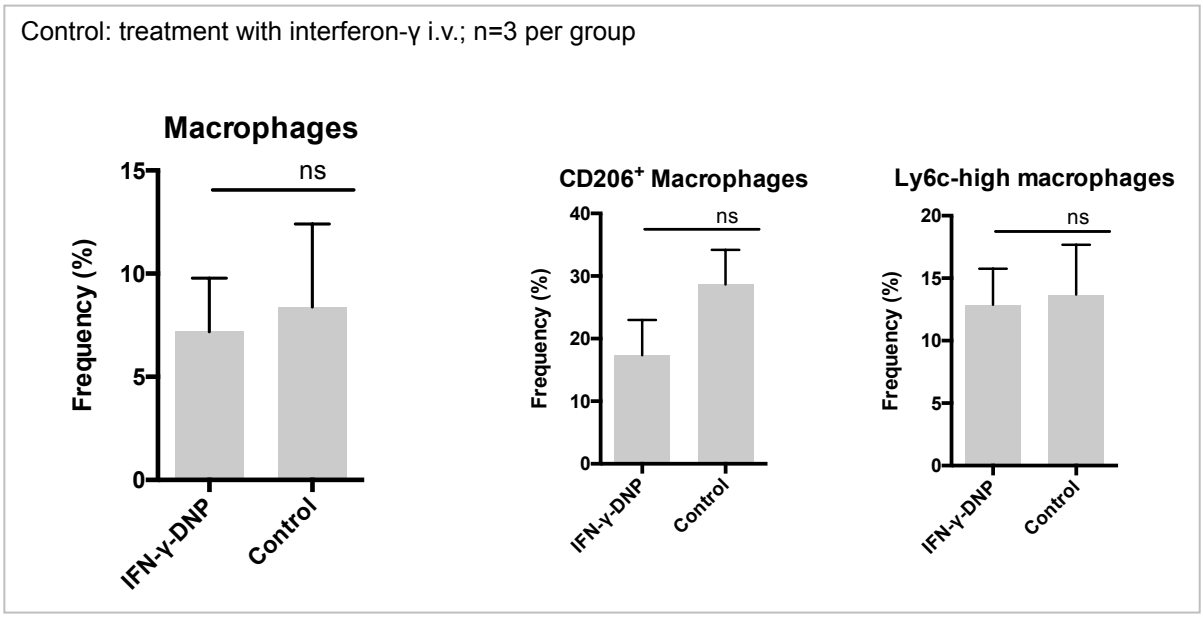

Figure **28**: Fluorescence Activated Cell Sorting of murine liver macrophages after intravenous injection of interferon γ-carrying DNP in C57BL/6 mice with B16F10 liver metastasis

FACS Analysis was performed after organ harvest and liver preparation as described above, counting the CD206, positive macrophages representing alternatively activated

macrophages, as well as Ly6c-high macrophages, representing classically activated macrophages. To proof statistical significance one-way ANOVA and Dunnett's multiple comparisons test with PBS as reference group was performed in graphpad prism. Previously C57BL/6 mice with B16F10 liver metastasis were treated with retroorbital injection of 400µg PEGylated IFN-γ-DNP (carrying 400ng IFN-γ in 300 µl PBS) on day 1, 3, 5, 7, 9. In the control group the injection was performed with 300 µl PBS containing 1.33 µg/ml IFN-γ (dose: 400 ng IFN-γ per animal per injection). The sacrifice by cervical dislocation and organ harvest was performed on day 14. IFN-γ-DNP group: 2 animals had to be sacrificed on day 12; Control group: 2 animals died during experiment, 2 animals had to be sacrificed on day 12. IFN-γ: Interferon-γ; IFN-DNP/ IFN-γ-DNP: Interferon-γ loaded dextran-based nanoparticles; ns: not significant.

V. DISCUSSION

Interferon-γ alone fails to polarize and repolarize bone marrow derived macrophages

TAMs cause a tumour promoting type ‘inflammation’ in the tumour microenvironment (8) by reciprocal interactions with cancer cells, promoting primary tumour growth, metastasis and suppressing anti-tumour immune responses (17). In previous studies INF-γ could reverse immunosuppressive and pro-tumour properties of TAMs (73) representing a promising therapeutic approach. My first cell culture experiment using Q-PCR as readout confirmed that IFN-γ and LPS are suitable to polarize and repolarize macrophages towards an anti-cancer M1 phenotype. Thus, LPS and IFN-γ in combination with LPS induced a significant increase of the M1 specific marker genes TNFα, IL-6 and CD38 in unpolarized and in M2-polarized macrophages and a significant decrease of the M2 specific marker genes Mrc1 (CD206) in unpolarized (M0), and of Egr2 in M2 polarized macrophages. The treatment with IFN-γ alone had no effect on macrophage polarization. This result seems to contradict several studies showing polarization and repolarization of macrophages by a single INF-γ treatment. However, some of those used costimulation with the toll-like receptor (TLR)-4 agonist LPS (73) or were early studies, which cannot be interpreted without limitations (84), because they usually employed peritoneal macrophages (42, 85) or IFN-γ with possible residual LPS. Nevertheless, as described in previous studies, the combination of LPS and IFN-γ led to a clear M1-type polarization, possibly due to the above-mentioned priming ability of IFN-γ to work as an activator of a yet insufficient subset of pro- inflammatory genes (69, 86, 87) which is then complemented and enhanced by TLR mediated signalling.

PEGylated interferon-γ-loaded dextran-nanoparticles polarized bone marrow derived macrophages towards and M1-phenotype only in combination with LPS

The findings from the first experiment continued while testing PEGylated (attached PEG-chains (2 kDa)) IFN-γ-DNP.

The result of previous studies that IFN-γ-DNPs are in principle suitable and nontoxic as a drug carrier for the polarization of macrophages (75) could be demonstrated by the resazurin assay, as well as by sufficient phagocytosis of the dye-labelled DNPs. It was noticeable that the intracellular fluorescence intensity, indicating efficient cellular uptake, increased after uptake of empty and INF-γ-loaded pegylated DNPs, but not after incubation with pegylated LPS-DNPs. The likely reason is impeded phagocytosis due to the bulky PEG-groups decorating the DNPs, also increasing hydrophilicity due to OH-groups.

Testing against empty DNPs the treatment with INF-γ-DNPs plus LPS, the combination of IFN-γ and LPS and the combination of LPS-DNP and INF-γ-DNP induced an increase in *tnfa, cd38 and mhcII* transcripts in unpolarized macrophages. In M2 polarized macrophages INF-γ-DNP treatment combined with LPS loaded DNPs led to a similar significant upregulation of the M1 marker genes. Furthermore, INF-γ-DNPs combined with LPS increased TNFα protein expression. By comparing

nanoparticle treatment with LPS-DNPs combined with IFN-γ-DNPs, to IFN-γ + LPS as reference treatment, a significant increase of M1 specific markers such as TNFα could be observed. As described in the previous section, INF-γ-DNPs as well as INF-γ alone required a costimulation with LPS (69, 86, 87). DNP-encapsulated cytokines lead to a significantly higher increase in M1 specific markers, possibly due to an improved phagocytotic uptake. This is in line with previous studies on nanoparticles and especially on dextran nanoparticles as shown in an earlier study of our institute (75), but could not yet be shown for INF-γ-DNPs in particular. Furthermore INF-γ-DNPs could have a positive effect on metabolic activity because of dextran serving as an additional source of energy (69). Nonetheless single empty nanoparticle treatment, as mentioned above, did not induce a polarizing effect, while the combination of DNPs with cytokines (LPS) wars effective.
The increase of *il10* and *mrc1* transcripts in unpolarized M0 macrophages treated with INF-γ-DNP and LPS-DNP in comparison to the PBS group (heatmap) were not expected. Since increased *mrc1* was not found in the group of M2 polarized macrophages, and also not in comparison to empty DNPs, it is contrary to other results, which showed a reduction in the marker gene. One assumption would be that contamination of the sample had occurred, resulting in upregulation of mannose receptor (Mrc1, CD206) expression (88, 89). Another possibility would be that the phagocytosis initiated by the treatment leads to increased Mrc1 production, but this would contradict the results of the other experiments and the existing literature and therefore seems unlikely (51). The results of the IL-10 ELISA also showed increased amounts of IL-10 after INF-γ-DNP and LPS-DNP treatment. One possible explanation is that M1 macrophages produce IL-10 in the early stages of inflammation as a negative feedback loop to dampen uncontrolled inflammation (90) (see next subchapter).
The results of two additional cell culture experiments analysed by Taqman real-time QPCR indicate a significant increase in *tnfα*, *cd38*, *mhc2*, *inos and ly6c* for the combination of IFN-γ-DNPs and LPS, the combination of IFN-γ-DNPs and LPS-DNP, as well as a decrease of the M2-specific marker *mrc1*. In both experiments comparing native and polarized macrophages, polarized M2 macrophages appear to be more responsive to treatment. To date, hardly any studies are available to compare these findings. In the literature, M2 polarization of human macrophages has been found to promote internalization of silica nanoparticles (91). However, Foerster et al. published that the polarization of macrophages does not impair the uptake of PEGylated DNP (75). Nevertheless, an increased sensitivity of macrophages to environmental signals caused by polarization is conceivable. Besides this observation, the current experiments do not allow a precise analysis. A separate series of experiments would have to be carried out for this purpose.

PEGylated interferon-γ loaded dextran-based nanoparticles in combination with LPS trigger proinflammatory cytokine production

Analysis of the supernatants through ELISA of M2 macrophages treated with IFN-γ-DNP and IFN-γ only in combination with LPS, or LPS-DNPs vs LPS with empty

DNPs led to a significant production of TNFα. That IFN-γ-DNPs and IFN-γ alone were not able to switch the macrophages towards proinflammatory cytokine (TNFα) production was expected considering previous work (69, 73) that showed that IFN-γ only primes proinflammatory genes needed complementation by LPS. This was confirmed by mRNA analysis of marker gens by Q-PCR. Since TNFα is a cytokine that has been associated with tumour regression in cancer treatment (92) and which is produced by activated macrophages (93), it seems to be a suitable indicator of tumoridical activity, and LPS activation is a powerful component to induce TNFα production (94).
Interestingly, BMDM (M0 and M2 type) stimulated with LPS-DNPs, as well as the combination of IFN-γ, and LPS and LPS-DNPs and IFN-γ-DNPs, showed an increased production of IL-10. At first glance, this was a surprising result, because IL-10 is frequently used as a marker for M2 polarization. However, as shortly mentioned above, there is evidence that in early state of inflammation M1 macrophages produce IL-10, to protect the host against an uncontrolled immune response. More specifically, IL-10 is required to supress excess inflammation, and M2 macrophages and a subset of macrophages stimulated through Fc receptors produce high amounts of IL-10 (90, 95, 96). Moreover, IL-10 makes macrophages more sensitive to IL-4 and IL-13, finally bringing them closer to a M2 phenotype (90, 95, 96). How far this plays a role in tumour progression or generally fits in this theory remains to be a critically asked question.

PEGylated interferon-γ loaded dextran nanoparticles could change macrophages to a MHCII^{high} and CD206^{low} phenotype

Further characterisation via FACS showed an increased amount of classically activated macrophages indicated by a high MHCII expression and a decrease of CD206 expression after treatment with IFN-γ-DNPs and LPS-DNPs, as well as with the combination of IFN-γ and LPS. Interestingly IFN-γ-DNPs could change macrophages to a proinflammatory phenotype (MHCII^{high}, CD206^{low}), while IFN-γ treatment alone did not lead to a significant increase of MHCII but to a decrease of CD206. A lower level of CD206 positive macrophages is associated with controlled tumour growth of the B16F10 melanoma cell line (97).
An increased *mhc2* transcription could always be shown after combined treatment with IFN-γ-DNP or IFN-γ and LPS-DNP, as well as with IFN-γ and LPS. From this finding it can be concluded that solitary IFN-γ-DNPs are able to enhance MHCII and to reduce CD206 expression. For enhanced M1 specific *inos* transcription additional LPS stimulation appears to be necessary (97, 98). Whether the enhanced MHCII and reduced CD206 expression with IFN-γ-DNPs and as assessed by FACS, indicates that protein translation often does not correlate with transcript levels, especially when studies time windows are limited (87).
An additional analysis comparing the treated group against empty dextran-nanoparticles showed the same results, excluding a polarization effect by empty DNPs. Considering the positive polarization effect of LPS and LPS-DNPs alone and

in combination with IFN-γ-DNP, as well as IFN-γ, warrants further research on these agents.

Reverse transcription quantitative real-time PCR

As described above qPCR with SYBR-Green expression is a commonly used technology for fast and specific data acquisition regarding gene expression. However, multiple steps are necessary, bearing possible sources of error, like contamination with genomic DNA. The highly recommend DNAse digestion prior to cDNA synthesis is often performed as a routine step in qPCR experiments especially if primers are used that do not distinguish between genomic DNA and cDNA (99). In the experiments performed with the more specific Taqman PCR the previous results of SYBR-Green method could be confirmed as reliable, giving precise results due to high specificity. The literature recommends to optimize and cofirm the SYBR-Green PCR by Taqman PCR (100). This could only be partially proven by the experiments carried out, as some primers only led to a result using the Taqman PCR. However there may still be room for improvement in the quality of the qPCR analysis performed. Overall, comparable results were confirmed by the other methods, including Taqman PCR, FACS, and ELISA.
Even with an optimized qPCR a critical check of the used markers is necessary, since research in the field of macrophage characterization by amplification of marker genes is not certain enough. Thus, common markers like IL-6, Arg-1, SOCS2, Tgfb1 and Fizz1 (51) did not yield reliable results in all experiments. Taken together, optimized SYBR-Green qPCR is a useful method to analyse transcript levels, especially when performed with suitable primer sets and confirmed by Taqman PCR (100-102), but requires confirmation by protein-based methods like ELISA, Western blot and FACS

Attempt to explain the lack of effect of PEGylated interferon-γ loaded dextran nanoparticles in vivo

The *in vivo* results showed neither toxic effects of DNPs carrying IFN-γ compared to systemic IFN-γ injection nor a change in biometric data of healthy mice and mice with B16F10 liver metastases. Unfortunately, the in vivo study showed no change in the burden of melanoma metastatic to the liver, nor significant differences in M1 and M2 specific macrophage markers of the liver tissue, as determined by QPCR. Likewise, the FACS analysis for CD206 and Ly6c expression could not detect any significant difference of $CD206^{high}$ macrophages representing alternatively activated macrophages, as well as $Ly6c^{high}$ macrophages, representing classically activated macrophages between the treatment and the control group.
In conclusion IFN-γ-DNP did not inhibit growth of B16F10 liver metastases and did not polarize liver macrophages towards M1 in healthy and metastatic murine livers. However, as has been shown in prior studies, nanoparticles can be highly effective to deliver therapeutics especially to the liver (71). The performed cell culture experiments suggested that IFN-γ-DNPs alone are not potent enough to lead to proinflammatory gene expression but need coactivation through LPS, while IFN-γ-

DNPs could achieve a MHCII^{high}, CD206^{low} phenotype in vitro. Hence the first suggestion is that IFN-γ-DNP fail because of low therapeutic potential and lack of coactivation through LPS. Moreover, macrophages in vivo are under the influence of numerous simultaneous stimuli, so that it does not seem possible to induce a definitive tumour relevant phenotype in vitro. However, there are several ex vivo clinical studies that can connect changes in tumour macrophage polarization and clinical outcome (39, 40, (103, 104). Here, IFN-γ mediated changes of the tumour microenvironment appear to be a critical factor in clinical outcome of patients with melanoma that were treated with programmed death-1-directed (PD-1-directed) immune checkpoint blockade (103). Therefore, despite solitary treatment with IFN-γ-DNPs had no direct therapeutic effect, the additional activation of IFN-γ induced genes by IFN-γ-DNPs could improve the therapeutic outcome when combined with established therapies. In some studies B16 melanoma metastasis as a tumour model was seen critically, since M1 macrophages and Th1 helper cells play a minor role in defending against this low immunogenicity cancer (79).

Mouse model

The work of Foerster et al suggested that Balb/c mice produced a higher number of CD8+ CTLs, Ly6c monocyte-macrophages, representing Th1-cell activation and M1 macrophage polarization, compared to C57BL/6 mice after inducing melanoma metastasis (79). This was unexpected, since C57BL/6 mice show a more pronounced Th1/M1 phenotype (105-107), while Balb/c mice a rather Th2/M2 phenotype (46). In this work in the in vitro experiments BMDM from C57BL/6 mice were used and over all there was sufficient reliable data to compare both mouse strains, so further research is needed to clarify this issue. Last but not least the relatively low number of mice per group may likely have contributed to the lack of significance of the results.

Conclusion

In the experiments performed, dextran nanoparticles proved to be suitable drug carriers for addressing macrophages, as they are not toxic *in vitro* and *in vivo,* and as they are well phagocytosed by macrophages. Analysis by qPCR indicates that despite different assumptions IFN-γ-DNPs alone do not induce polarization/repolarization of tumour associated macrophages to an M1 phenotype *in vitro*, but require LPS as an additional stimulus. Certain studies suggested that priming of regulatory elements of gene transcription by IFN-γ alone does not necessarily lead to a significantly enhanced pro-inflammatory gene transcription, but only primes macrophages for inflammatory immune response after TLR stimulation, such as through LPS and TLR-4 (69, 86). The increased production of TNFα, measured by ELISA, could also only be achieved by IFN-γ-DNPs combined with LPS treatment. As assessed by FACS analysis of BMDM, IFN-γ-DNP treatment induces an M1 phenotype characterized by increased MHCII and decreased CD206 expression, suggesting that IFN-γ-DNPs, despite in part qPCR results to the contrary, exerted a partial polarizing effect. However, to what extent this affects M1

specific macrophage functions could not be conclusively clarified in the present study, and would require additional functional studies, such as cocultures with CD8+ T cells and melanoma cells. With regard to the effect of IFN-γ-DNPs on gene expression, it is reasonable to assume that there are still undiscovered interactions between different signalling pathways in which negative feedback and feedforward loops are involved. In addition the complexity of macrophage characterisation due to the many different subtypes and their plasticity makes it difficult to define functional properties in simple polarization assays in vitro. In this study especially *tnfa*, *cd38*, *mhc2*, *inos* and *ly6c* were confirmed as M1 marker genes and *egr2* and *mrc1 /cd206* as M2 marker genes. There is potential to improve the characterization of macrophages by qPCR or Taqman PCR for additional marker genes.
Although IFN-γ-DNPs were able to generate a MHCII ^{high} CD206 ^{low} phenotype *in vitro*, as detected by FACS, no therapeutic effect was observed *in vivo*. IFN-γ-DNPs did not inhibit growth of B16F10 liver metastases and did not polarize liver macrophages towards M1 in healthy and metastatic murine livers. However, it has been shown in prior studies that IFN-γ alone can change tumour macrophage polarization and clinical outcome (39, 40, (103, 104). Thus, it may well be possible that IFN-γ alone may have a more pronounced anti-cancer effect in tumour models other than the highly aggressive murine B16F10 melanoma that has low immunogenicity. On the basis of the observed findings, further research could investigate the potential therapeutic effect of PEGylated LPS-DNP especially in combination with IFN-γ-DNPs in combination with e.g. classical chemotherapy *in vitro* and *in vivo*.

VI. SUMMARY

The immune system, comprising cellular and humoral elements, is crucial in both malignancy progression and regression. Macrophage progenitors develop in the bone marrow and differentiate into various subtypes with diverse target tissues and functions. In the context of malignant tumours, two major subclasses are distinguished: TAMs (Tumour associated macrophages), which resemble the M2 phenotype and tumouricidal proinflammatory M1 macrophages. TAMs contribute to tumour-promoting immunosuppression and vascularization in the tumour microenvironment. This negatively affects primary tumour growth, metastasis, and therapy response. Regarding macrophage differentiation, interferon-γ (IFN-γ) is a potent cytokine to support M1 polarization and is relevant to immunological tumour defence. Nanoparticles can serve as carriers to reduce the side effects of cytokine therapy by enhancing the uptake of the active substance in the target tissue, while sparing unrelated tissues. Dextran nanoparticles (DNPs) are taken up by macrophages *in vitro* without any toxic impact. *In vivo*, DNP accumulate mainly in the liver, where they are prominently taken up by macrophages.

Until now, the efficacy of interferon-γ (IFN-γ) loaded DNPs to induce M1-type polarization/repolarization of TAMs *in vitro* and a possible therapeutic effect *in vivo* has not been studied. The aim of this thesis was to study if IFN-γ-DNP affect the polarization of bone marrow derived macrophages of Balb/c and C57BL/6 mice *in vitro* and whether they have a positive therapeutic effect in a melanoma metastasis model *in vivo*.

Toxicity of IFN-γ-DNP was excluded in *in vitro* experiments with primary macrophages derived from wild-type mice. Using quantitative real-time polymerase chain reaction (qPCR), the genetic profiles of native and *in vitro* M2 differentiated macrophages subsequently treated with IFN-γ and IFN-γ-DNP were analysed. Despite different assumptions, both IFN-γ and IFN-γ-DNP required costimulation with lipopolysaccharide (LPS) to significantly increased the expression of tumour necrosis factor α (*tnfa*), cluster of differentiation 38 (*cd38*), class II major histocompatibility complex molecules (*mhc2*),inducible nitric oxide synthase (*inos*) and lymphocyte antigen 6 complex (*ly6c*), all M1 marker genes, and upregulated the expression of early growth response protein (*egr2*) and mannose receptor, cluster of differentiation 206 (*cd206*/*mrc1*), both M2 marker genes. Macrophages treated with IFN-γ-DNP and LPS-loaded dextran nanoparticles (LPS-DNP) transcribed significantly more mRNA of specific M1 marker genes and reduced the expression of M2-specific genes compared to macrophages treated with IFN-γ and LPS alone. Therefore, it may be concluded that IFN-γ (IFN-γ-DNP) and LPS have a synergistic effect towards M1-type polarization due to the priming ability of IFN-γ. This effect could be increased with enhanced delivery and uptake of IFN-γ loaded into DNP. Furthermore, an increased metabolic activity due to dextran as an additional source of energy may also contribute. However, empty DNP (eDNP) alone had no polarizing effect. Single IFN-γ-DNP treatment induced an M1 phenotype also as characterized by fluorescence-activated cell sorting (FACS)-analysis showed an

increased MHCII and decreased CD206 expression. In contrast, coactivation with LPS was required to detect a significant change in the mRNA expression of *mhc2* and *mrc1* by qPCR.
In addition, the combination of IFN-γ-DNP and LPS, LPS as well as LPS-DNP, led to an increased tumour necrosis factor α (TNFα) production, as determined by enzyme-linked immunosorbent assay (ELISA), while the increased interleukin-10 (previous described as M2-type marker) content in the cell culture supernatant can presumably be explained by an increased production of this cytokine that can occur initially during M1 macrophage polarization.
The DNPs were successfully tested for tolerability in a mouse (C57BL/6) model of liver metastasis using B16F10 melanoma cells. Although IFN-γ-DNPs generated a MHCII ^{high} CD206 ^{low} phenotype *in vitro*, as detected by FACS, no therapeutic effect was observed *in vivo*. Treatment with IFN-γ-DNP was neither able to inhibit the growth of liver metastases nor to induce a polarization of macrophages/TAMs in vivo towards a tumouricidal M1 type in healthy or metastatic livers.
Based on the observed results, further research may investigate the potential therapeutic effect of longer lived and shielded PEGylated LPS-DNP, especially combined with IFN-γ-DNP, *in vitro* and *in vivo*.
In conclusion, although IFN-γ-DNP alone did not have a therapeutic anti-tumour effect *in vivo*, IFN-γ-DNP, particularly in combination with LPS, demonstrated promising results in polarizing and repolarizing bone marrow-derived macrophages to a tumouricidal phenotype *in vitro*.

VII. ZUSAMMENFASSUNG

Das Immunsystem, bestehend aus humoralen und zellulären Komponenten, spielt eine entscheidende Rolle, sowohl bezüglich des Progresses, als auch des Regresses maligner Tumore. Im Hinblick auf die an der Tumorabwehr beteiligten Immunzellen nehmen Makrophagen eine zentrale Stellung ein. Die Progenitorzellen der Makrophagen entstehen im Knochenmark und zirkulieren in der Blutbahn, bis sie anschließend in die verschiedenen Zielgewebe wandern, um sich dort zu spezialisierten Gewebsmakrophagen zu differenzieren. Im Kontext von bösartigen Tumoren unterscheidet man zwei große Subklassen: Zum einen Tumormakrophagen (TAM: tumor associated macrophages), welche dem M2 Phänotyp ähnlich sind, zum anderen proinflammatorische M1 Makrophagen, die das Tumorwachstum hemmen. TAMs begünstigen entscheidend die tumorfördernde Immunsuppression und Vaskularisierung im Tumormikromillieus, was das primäre Tumorwachstum, die Metastasierung und die Therapieantwort negativ beeinflusst. Die Differenzierung der Makrophagen wird maßgeblich durch das sie umgebende Milieu und die darin enthaltenen Zytokine beeinflusst. Interferon-γ (IFN-γ) ist ein potentes Zytokin, das eine M1 Polarisierung fördert und damit relevant für die immunologische Tumorabwehr ist. Nanopartikel als Transportmedium können die Nebenwirkungen der Zytokintherapie minimieren, indem sie die Aufnahme des Wirkstoffs im Zielgewebe maximieren, während unbeteiligte Gewebe umgangen werden. Es konnte gezeigt werden, dass dextranbasierte Nanopartikel von Makrophagen *in vitro* ohne jegliche toxische Wirkung aufgenommen werden und sich *in vivo* vor allem in der Leber anreichern, wo sie ebenfalls hauptsächlich von Makrophagen aufgenommen werden.
Die Effektivität IFN-γ-beladener dextranbasierter Nanopartikel (IFN-γ-DNP) eine M1-Typ Polarisierung/Repolarisierung tumorassoziierter Makrophagen *in vitro* zu induzieren, als auch *in vivo* einen möglichen therapeutischen Effekt zu erzielen wurde bisher nicht untersucht. Ziel dieser Arbeit war es, zu untersuchen, ob IFN-γ-DNP die Polarisierung von Makrophagen aus dem Knochenmark von Balb/c- und C57BL/6-Mäusen *in vitro* beeinflussen und ob sie in einem Melanom-Metastasierungs-Modell *in vivo* eine positive therapeutische Wirkung haben.
IFN-γ-DNP zeigten *in vitro* keinen toxischen Effekt gegenüber Makrophagen, die aus dem Knochenmark von Wildtyp-Mäusen extrahiert und kultiviert wurden. Mittels quantitativer Echtzeit-Polymerase-Kettenreaktion (qPCR) wurden die genetischen Profile der nativen und *in vitro* alternativ (M2) differenzierten und anschließend mit IFN-γ und IFN-γ-DNP behandelten Makrophagen untersucht. Entgegen der Erwartung transkribierten mit IFN-γ und IFN-γ-DNP behandelte Makrophagen nur unter ergänzender Stimulation mit Lipopolysacchariden (LPS) im Vergleich zur Kontrollgruppe signifikant vermehrt M1 spezifischer Marker-Gene, wie den Tumornekrosefaktor α (*tnfa*), das Cluster of Differentiation 38 (*cd38*), die Moleküle des Haupthistokompatibilitätskomplexes der Klasse II (*mhc2*), die Induzierbaren Stickoxid-Synthase (*inos*) und den Lymphozyten-Antigen 6-Komplex (*ly6c*). Early Growth Response Protein (*egr2*) und Mannose-Rezeptor, Cluster of Differentiation

206 (*cd206/mrc1*), beide M2 Marker-Gene, wurde vermindert transkribiert. Makrophagen, die mit IFN-γ-DNP und LPS oder LPS tragenden Dextran-Nanopartikeln (LPS-DNP) behandelt wurden, transkribierten signifikant mehr M1 spezifische Gene als die Makrophagen der Referenzgruppe, die nur die von Kombination IFN-γ und LPS erhielten. Daraus lässt sich schließen, dass IFN-γ (IFN-γ-DNP) und LPS, möglicherweise aufgrund der Priming-Fähigkeit von IFN-γ, eine synergistische Wirkung auf die M1-Typ-Polarisierung haben. Die vermehrte Verfügbarkeit und Aufnahme von in DNP gebundenem IFN-γ, verglichen mit ungebundenem IFN-γ, könnte diese Wirkung verstärken. Außerdem scheint die Stoffwechselaktivierung durch die dextranhaltigen Nanopartikel eine Rolle zu spielen, wobei jedoch ungeladene DNP (eDNP) Makrophagen nicht polarisierten.
Die Behandlung mit IFN-γ-DNP induzierte einen M1-Phänotyp, der auch durch fluoreszenzaktivierte Zellsortierung (FACS) charakterisiert wurde - die Analyse zeigte eine erhöhte MHCII- und eine verringerte CD206-Expression. Dagegen war eine Koaktivierung mit LPS erforderlich, um eine signifikante Änderung in der Expression von *mhc2* und *mrc1* mittels qPCR nachweisen zu können. Die Kombination von IFN-γ-DNP und LPS, sowohl LPS als auch LPS-DNP, führte zu einer erhöhten Produktion von Tumornekrosefaktor α (TNFα), die mittels Enzymgekoppelter Immunadsorptionstest ((EIA) engl. Enzyme-Linked Immunosorbent Assay (ELISA)) bestimmt wurde, wohingegen der erhöhte Interleukin-10 Gehalt (vorrangehend als M2-Typ Marker beschrieben) im Zellkulturüberstand vermutlich darauf zurückzuführen, dass auch während der M1-Polarisierung initial eine vermehrte Produktion diese Zytokins auftreten kann.
Die Verträglichkeit der DNP wurde erfolgreich in einem Mausmodell (C57BL/6) für Lebermetastasen unter Verwendung von B16F10 Melanomzellen getestet. Obwohl IFN-γ-DNP *in vitro* einen Phänotypenwechsel ($MHCII^{high}$, $CD206^{low}$ induzierten, konnte *in vivo* keine therapeutische Wirkung beobachtet werden. Eine Behandlung mit IFN-γ-DNP konnte weder das Wachstum der Lebermetastasen hemmen, noch in gesunden oder Metastasen-Lebern eine Polarisierung der Makrophagen/TAM in Richtung eines tumorhemmenden M1-Typs erreichen.
Basierend auf den beobachteten Ergebnissen könnten weitere Forschungsarbeiten die potenziellen therapeutische Wirkung von langlebigerem und geschütztem PEGyliertem LPS-DNP, insbesondere in Kombination mit IFN-γ-DNP *in vitro* und *in vivo* untersuchen.
Zusammenfassend lässt sich sagen, dass IFN-γ-DNP allein zwar keine therapeutische anti-tumorale Wirkung *in vivo* hatte, dennoch IFN-γ-DNP *in vitro*, insbesondere in Kombination mit LPS, eine Polarisierung und Repolarisierung nativer und M2 differenzierter Makrophagen in Richtung eines tumorkritischen Phänotyps initiierte.

VIII. LITERATURE

1. Balkwill F, Mantovani A. Inflammation and cancer: back to Virchow? The Lancet. 2001;357(9255):539-45.

2. Mantovani A, Ponzetta A, Inforzato A, Jaillon S. Innate immunity, inflammation and tumour progression: double-edged swords. J Intern Med. 2019;285(5):524-32.

3. Sica A, Allavena P, Mantovani A. Cancer related inflammation: the macrophage connection. Cancer Lett. 2008;267(2):204-15.

4. Binnemars-Postma K, Storm G, Prakash J. Nanomedicine Strategies to Target Tumor-Associated Macrophages. Int J Mol Sci. 2017;18(5):979.

5. Mantovani A SS, Locati M, Allavena P, Sica A. Macrophage polarization: tumor-associated macrophages as a paradigm for polarized M2 mononuclear phagocytes. Trends Immunol. 2002;23(11):549-55.

6. Hanahan D, Weinberg RA. Hallmarks of cancer: the next generation. Cell. 2011;144(5):646-74.

7. Allavena P SA, Solinas G, Porta C, Mantovani A. The inflammatory micro-environment in tumor progression: the role of tumor-associated macrophages. Crit Rev Oncol Hematol. 2008;66(1):1-9.

8. Sica A, Larghi P, Mancino A, Rubino L, Porta C, Totaro MG, et al. Macrophage polarization in tumour progression. Semin Cancer Biol. 2008;18(5):349-55.

9. Murray PJ, Allen JE, Biswas SK, Fisher EA, Gilroy DW, Goerdt S, et al. Macrophage activation and polarization: nomenclature and experimental guidelines. Immunity. 2014;41(1):14-20.

10. Qian BZ, Pollard JW. Macrophage diversity enhances tumor progression and metastasis. Cell. 2010;141(1):39-51.

11. Hanahan D, Weinberg RA. The Hallmarks of Cancer. Cell. 2000;100(1):57–70.

12. Grivennikov SI, Greten FR, Karin M. Immunity, inflammation, and cancer. Cell. 2010;140(6):883-99.

13. Ferrara N. Pathways mediating VEGF-independent tumor angiogenesis. Cytokine Growth Factor Rev. 2010;21(1):21–6.

14. Birkeland SA, Storm HH, Lamm LU, Barlow L, Blohmé I, Forsberg B, et al. Cancer risk after renal transplantation in the Nordic countries, 1964-1986. Int J Cancer. 1995 Jan 17;60(2):183-9.

15. Pages F, Galon J, Dieu-Nosjean MC, Tartour E, Sautes-Fridman C, Fridman WH. Immune infiltration in human tumors: a prognostic factor that should not be ignored. Oncogene. 2010;29(8):1093-102.

16. Jakubowska K, Koda M, Kisielewski W, Kanczuga-Koda L, Famulski W. Prognostic significance of inflammatory cell response in patients with colorectal cancer. Oncol Lett. 2019;18(1):783-91.

17. Berx G, van Roy F. Involvement of members of the cadherin superfamily in cancer. Cold Spring Harb Perspect Biol. 2009;1(6):a003129.

18. Egeblad M, Ewald AJ, Askautrud HA, Truitt ML, Welm BE, Bainbridge E, et al. Visualizing stromal cell dynamics in different tumor microenvironments by spinning disk confocal microscopy. Dis Model Mech. 2008;1(2-3):155–67.

19. Wyckoff J, Wang W, Lin EY, Wang Y, Pixley F, Stanley ER, et al. A Paracrine Loop between Tumor Cells and Macrophages Is Required for Tumor Cell Migration in Mammary Tumors. Cancer Res. 2004;64(19):7022-9.

20. Hagemann T, Wilson J, Kulbe H, Li NF, Leinster DA, Charles K, et al. Macrophages induce invasiveness of epithelial cancer cells via NF-kappa B and JNK. J Immunol. 2005;175(2):1197-205.

21. Coghlin C, Murray GI. Current and emerging concepts in tumour metastasis. J Pathol. 2010;222(1):1-15.

22. Jarosz-Biej M, Smolarczyk R, Cichon T, Kulach N. Tumor Microenvironment as A "Game Changer" in Cancer Radiotherapy. Int J Mol Sci. 2019;20(13).

23. Andrade RGD, Reis B, Costas B, Lima SAC, Reis S. Modulation of Macrophages M1/M2 Polarization Using Carbohydrate-Functionalized Polymeric Nanoparticles. Polymers (Basel). 2020;13(1):1-18.

24. Andon FT DE, Maeda A, Erreni M, Mantovani A, Alonso MJ, Allavena P. Targeting tumor associated macrophages: The new challenge for nanomedicine. Semin Immunol. 2017;34(6):103-13.

25. Kaps L, Schuppan D. Targeting Cancer Associated Fibroblasts in Liver Fibrosis and Liver Cancer Using Nanocarriers. Cells. 2020;9(9):2027.

26. DeNardo DG, Ruffell B. Macrophages as regulators of tumour immunity and immunotherapy. Nat Rev Immunol. 2019;19(6):369–82.

27. Singh Y, Pawar VK, Meher JG, Raval K, Kumar A, Shrivastava R, et al. Targeting tumor associated macrophages (TAMs) via nanocarriers. J Control Release. 2017;254:92-106.

28. Lewis CE, Pollard JW. Distinct role of macrophages in different tumor microenvironments. Cancer Res. 2006;66(2):605-12.

29. Cao L, Che X, Qiu X, Li Z, Yang B, Wang S, et al. M2 macrophage infiltration into tumor islets leads to poor prognosis in non-small-cell lung cancer. Cancer Manag Res. 2019;11(1):6125-38.

30. Biswas SK, Allavena P, Mantovani A. Tumor-associated macrophages: functional diversity, clinical significance, and open questions. Semin Immunopathol. 2013;35(5):585-600.

31. Ruffell B, Coussens LM. Macrophages and therapeutic resistance in cancer. Cancer Cell. 2015;27(4):462-72.

32. Shiao SL, Ruffell B, DeNardo DG, Faddegon BA, Park CC, Coussens LM. TH2-Polarized CD4(+) T Cells and Macrophages Limit Efficacy of Radiotherapy. Cancer Immunol Res. 2015;3(5):518-25.

33. Arlauckas SP, Garris CS, Kohler RH, Kitaoka M, Cuccarese MF, Yang KS, et al. In vivo imaging reveals a tumor-associated macrophage-mediated resistance pathway in anti-PD-1 therapy. Sci Transl Med. 2017;9(389):eaal3604.

34. Ruffell B, Chang-Strachan D, Chan V, Rosenbusch A, Ho CM, Pryer N, et al. Macrophage IL-10 blocks CD8+ T cell-dependent responses to chemotherapy by suppressing IL-12 expression in intratumoral dendritic cells. Cancer Cell. 2014;26(5):623-37.

35. Le DT, Lutz E, Uram JN, Sugar EA, Onners B, Solt S, et al. Evaluation of ipilimumab in combination with allogeneic pancreatic tumor cells transfected with a GM-CSF gene in previously treated pancreatic cancer. J Immunother. 2013;36(7):382-9.

36. Zhou L, Li Y, Gao W, Huangfu H, Wen S, Zhang C, et al. Assessment of tumor-associated immune cells in laryngeal squamous cell carcinoma. J Cancer Res Clin Oncol. 2019;145(7):1761-72.

37. Yang L, Sun J, Liu Q, Zhu R, Yang Q, Hua J, et al. Synergetic Functional Nanocomposites Enhance Immunotherapy in Solid Tumors by Remodeling the Immunoenvironment. Adv Sci (Weinh). 2019;6(8):1802012.

38. Mantovani A, Marchesi F, Malesci A, Laghi L, Allavena P. Tumour-associated macrophages as treatment targets in oncology. Nat Rev Clin Oncol. 2017;14(7):399-416.

39. Zhu Y, Herndon JM, Sojka DK, Kim KW, Knolhoff BL, Zuo C, et al. Tissue-Resident Macrophages in Pancreatic Ductal Adenocarcinoma Originate from Embryonic Hematopoiesis and Promote Tumor Progression. Immunity. 2017;47(2):323-38.

40. Beatty GL, Chiorean EG, Fishman MP, Saboury B, Teitelbaum UR, Sun W, et al. CD40 Agonists Alter Tumor Stroma and Show Efficacy Against Pancreatic Carcinoma in Mice and Humans. Science. 2011;331(6024):1612-6.

41. Guerriero JL, Sotayo A, Ponichtera HE, Castrillon JA, Pourzia AL, Schad S, et al. Class IIa HDAC inhibition reduces breast tumours and metastases through anti-tumour macrophages. Nature. 2017;543(7645):428-32.

42. Nathan CF, Murray HW, Wiebe ME, Rubin BY. Identification of interferon-gamma as the lymphokine that activates human macrophage oxidative metabolism and antimicrobial activity. J Exp Med. 1983;158(3):670-89.

43. Celada A, Gray PW, Rinderknecht E, RD S. Evidence for a gamma-interferon receptor that regulates macrophage tumoricidal activity. J Exp Med. 1984 Jul 1;160(1):55-74.

44. Stein M, Keshav S, Harris N, Gordon S. Interleukin 4 potently enhances murine macrophage mannose receptor activity: a marker of alternative immunologic macrophage activation. J Exp Med. 1992;176(1):287-92.

45. Doyle AG, Herbein G, Montaner LJ, Minty AJ, Caput D, Ferrara P, et al. Interleukin-13 alters the activation state of murine macrophages in vitro: comparison with interleukin-4 and interferon-y. Eur J Immunol. 1994;24(6):1441–5.

46. Mills CD, Kincaid K, Alt JM, Heilman MJ, Hill AM. Pillars Article: M-1/M-2 Macrophages and the Th1/Th2 Paradigm. J. Immunol. 2000.164: 6166-6173. Reprinted in: J Immunol. 2017;199(7):2194-201.

47. Ying W, Cheruku PS, Bazer FW, Safe SH, Zhou B. Investigation of macrophage polarization using bone marrow derived macrophages. J Vis Exp. 2013 Jun 23(76):50323.

48. MacMicking J, Xie QW, Nathan C. Nitric oxide and macrophage function. Annual Review of Immunology. 1997;15:323-50.

49. Miao X, Leng X, Zhang Q. The Current State of Nanoparticle-Induced Macrophage Polarization and Reprogramming Research. Int J Mol Sci. 2017;18(2):336.

50. Mantovani A, Sica A, Sozzani S, Allavena P, Vecchi A, Locati M. The chemokine system in diverse forms of macrophage activation and polarization. Trends Immunol. 2004;25(12):677-86.

51. Jablonski KA, Amici SA, Webb LM, Ruiz-Rosado Jde D, Popovich PG, Partida-Sanchez S, et al. Novel Markers to Delineate Murine M1 and M2 Macrophages. PLoS One. 2015;10(12):e0145342.

52. Altin JG SE. The role of CD45 and CD45 assoiated molecules in T-cell activation. Immunology and Cell Biology. 1997;75(5):430-44.

53. Lin HH, Faunce DE, Stacey M, Terajewicz A, Nakamura T, Zhang-Hoover J, et al. The macrophage F4/80 receptor is required for the induction of antigen-specific efferent regulatory T cells in peripheral tolerance. J Exp Med. 2005;201(10):1615-25.

54. Brown JM. Vasculogenesis: a crucial player in the resistance of solid tumours to radiotherapy. Br J Radiol. 2014;87(1035):20130686.

55. NIH National Library of Medicine, The National Center for Biotechnology Information. Il6 interleukin 6 [Mus musculus (house mouse)], Gene ID: 16193

[Internet]. 2015, Last update 07-21-2020 [07-20-2020]. Available from: https://www.ncbi.nlm.nih.gov/gene/16193.

56. NIH National Library of Medicine, The National Center for Biotechnology Information. Egr2 early growth response 2 [Mus musculus (house mouse)] Gene ID: 13654 [Internet] 2020, Last update 07-31-2020 [07-31-2020]. Available from: https://www.ncbi.nlm.nih.gov/gene/13654.

57. NIH National Library of Medicine, The National Center for Biotechnology Information. Tnf tumor necrosis factor [Mus musculus (house mouse)] Gene ID: 21926 [Internet]. 2020, Last update 07-26-2020 [07-20-2020]. Available from: https://www.ncbi.nlm.nih.gov/gene/21926.

58. Mace KF, Ehrke MJ, Hori K, Maccubbin DL, Mihich E. Role of tumor necrosis factor in macrophage activation and tumoricidal activity. Cancer Res. 1988;48(19):5427-32.

59. Parameswaran N, Patial S. Tumor Necrosis Factor-α Signaling in Macrophages. Crit Rev Eukaryot Gene Expr. 2010;20(2):87–103.

60. NIH National Library of Medicine, The National Center for Biotechnology Information. Mrc1 mannose receptor, C type 1 [Mus musculus (house mouse)] Gene ID: 17533 [Internet]. 2020, Last update 07-14-2020 [07-31-2020]. Available from: https://www.ncbi.nlm.nih.gov/gene/17533.

61. NIH National Library of Medicine, The National Center for Biotechnology Information. Ly6c1 lymphocyte antigen 6 complex, locus C1 [Mus musculus (house mouse)] Gene ID: 17067 [Internet]. 2014, Last update 07-26-2020 [07-20-2020]. Available from: https://www.ncbi.nlm.nih.gov/gene/17067.

62. NIH National Library of Medicine, The National Center for Biotechnology Information. Tgfb1 transforming growth factor, beta 1 [Mus musculus (house mouse)], Gene ID: 21803 [Internet]. 2016, Last update 07-26-2020 [07-20-2020]. Available from: https://www.ncbi.nlm.nih.gov/gene/21803.

63. NIH National Library of Medicine, The National Center for Biotechnology Information. H2 histocompatibility-2, MHC [Mus musculus (house mouse)],Gene ID: 111364 [Internet]. 2020, Last update 07-14-2020 [07-20-2020]. Available from: https://www.ncbi.nlm.nih.gov/gene/111364.

64. NIH National Library of Medicine, The National Center for Biotechnology Information. Il10 interleukin 10 [Mus musculus (house mouse)], Gene ID: 16153 [Internet]. 2015, Last update 07-19-2020 [07-31-2020]. Available from: https://www.ncbi.nlm.nih.gov/gene/16153.

65. NIH National Library of Medicine, The National Center for Biotechnology Information. Nos2 nitric oxide synthase 2, inducible [Mus musculus (house mouse)] Gene ID: 18126 [Internet]. 2015, Last update 07-21-2020 [07-20-2020]. Available from: https://www.ncbi.nlm.nih.gov/gene/18126.

66. NIH National Library of Medicine, The National Center for Biotechnology Information. Arg1 arginase, liver [Mus musculus (house mouse)] Gene ID: 11846 [Internet]. 2020, Last update 07-26-2020 [07-31-2020]. Available from: https://www.ncbi.nlm.nih.gov/gene/11846.

67. Glaria E, Valledor AF. Roles of CD38 in the Immune Response to Infection. Cells. 2020;9(1):228.

68. Chistiakov DA, Killingsworth MC, Myasoedova VA, Orekhov AN, Bobryshev YV. CD68/macrosialin: not just a histochemical marker. Lab Invest. 2017;97(1):4-13.

69. Ivashkiv LB. IFNgamma: signalling, epigenetics and roles in immunity, metabolism, disease and cancer immunotherapy. Nat Rev Immunol. 2018;18(9):545-58.

70. Locati M, Curtale G, Mantovani A. Diversity, Mechanisms, and Significance of Macrophage Plasticity. Annu Rev Pathol. 2020;15:123–47.

71. Ramirez-Carrozzi VR, Nazarian AA, Li CC, Gore SL, Sridharan R, Imbalzano AN, et al. Selective and antagonistic functions of SWI/SNF and Mi-2beta nucleosome remodeling complexes during an inflammatory response. Genes Dev. 2006;20(3):282–96.

72. Foster SL, Medzhitov R. Gene-specific control of the TLR-induced inflammatory response. Clin Immunol. 2009;130(1):7-15.

73. Duluc D, Corvaisier M, Blanchard S, Catala L, Descamps P, Gamelin E, et al. Interferon-gamma reverses the immunosuppressive and protumoral properties and prevents the generation of human tumor-associated macrophages. Int J Cancer. 2009;125(2):367–73.

74. Wich PR, Fréchet JMJ. Degradable Dextran Particles for Gene Delivery Applications. Australian Journal of Chemistry. 2012;65(1):15-9.

75. Foerster F, Bamberger D, Schupp J, Weilbächer M, Kaps L, Strobl S, et al. Dextran-based therapeutic nanoparticles for hepatic drug delivery. Nanomedicine (Lond). 2016;11(20):2663–77.

76. Wang Y, Lin YX, Qiao SL, An HW, Ma Y, Qiao ZY, et al. Polymeric nanoparticles promote macrophage reversal from M2 to M1 phenotypes in the tumor microenvironment. Biomaterials. 2017;112(1):153-63.

77. Foerster F, Baumhoefner C, Konhaeuser M, Aslam M, Schupp J, Tuettenberg A, et al. Evaluation of dextran-based nanoparticles for hepatic macrophage repolarization in liver cancer. Hepatology. 2017;66(S1):359.

78. Bustin SA, Benes V, Garson JA, Hellemans J, Huggett J, Kubista M, et al. The MIQE guidelines: minimum information for publication of quantitative real-time PCR experiments. Clin Chem. 2009;55(4):611-22.

79. Foerster F, Boegel S, Heck R, Pickert G, Russel N, Rosigkeit S, et al. Enhanced protection of C57 BL/6 vs Balb/c mice to melanoma liver metastasis is mediated by NK cells. Oncoimmunology. 2018;7(4):e1409929.

80. Box GM, Eccles SA. Simple Experimental and Spontaneous Metastasis Assays in Mice. In: Wells CM, Parsons M, editors. Cell Migration: Developmental Methods and Protocols. Totowa, NJ: Humana Press; 2011. p. 311-29.

81. Cohen JL, Schubert S, Wich PR, Cui L, Cohen JA, Mynar JL, et al. Acid-degradable cationic dextran particles for the delivery of siRNA therapeutics. Bioconjug Chem. 2011;22(6):1056–65.

82. Bachelder EM, Beaudette TT, Broaders KE, Dashe J, Frechet JM. Acetal-derivatized dextran: an acid-responsive biodegradable material for therapeutic applications. J Am Chem Soc. 2008;130(32):10494-5.

83. Bas A, Forsberg G, Hammarstroem S, Hammarstroem M-L. Utility of the Housekeeping Genes 18S rRNA, b-Actin and Glyceraldehyde-3-Phosphate-Dehydrogenase for Normalization in Real-Time Quantitative Reverse Transcriptase-Polymerase Chain Reaction Analysis of Gene Expression in Human T Lymphocytes. Scandinavian Journal of Immunology. 2004;59(6):566–73.

84. Kalagara R, Gao W, Glenn HL, Ziegler C, Belmont L, Meldrum DR. Identification of stable reference genes for lipopolysaccharide-stimulated macrophage gene expression studies. Biol Methods Protoc. 2016 Dec 27;1(1):bpw005.

85. Idriss HT, Naismith JH. TNF alpha and the TNF receptor superfamily: structure-function relationship(s). Microsc Res Tech. 2000;50(3):184-95.

86. Müller E, Christopoulos PF, Halder S, Lunde A, Beraki K, Speth M, et al. Toll-Like Receptor Ligands and Interferon-γ Synergize for Induction of Antitumor M1 Macrophages. Front Immunol. 2017 Oct 26;8:1383.

87. Hu X, Ivashkiv LB. Cross-regulation of signaling pathways by interferon-gamma: implications for immune responses and autoimmune diseases. Immunity. 2009;31(4):539-50.

88. East L, Isacke CM. The mannose receptor family. Biochim Biophys Acta. 2002;1572(2-3):364–86.

89. Martinez-Pomares L, Linehan SA, Taylor PR, Gordon S. Binding properties of the mannose receptor. Immunobiology. Immunobiology 2001;204(5):527-35.

90. Edwards JP, Zhang X, Frauwirth KA, Mosser DM. Biochemical and functional characterization of three activated macrophage populations. J Leukoc Biol. 2006;80(6):1298–307.

91. Hoppstadter J, Seif M, Dembek A, Cavelius C, Huwer H, Kraegeloh A, et al. M2 polarization enhances silica nanoparticle uptake by macrophages. Front Pharmacol. 2015 Mar 23;6:55.

92. Marucha PT, Crespin TR, Shelby RA, Andersen BL. TNF-alpha levels in cancer patients relate to social variables. Brain Behav Immun. 2005;19(6):521-5.

93. Horiuchi T, Mitoma H, Harashima S, Tsukamoto H, Shimoda T. Transmembrane TNF-alpha: structure, function and interaction with anti-TNF agents. Rheumatology (Oxford). 2010;49(7):1215-28.

94. MacEwan DJ. TNF ligands and receptors - a matter of life and death. Br J Pharmacol. 2002;135(4):855-75.

95. Lang R, Patel D, Morris JJ, Rutschman RL, Murray PJ. Shaping gene expression in activated and resting primary macrophages by IL-10. J Immunol. 2002;169(5):2253-63.

96. Murray PJ. Macrophage Polarization. Annu Rev Physiol. 2017;79:541-66.

97. Paul S, Chhatar S, Mishra A, Lal G. Natural killer T cell activation increases iNOS(+)CD206(-) M1 macrophage and controls the growth of solid tumor. J Immunother Cancer. 2019;7(1):208.

98. Xaus J, Comalada M, Barrachina M, Herrero C, Goñalons E, Soler C, et al. The Expression of MHC Class II Genes in Macrophages Is Cell Cycle Dependent. The Journal of Immunology. 2000;165(11):6364-71.

99. Huang Z, Fasco MJ, LS. K. Optimization of Dnase I removal of contaminating DNA from RNA for use in quantitative RNA-PCR. Biotechniques. 1996 Jun;20(6):1012-4,6,8-20.

100. Tajadini M, Panjehpour M, Javanmard SH. Comparison of SYBR Green and TaqMan methods in quantitative real-time polymerase chain reaction analysis of four adenosine receptor subtypes. Adv Biomed Res. 2014 Feb 28;3(1):85.

101. Arikawa E, Sun Y, Wang J, Zhou Q, Ning B, Dial SL, et al. Cross-platform comparison of SYBR Green real-time PCR with TaqMan PCR, microarrays and other gene expression measurement technologies evaluated in the MicroArray Quality Control (MAQC) study. BMC Genomics. 2008;9(2):328-46.

102. Tao Y, Yue Y, Qiu G, Ji Z, Spillman M, Gai Z, et al. Comparison of analytical sensitivity and efficiency for SARS-CoV-2 primer sets by TaqMan-based and SYBR Green-based RT-qPCR. Appl Microbiol Biotechnol. 2022;106(5-6):2207-18.

103. Ayers M, Lunceford J, Nebozhyn M, Murphy E, Loboda A, Kaufman DR, et al. IFN-gamma-related mRNA profile predicts clinical response to PD-1 blockade. J Clin Invest. 2017;127(8):2930-40.

104. Yamamoto N, Zou JP, Li XF, Takenaka H, Noda S, Fujii T, et al. Regulatory mechanisms for production of IFN-gamma and TNF by antitumor T cells or macrophages in the tumor-bearing state. J Immunol. 1995 154(4):2281-90.

105. Quail DF, Joyce JA. Microenvironmental regulation of tumor progression and metastasis. Nat Med. 2013;19(11):1423-37.

106. Johansson M, Denardo DG, Coussens LM. Polarized immune responses differentially regulate cancer development. Immunol Rev. 2008;222:145-54.

107. Biswas SK, Mantovani A. Macrophage plasticity and interaction with lymphocyte subsets: cancer as a paradigm. Nat Immunol. 2010;11(10):889-96.

IX. ACKNOWLEDGEMENTS

I would like to thank Univ.-Prof. Dr. Dr. Detlef Schuppan for being my supervisor, his support and the opportunity to write my MD thesis in his Institute.

I thank PD Dr. med. (Ernst)_Friedrich_(Christoph) Foerster for directly supervising my MD thesis, for the great support throughout the entire work process and the tireless willingness to answer my questions.

I am grateful to all the members of the Institute of Translational Immunology (TIM) who were always there to help me learn and perform the experimental work. Especially would thank … for sharing her knowledge and teaching in cell culture. …, … and … for their help to prepair histological sections and immunohistochemical staining.

I would like to thank … (Institute of Pharmacy and Biochemistry, Johannes Gutenberg-University, Mainz) for providing the dextran-based nanoparticles.

Finally, I would like to thank my family, friends and my husband for their endless patience and support.

Part of this work was published as: abstract 'Evaluation of dextran-based nanoparticles for hepatic macrophage repolarization in liver cancer', (Foerster F. et al., Hepatology, 2017(77))

and presented as poster abstract: 'Evaluation of dextran-based nanoparticles for hepatic macrophage repolarization in liver cancer' at the 68th Annual Meeting of the American-Association-for-the-Study-of-Liver-Diseases (AASLD) / Liver Meeting, DC, Washington, 20 October 2017 - 24 October 2017.

X. CURRICULUM VITAE

Personal data

Name	Carlotta Baumhöfner
Date of birth	08-29-1993
Place of birth	Frankfurt am Main
Father	Axel Baumhöfner
Mother	Corinna Baumhöfner

Academic career

05-14-2020	Approbation
10/2013 – 05/2020	Medicine, Johannes Gutenberg University Mainz
09/2015	First part of state medical examination
04/2019	Second part tate medical examination
05/2020	Third part of statemedical examination
2012	Abitur, grammar school "Leibnizschule", Offenbach am Main
2003	Grammar school “Leibnizschule“, Offenbach am Main
2000 - 2003	Elementary school “Ernst-Reuter-Schule“, Offenbach am Main
1999 - 2000	Elementary school “Dahlmannschule“, Frankfurt am Main

Professional experience, Clinical experience

Since 09/2021	Assistant Physician in Internal Medicine at the Department of Gastroenterology, Klinikum Hanau, Hanau
08/2020 – 08/2021	Assistant Physician in Internal Medicine at the Department of Gastroenterology, Gastroenterological Tumour Therapy and Diabetology Gemeinschaftsklinikum Mittelrhein, Kemperhof Koblenz
2019 - 2020	Practical year at the Gemeinschaftsklinikum Mittelrhein, Kemperhof Koblenz First tertial: Surgery Second tertial: Gynecology Third tertial: Internal Medicine

2015 - 2019	Employment as a medical student for a temporary job, vascular surgery St. Josefs-Hospital Wiesbaden
2018	Clinical traineeship in anesthesia at the ambulatory surgery center of the BG Klinikum Hamburg
2017	Clinical traineeship at the joint practice of Dr. Koffler and Theobald for pediatrics and adolescent medicine in Mainz
2017	Clinical traineeship in gynecology, St.Josefs-Hospital Wiesbaden
2016	Clinical traineeship in internal medicine, Katholisches Klinikum, Mainz
2012 - 2013	Temporary employment at Lion and Fishes GmbH in the area of sales and marketing

Internships

2013	Nursing internship at Clementine Children's Hospital Frankfurt, newborns and infants
2013	Nursing internship at Ketteler Hospital Offenbach, surgical ward
01/2013	Internship at Fletcher Allen Health Care Institute, Department of Radiology, Burlington, Vermont, USA
2012	Nursing internship at Klinikum Offenbach, neurosurgery ward
2010	Internship in architecture, whitedesign, Bristol, UK
2008	Internship in exhibition and furniture construction, Spacewood GmbH, Frankfurt am Main